Phytoplankton functional traits under the impact of environmental change: From single cells to communities

Dissertation zur Erlangung des Grades eines

Doktors der Naturwissenschaften

- Dr. rer. nat. -

Fachbereich 2 Biologie/Chemie

Vorgelegt von

Elisabeth Groß

Universität Bremen

April 2022

ALFRED-WEGENER-INSTITUT
HELMHOLTZ-ZENTRUM FÜR POLAR- UND MEERESFORSCHUNG

GEFÖRDERT VOM
Bundesministerium
für Bildung
und Forschung

Prüfungsausschuss:

1. Gutachter: Prof. Dr. Tilmann Harder (Meereschemie, Universität Bremen)

2. Gutachter: PD Dr. Cédric Meunier (PlanktoSERV, Shelf Sea System Ecology, Alfred-Wegener-Institut, Helmholtz-Zentrum für Polar-und Meeresforschung, Biologische Anstalt Helgoland)

1. Prüfer: Prof. Dr. Marko Rohlfs (Populations- und Evolutionsökologie, Universität Bremen)

2. Prüferin: Dr. Marlis Reich (Molekulare Ökologie, Universität Bremen)

Tag des Promotionskolloquiums: 13. Juni 2022

Contents

Contents ..... **i**

List of figures ..... **iv**

List of tables ..... **vi**

Frequently used abbreviations ..... **vii**

Thesis summary ..... **ix**

Zusammenfassung ..... **xi**

Chapter 1. General introduction **1**

1.1. Phytoplankton ecology, from diversity to trait-based approaches *1*
1.2. Impacts of global change on coastal marine phytoplankton *3*
1.3. Single-cell and single-strain responses *5*
1.4. Population and community responses *7*

Aims of the thesis **10**

Publications and manuscripts **12**

Chapter 2. Environmental impacts on single-cell variation within a ubiquitous diatom: the role of growth rate **15**

2.1. Introduction *17*
2.2. Materials and methods *20*
2.3. Results *24*
2.4. Discussion *31*
2.5. Conclusion *35*

Supplementary material *36*

Chapter 3. Global change induces oxidative stress and alters the carbon metabolism of phytoplankton **39**

3.1. Introduction *41*
3.2. Materials and methods *43*
3.3. Results *51*
3.4. Discussion *56*
Supplementary material *61*

Chapter 4. The impact of marine heatwaves under two dissolved N:P ratios on the physiology of the diatom *Phaeodactylum tricornutum* **67**

4.1. Introduction *69*
4.2. Materials and methods *71*
4.3. Results *75*
4.4. Discussion *80*
Supplementary material *84*

Chapter 5. Extreme weather events: potential consequences of abrupt increases in river discharge on North Sea phytoplankton communities. **85**

5.1. Introduction *87*
5.2. Materials and methods *90*
5.3. Results *95*
5.4. Discussion *103*
5.5. Conclusion *107*
Supplementary material *109*

Chapter 6. General discussion **115**

6.1. Rising average temperature, pCO_2, and dissolved N:P ratio – phytoplankton living under future environmental conditions *116*
6.1.1. Growth rate 117

6.1.2. Trait variability 118
6.1.3. Strain-specific responses 120
6.1.4. Synthesis 120
6.2. Extreme weather events – Phytoplankton coping with extremes 121
6.2.1. Heatwaves 122
6.2.2. Increased river discharge 123
6.2.3. Synthesis 124
6.3. Potential consequences for ecosystem functioning 125

Bibliography 127

Acknowledgments 151

List of figures

Figure 1.1: Correlation between phytoplankton traits and ecological functions 3

Figure 2.1: Growth rates, cell size, and chlorophyll *a* content of *T. weissflogii* 26
Figure 2.2: Principal component analysis 28
Figure 2.3: Cellular protein content of *T. weissflogii* 28
Figure 2.4: Cell size and chlorophyll *a* content of *T. weissflogii* 30
Figure 2.5: Cell size variability over growth rate of *T. weissflogii* 31

Figure 3.1: Antioxidant enzymatic response and oxidative stress. 52
Figure 3.2: Alternative oxidase activity and carotenoids 52
Figure 3.3: Carbon fluxes in the *Phaeodactylum tricornutum* 54
Figure 3.4: Cellular carbon content and *Phaeodactylum tricornutum* specific growth rate ... 54
Figure 3.5: Principal component analysis 56

Figure 4.1: Schematic overview of the experimental setup 73
Figure 4.2: Routine rate and AOX activity of *P. tricornutum* 77
Figure 4.3: Growth rate of *P. tricornutum* 78
Figure 4.4: Cell size of *P. tricornutum* 78
Figure 4.5: POC of *P. tricornutum* 79

Figure 5.1: Location of the transect with the three sampling stations in the North Sea 91
Figure 5.2: Growth rate of phytoplankton communities 96
Figure 5.3: Relative abundances before incubation 98
Figure 5.4: Phytoplankton community composition after incubation 99
Figure 5.5: Cell volume of phytoplankton communities before incubation 100
Figure 5.6: Cell volume of phytoplankton communities after incubation 100
Figure 5.7: Molar C:N, C:P, N:P ratios of initial community 101
Figure 5.8: Molar C:N, C:P, N:P ratios of phytoplankton communities after incubation 102

Supplementary figures

Suppl. Figure 2.1: Growth curve of *T. weissflogii* 36
Suppl. Figure 2.2: Lipid and protein contentof *T. weissflogii* over growth rate 36

Suppl. Figure 3.1: Dissolved inorganic nutrients 61
Suppl. Figure 3.2: Biomarker of oxidative stress 62
Suppl. Figure 3.3: Biomarkers of enzymatic antioxidant response 62
Suppl. Figure 3.4: Cellular carotenoids concentration 63

Suppl. Figure 5.1: Absolute abundances at station 1 before and after incubation. 109
Suppl. Figure 5.2: Absolute abundances at station 2 before and after incubation 110
Suppl. Figure 5.3: Absolute abundances at station 3 before and after incubation 110
Suppl. Figure 5.4: POC, PON, POP of initial community samples 111

List of tables

Table 3.1: Rapid light curve fitted parameters 53

Table 4.1: ANOVA results of best-fit model of total respiration and AOX activity of *P. tricornutum* 76

Table 5.1: Dissolved and total nutrient concentrations before and after 72-hours of experimental incubation 90
Table 5.2: Two-way analysis of variance growth rate 93
Table 5.3: Two-way analysis of variance molar ratios 101

Supplementary tables

Suppl. Table 2.1: DIN and DIP 37

Suppl. Table 3.1: Seawater carbonate chemistry. 63

Suppl. Table 4.1: DIN and DIP in two temperature and two dissolved nutrient treatments 84

Suppl. Table 5.1: Results of Tukey's *post-hoc* comparison after two-way ANOVA of average cell volume of phytoplankton communities after incubation 112
Suppl. Table 5.2: Results of Tukey's *post-hoc* comparison after two-way ANOVA of molar C:N, C:P, N:P ratio of phytoplankton communities after incubation 113

Frequently used abbreviations

ANOVA: Analysis of variance

AOX: Alternative oxidase

Chl *a*: Chlorophyll *a*

CWM: Community weighted mean

DIC: Dissolved inorganic carbon

DIN: Dissolved inorganic nitrogen

DIP: Dissolved inorganic phosphorus

DOC: Dissolved organic carbon

ETC: Electron transport chain

FSC: Forward scatter

IPCC: Intergovernmental Panel on Climate Change

KCN: Potassium cyanide

N: Nitrogen

P: Phosphorus

PCA: Principal component analysis

***p*CO$_2$**: Partial pressure of carbon dioxide

POC: Particulate organic carbon

PON: Particulate organic nitrogen

POP: Particulate organic phosphorus

RCP: Representative concentration pathways

SHAM: Salicylhydroxamic acid

Thesis summary

Phytoplankton are responsible for half of the total oxygen production on Earth and play an important role in ocean productivity as the base of most aquatic food webs. However, human activities are leading to changes in marine abiotic parameters, and phytoplankton are facing simultaneous changes in temperature, partial pressure of carbon dioxide (pCO_2), and dissolved nutrient concentrations, as well as more frequent and intense extreme weather events such as heatwaves and increasing river discharge. In my thesis, I applied trait-based approaches to investigate these effects in several multiple driver experiments at different ecological scales, from individual phytoplankton cells to populations to entire phytoplankton communities.

To assess the impact of long-term changes in average environmental conditions, two model diatom species were exposed to a simultaneous increase in temperature, pCO_2, and shifting dissolved nitrogen:phosphorous (N:P) ratios. The scenarios were chosen based on predictions by the Intergovernmental Panel on Climate Change (IPCC) and nutrient regime shifts expected for the end of the century. The results of my thesis indicate that temperature was the most important driver affecting phytoplankton growth and other functional traits. For phytoplankton species currently growing below their thermal limits, growth rates will likely increase with projected temperature rises of + 1.5 or + 3 °C, but the magnitude of this growth enhancement may be dampened by simultaneous increases in pCO_2 and N:P ratios. Increasing growth rates within cultures of the ubiquitous diatom species *Thalassiosira weissflogii* caused a decline in the variability of cellular chlorophyll *a* content and a decline in cell-to-cell variability in cell size, the latter of which can only be explained by a decrease in phenotypic plasticity. Furthermore, increasing temperatures and pCO_2 caused an overall decrease in cell-to-cell variability of cell size, which was not correlated with growth rate. The decrease in trait variability could reduce the potential for phytoplankton to cope with changes in environmental conditions. In addition, higher temperatures, pCO_2, and dissolved N:P ratios caused an increase in the alternative oxidase (AOX) pathway of the diatom *Phaeodactylum tricornutum* and an increased ratio between photoprotective and light-harvesting pigments, indicating cellular stress.

Besides long-term changes in average environmental conditions, abrupt changes caused by extreme weather events may also alter the functional properties of phytoplankton. The impact of a marine heatwave was investigated in my thesis using the diatom *P. tricornutum* in combination with an increase in dissolved N:P ratio. Cellular responses were measured directly after a + 5 °C temperature increase and after a 5-day acclimation period. AOX was also examined as a stress marker, but this time, no increase in AOX activity due to the abrupt increase in temperature was observed. Most changes in cellular traits were rather observed after acclimation to higher temperatures, such as an increase in growth rate and cellular particular organic carbon (POC) content. In contrast, cell size and cellular lipid content decreased. These results indicate that phytoplankton cells might have the potential to buffer environmental fluctuations such as marine heatwaves yet undergo significant changes in their traits.

Finally, I investigated the potential impact of increased river discharge on natural North Sea phytoplankton communities. The experiment was on board the research vessel Pelagia at three different stations with increasing distances from the coast. Pulses of nutrient-rich freshwater, resulting in an abrupt increase in nutrient concentrations and a decrease in salinity, caused an increase in community growth rates but also decreased phytoplankton cell size within the different phytoplankton groups and a decrease in cellular N:P ratio. At the same time, no strong negative effect of decreasing salinity was observed, indicating a large salinity tolerance of North Sea phytoplankton communities, although it appears that while phytoplankton benefit from nutrient additions, this is no longer the case when accompanied by a more drastic decrease in salinity. Overall, responses of phytoplankton communities depended more on the initial community structure at each sampling site than on the origin of the communities. Still, an abrupt increase in river discharge might have the potential to restructure phytoplankton communities and modulate short-term responses in higher trophic levels.

This thesis provides a comprehensive picture of the effects of different types of environmental changes on the functional traits of phytoplankton, from single cells to phytoplankton communities. Long-term environmental changes, as well as short-term extreme weather events, can lead to substantial changes in growth rates, cell size, and the biochemical composition of phytoplankton, which have the potential to alter marine food webs and biogeochemical cycling.

Zusammenfassung

Phytoplankton ist für die Hälfte der gesamten Sauerstoffproduktion auf der Erde verantwortlich und spielt als Grundlage der meisten aquatischen Nahrungsnetze eine wichtige Rolle für die Produktivität der Ozeane. Menschliche Aktivitäten führen jedoch zu Veränderungen der abiotischen Parameter im Meer, und Phytoplankton ist mit gleichzeitigen Veränderungen der Temperatur, des Partialdrucks von Kohlendioxid (pCO_2) und der Konzentration gelöster Nährstoffe sowie mit häufigeren und intensiveren extremen Wetterereignissen wie Hitzewellen und zunehmenden Flusseinträgen konfrontiert. In meiner Dissertation habe ich eigenschaftsbasierte Ansätze angewandt, um diese Auswirkungen in mehreren Experimenten mit simultanen Änderungen der abiotischen Parameter auf verschiedenen ökologischen Ebenen zu untersuchen, von einzelnen Phytoplanktonzellen über Populationen bis hin zu ganzen Phytoplanktongemeinschaften.

Um die Auswirkungen langfristiger Veränderungen der durchschnittlichen Umweltbedingungen zu bewerten, wurden zwei Modell-Kieselalgenarten einem gleichzeitigen Anstieg der Temperatur, des pCO_2 und einer Verschiebung des Verhältnisses von gelöstem Stickstoff:Phosphor (N:P) ausgesetzt. Die Szenarien wurden auf der Grundlage der Vorhersagen des „Intergovernmental Panel on Climate Change“ (IPCC) und der für das Ende des Jahrhunderts erwarteten Verschiebung der Nährstoffverhältnisse ausgewählt. Die Ergebnisse meiner Dissertation zeigen, dass die Temperatur der wichtigste Einflussfaktor auf das Wachstum des Phytoplanktons und andere funktionelle Merkmale ist. Für Phytoplanktonarten, die derzeit unterhalb ihrer thermischen Grenzen wachsen, werden die Wachstumsraten bei einem prognostizierten Temperaturanstieg von + 1,5 oder + 3 °C wahrscheinlich zunehmen, aber das Ausmaß dieser Wachstumssteigerung könnte durch den gleichzeitigen Anstieg von pCO_2 und N:P-Verhältnissen gedämpft werden. Steigende Wachstumsraten in Kulturen der weit verbreiteten Kieselalgenart *Thalassiosira weissflogii* führten zu einem Rückgang der Variabilität des zellulären Chlorophyll-a-Gehalts und zu einem Rückgang der Variabilität der Zellgröße zwischen den einzelnen Zellen, wobei letzteres nur durch eine Abnahme der phänotypischen Plastizität erklärt werden kann. Darüber hinaus verursachten steigende Temperaturen und pCO_2 einen Gesamtrückgang der Variabilität der

Zellgröße zwischen den einzelnen Zellen, der nicht mit der Wachstumsrate korreliert war. Der Rückgang der Merkmalsvariabilität könnte das Potenzial des Phytoplanktons verringern, sich an veränderte Umweltbedingungen anzupassen. Darüber hinaus verursachten höhere Temperaturen, pCO_2 und das Verhältnis von gelöstem N:P einen Anstieg des alternativen Oxidase-Stoffwechsels (AOX) der Kieselalge *Phaeodactylum tricornutum* und ein erhöhtes Verhältnis zwischen photoprotektiven und lichtsammelnden Pigmenten, was auf zellulären Stress hinweist.

Neben langfristigen Veränderungen der durchschnittlichen Umweltbedingungen können auch abrupte Veränderungen durch extreme Wetterereignisse die funktionellen Eigenschaften des Phytoplanktons verändern. Die Auswirkungen einer marinen Hitzewelle wurden in meiner Dissertation am Beispiel der Kieselalge *P. tricornutum* in Verbindung mit einem Anstieg des Verhältnisses von gelöstem N:P untersucht. Die zellulären Reaktionen wurden direkt nach einem Temperaturanstieg um 5 °C und nach einer fünftägigen Akklimatisierungsphase gemessen. Auch in diesem Versuch wurde AOX als Stressmarker untersucht, aber in diesem Fall wurde kein Anstieg der AOX-Aktivität aufgrund des abrupten Temperaturanstiegs beobachtet. Die meisten Veränderungen der zellulären Merkmale wurden vielmehr nach der Akklimatisierung an höhere Temperaturen beobachtet, wie z. B. ein Anstieg der Wachstumsrate und des zellulären Gehalts an besonderem organischem Kohlenstoff (POC). Im Gegensatz dazu nahmen die Zellgröße und der zelluläre Lipidgehalt ab. Diese Ergebnisse deuten darauf hin, dass Phytoplanktonzellen das Potenzial haben könnten, Umweltschwankungen wie marine Hitzewellen abzupuffern, dabei aber erhebliche Veränderungen in ihren Eigenschaften erfahren.

Abschließend untersuchte ich die potentiellen Auswirkungen erhöhter Flusseinträge auf natürliche Phytoplanktongemeinschaften der Nordsee. Das Experiment fand an Bord des Forschungsschiffs Pelagia an drei verschiedenen Stationen mit zunehmender Entfernung von der Küste statt. Pulse von nährstoffreichem Süßwasser, die zu einem abrupten Anstieg der Nährstoffkonzentrationen und einer Abnahme des Salzgehalts führten, bewirkten einen Anstieg der Wachstumsraten der Gemeinschaften, aber auch eine Abnahme der Zellgröße des Phytoplanktons innerhalb der verschiedenen Phytoplanktongruppen und eine Abnahme des N:P-Verhältnisses in den Zellen. Gleichzeitig wurde keine starke negative Auswirkung des

abnehmenden Salzgehalts beobachtet, was auf eine große Salinitätstoleranz der Phytoplanktongemeinschaften in der Nordsee hindeutet, obwohl es scheint, dass das Phytoplankton zwar von der Nährstoffzufuhr profitiert, dies aber nicht mehr der Fall ist, wenn sie mit einer drastischeren Abnahme des Salzgehalts einhergeht. Insgesamt hingen die Reaktionen der Phytoplanktongemeinschaften mehr von der ursprünglichen Struktur der Gemeinschaften an den einzelnen Probenahmestellen ab als vom Ursprung der Gemeinschaften. Dennoch könnte ein abrupter Anstieg von Flusseinträgen das Potenzial haben, Phytoplanktongemeinschaften umzustrukturieren und kurzfristige Reaktionen in höheren trophischen Ebenen zu beeinflussen.

Diese Dissertation liefert ein umfangreiches Bild der Auswirkungen verschiedener Arten von Umweltveränderungen auf die funktionellen Eigenschaften des Phytoplanktons, von einzelnen Zellen bis hin zu Phytoplanktongemeinschaften. Langfristige Umweltveränderungen sowie kurzfristige extreme Wetterereignisse können zu erheblichen Veränderungen der Wachstumsraten, der Zellgröße und der biochemischen Zusammensetzung des Phytoplanktons führen, welche das Potenzial haben, marine Nahrungsnetze und biogeochemische Kreisläufe zu verändern.

Chapter 1

General introduction

1.1. Phytoplankton ecology, from diversity to trait-based approaches

Phytoplankton are an essential component of aquatic life but also for life on Earth in general. They play a key role in the cycling of carbon and nutrients and, at the same time, are responsible for about half of the worldwide oxygen production. Phytoplankton use inorganic and, to some extent, organic nutrients and convert them into biomass through photosynthetic processes. This biomass can either be transported to deeper water layers by sinking phytoplankton cells, or it is available to grazers, allowing energy and nutrients to be transferred through the food web to higher trophic levels. Phytoplankton are particularly diverse organisms, with cell sizes ranging over several orders of magnitude, from less than 2 µm for nanophytoplankton up to 200 µm for microphytoplankton. In addition, individual cells can form chains or colonies and/or have spines to protect themselves from predators, and mixotrophic species can take up organic biomass, thereby widening the spectrum of available resources. This wide diversity in size, shape, and life history allows phytoplankton to occupy a broad range of ecological niches. For decades, scientists have developed ecological frameworks to synthesize this diversity and facilitate the study of phytoplankton-environment interactions.

As early as in 1961, Hutchinson raised the question of how phytoplankton species, in their great diversity, can coexist in a relatively unstructured environment where they often compete for the same resources (Hutchinson, 1961). This paradox of the plankton indeed contradicted the competitive exclusion principle which posits that when two species compete for the same resource, one will be driven to extinction (Hardin, 1960). However, guided in part by Tilman's mechanistic theory of resource competition (Tilman, 1977, Tilman, 1985) and Connell's intermediate disturbance hypothesis (Connell, 1978), we now know that the aquatic environment in which phytoplankton grow is not as unstructured as initially thought (Abraham,

1998), and several ecological approaches and syntheses have increased our understanding of phytoplankton dynamics and diversity over the past decades. In 1978, Margalef proposed a model, now commonly known as Margalef's Mandala, which considers dissolved nutrient concentration and turbidity as driving forces for phytoplankton community composition and biomass variation in space and time (Margalef, 1978). The mandala not only relates diatom and dinoflagellate life forms to physical and nutritional forces but also incorporates the ecological concept of the *r* and *K* strategies, which describe the trade-off between growth and production versus maintenance and efficiency in resource acquisition. Whereas diatoms generally have high reproduction rates and thrive at high dissolved nutrient concentrations and high turbulence, dinoflagellates favor maintenance and are more competitive under nutrient-poor and low-turbulence conditions, which has led Margalef to qualify diatoms as *r*-strategists and dinoflagellates as *K*-strategists. Phytoplankton also differ in their life history strategies, and three major nutrient acquisition strategies have been identified (Sommer, 1984): (1) velocity-adapted species, or *r*-strategists, which have high maximum nutrient uptake rates and high maximum growth rates, enabling them to make efficient use of nutrient pulses, (2) storage-adapted species, which have high nutrient uptake rates but relatively low maximum growth rates and which can store nutrients, and (3) affinity-adapted species, or *K*-strategists, which efficiently take up and assimilate growth-limiting nutrients even at low concentrations, a strategy that is advantageous in oligotrophic environments.

Based on this earlier work, in the early 21st century Elena Litchman created a more formal, overarching framework for a trait-based approach to phytoplankton ecology that relates ecological functions (reproduction, resource acquisition, predator avoidance) to trait types (life history, behavioral, physiological, morphological) and considers associated trait-offs (Fig. 1.1, Litchman & Klausmeier, 2008). More specifically, the combination of traits determines the resource acquisition, survival, and reproductive success of organisms under specific environmental conditions and thereby defines ecological niches. In the broadness of traits that characterize phytoplankton cells, a few master traits, like cell size and maximum growth rate, appear to be a key determinant of ecological success as they are significantly correlated with many other ecophysiological traits such as nutrient and light utilization and grazer resistance (Litchman *et al.*, 2010). Hence, the functional classification of phytoplankton not only helps to capture and understand the wide diversity of phytoplankton but can also be used to assess how

environmental changes may alter phytoplankton dynamics. This is especially important in the context of global change because human-induced environmental alterations can alter phytoplankton functional structure, which highlights the need to understand how phytoplankton can respond to changes in environmental conditions.

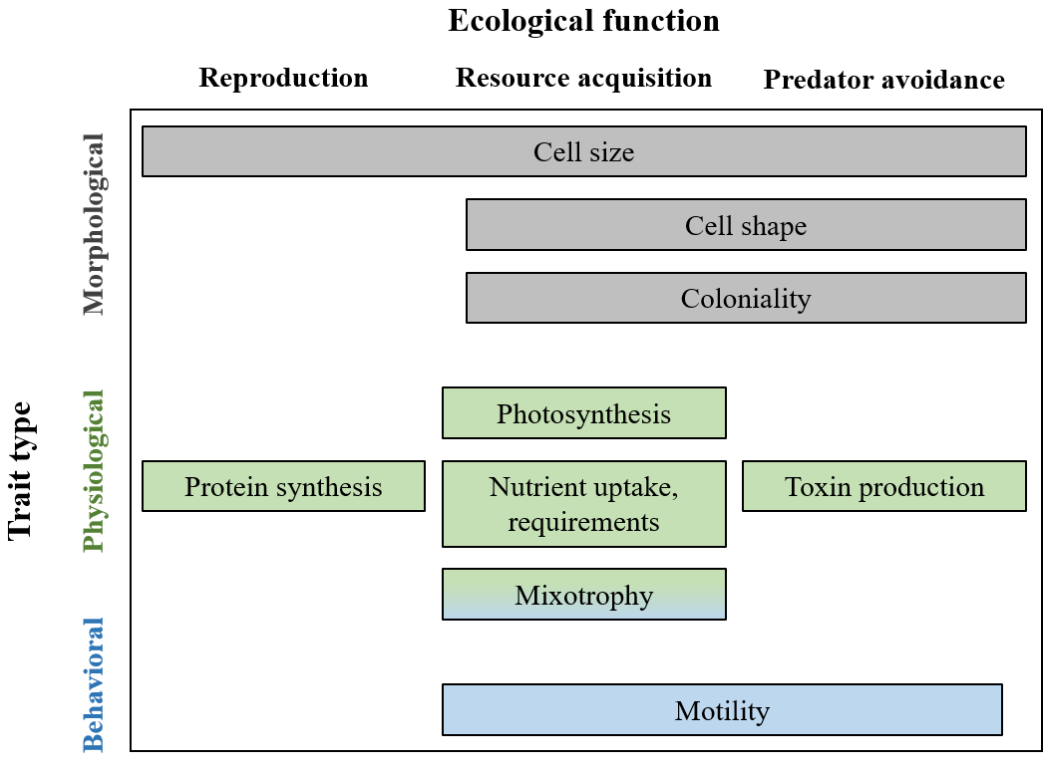

Figure 1.1: Correlation between phytoplankton traits and ecological functions. Modified after Litchman and Klausmeier (2008)

1.2. Impacts of global change on coastal marine phytoplankton

As a consequence of human activities, greenhouse gas concentrations have dramatically increased over the past decades. Depending on the scenarios developed by the Intergovernmental Panel on Climate Change (IPCC), temperatures will increase by 0.6–4.0 °C by 2100 (Collins *et al.*, 2013). However, warming is not uniform across the globe, and analyses of long-term data series have shown that marine coastal areas can warm faster than the global average (Wiltshire *et al.*, 2010). Numerous studies have shown that warming may have profound implications for coastal marine ecosystems (Wernberg *et al.*, 2012, Harley *et al.*, 2006), but recent work identified that changes in seawater chemistry might be even more

important than changes in temperature for the performance and survival of many organisms (Harley et al., 2006, Alvarez-Fernandez *et al.*, 2018, Doney, 2010). This observation is particularly important as coastal systems are among the most productive but most sensitive areas to environmental change (Halpern *et al.*, 2008). The alteration of coastal biogeochemical cycles is largely driven by nutrient runoffs originating from urban, agricultural, and industrial activities. For instance, nitrogen (N) and phosphorus (P) concentrations dramatically increased in European coastal waters from the 1960s until the 1980s (Grizzetti *et al.*, 2012). While national and regional regulations have successfully reduced N and P inputs into coastal areas, an analysis of the effects of European environmental policies shows that measures to reduce P were more successful than those tackling N. As a consequence, the N:P ratio in European coastal waters has steadily increased, and coastal systems are becoming increasingly P-limited (Grizzetti et al., 2012, Peñuelas *et al.*, 2013, Peñuelas *et al.*, 2012). Moreover, the main source of P fertilizers used in modern agriculture is mined phosphate rock, a non-renewable resource. Under a continuously increasing demand, the reserves may be depleted in 50-100 years (Cordell *et al.*, 2009), which may further increase P-limitation in coastal systems in the future. In addition, phytoplankton are not only facing gradual changes in abiotic parameters but also have to cope with extreme weather events, such as heavy precipitation or heatwaves, which are predicted to increase in frequency and intensity. While river discharges supply dissolved nutrients that are essential for phytoplankton growth, heavy precipitation events can lead to a disproportional input of nutrient-rich freshwater associated with strong local decreases in salinity. The rapid increase in seawater temperature due to heatwaves can drastically impact marine organisms, for instance, by causing cryptic loss of genetic diversity (Gurgel *et al.*, 2020) or by promoting local extinction of a species (Thomsen *et al.*, 2019).

As primary producers, phytoplankton are directly affected by changes in abiotic parameters. As described above, anthropogenic activities lead to simultaneous shifts in multiple environmental drivers, which exerts significant pressure on phytoplankton and alter these organisms at different organizational levels, from single individuals to whole communities. Consequently, the response of marine phytoplankton to changes in environmental conditions can be assessed at these different levels. Firstly, cellular phenotypic plasticity plays a key role, as the tolerance range of individual cells determines how single strains cope with changing environmental conditions (Collins et al., 2013, Sett *et al.*, 2014). Secondly, the sum of the

tolerance ranges of different strains within a population determines whether the population can cope with environmental change (Godhe & Rynearson, 2017). And third, change in community composition can occur when altered abiotic conditions lead to species selection. The previously introduced trait-based approaches have been successfully used to assess the impact of environmental change on phytoplankton, from the single-cell and population to the community level.

1.3. Single-cell and single-strain responses

Trait responses on the population or community level have received much attention (see below), but the reaction of individual phytoplankton cells to varying environmental conditions is still understudied. While this discrepancy is understandable and arises from the difficulty of measuring organisms smaller than 200µm individually, this organizational level should receive more attention as it is first and foremost responses of individuals which ultimately determine the ecological success of a species. So far, studies that investigated phytoplankton responses on a single-cell level have mainly been found in the field of metabolomics, assessing the biochemical composition and responses of individual cells using Fourier transform infrared (FTIR) spectroscopy and mass spectrometry (Jaschinski *et al.*, 2014, Pogorzelec *et al.*, 2017, Heraud *et al.*, 2005, Wagner *et al.*, 2010). Interestingly, these studies have shown that a substantial degree of variation exists between individual cells of a single strain, thereby highlighting the ecological importance of measuring single phytoplankton cells. For phytoplankton, in nature, it is indeed individuals that interact with each other, for example, through predator-prey relationships, not populations or communities. Quantifying the extent to which the biochemical composition of phytoplankton is affected by global change is relevant as it drives, for instance, the fitness of herbivorous consumers (Sterner & Elser, 2002). Because phytoplankton obtain solar energy and nutrients from different, uncoupled sources within their environment, these organisms developed strategies to store resources, as the availability of one resource does not guarantee that of another one. When nutrient availability or light conditions change, acquisition and storage create the potential for large variations in the biochemical composition of phytoplankton. Due to their large plasticity in biochemical composition, Phytoplankton can be defined as conformers (Meunier et al. 2014). Alterations of phytoplankton cellular biochemical composition are not anodyne as they can lead to nutritional

mismatches between the metabolic demands of herbivorous consumers and the quality of phytoplankton they consume. These mismatches can have far-reaching consequences for food webs as they do not only affect the abundance and persistence of single herbivore populations but also significantly influence interaction strengths and trophic transfer efficiencies of energy within food webs (Sterner & Elser, 2002).

Other studies on phenotypic trait plasticity, with a broader ecological perspective, compared the reaction of different strains with each other under different environmental conditions. For instance, Kremp *et al.* (2012) tested the effect of increasing temperature and partial pressure of carbon dioxide (pCO_2) on two traits, growth rate, and toxin production, of several strains of two algal species from different locations. This study shows that the origin of the strains plays a large role in the reaction to the treatments. Whereas strains of *Skeletonema marinio* originating from the North West Adriatic showed no clear pattern in response, the strains isolated from Skagerrak responded more homogenously to the treatments with a positive correlation between growth rate and temperature. Also, the second species studied, *Alexandrium ostenfeldii*, showed a strain-specific response in terms of growth rate and toxin production. Hattich *et al.* (2017) investigated the impact of ocean acidification on several genotypes of three phytoplankton species. Even though all three species, *Emiliania huxleyi*, *Gephyrocapsa oceanica*, and *Chaetoceros affinis*, mostly buffered the effect of higher pCO_2, the response range of different genotypes of a species varied.

Overall, these examples highlight that a substantial degree of variation exists in the functional responses of individual cells within a strain as well as of individual strains within a population to varying environmental conditions. Despite the obvious importance of studying the impact of global change at these organizational levels, there is still a paucity of studies adopting a trait-based approach to assess how phytoplankton cells react to changes in their environmental conditions but also how different traits are linked with each other (Meunier *et al.*, 2017). An important trait that is closely linked to other cellular parameters such as cell size or elemental stoichiometry (Finkel *et al.*, 2010) and can therefore be considered a master trait is growth rate. Since the growth rate of phytoplankton is affected by several environmental parameters like temperature or pCO_2 (Collins *et al.*, 2014, Cross *et al.*, 2015), changes in growth rate are likely to affect the other traits indirectly. However, the link between environmental

conditions, growth rate, and cellular traits remain poorly understood. Therefore, this thesis aims to contribute to filling the knowledge gaps on how multiple, interlinked, functional traits of individual phytoplankton strains respond to simultaneous changes in abiotic parameters and to what extent single-cell variation is affected.

1.4. Population and community responses

Compared to studies quantifying the responses of single cells or strains to global change drivers, considerably more work has been conducted on phytoplankton populations (reviewed by Gao *et al.*, 2018, reviewed by Van de Waal & Litchman, 2020). Earlier studies focused primarily on the influence of changes in temperature, pCO_2, and nutrient availability, mostly as individual drivers, while only fairly recently, interactions between multiple drivers have been considered (reviewed by Gunderson *et al.*, 2016). Because temperature drives metabolic activities, growth rate is often considered a response trait, and multiple studies have observed a direct link between temperature and growth rates in phytoplankton populations. Montagnes and Franklin (2001) showed that for all eight diatoms and both flagellates investigated, the growth rate increased linearly with temperature. Also, Kremer *et al.* (2017), who analyzed a dataset of more than 4200 growth rate measurements, showed a strong positive correlation between temperature and population growth rate. However, growth rate is also affected by other abiotic parameters such as pCO_2. As Rubisco, the enzyme that catalyzes inorganic carbon, is not saturated under current CO_2 concentrations, it is generally expected that increasing pCO_2 leads to increasing growth rates (Badger *et al.*, 1998). The response to changes in pCO_2, however, often strongly correlates to other parameters such as temperature (reviewed by Häder & Gao, 2015), nutrient concentrations (Flynn *et al.*, 2015), or light intensity (Seifert *et al.*, 2020). Another trait that has been frequently investigated is cell size. Cell size is linked to nutrient uptake capacities, growth and metabolic rates, and even the storage capacities of phytoplankton cells (Finkel et al., 2010). Marañón *et al.* (2013) investigated, among other things, nutrient uptake rates of 22 phytoplankton species and found a strong linear correlation with cell size, showing higher nutrient uptake rates the larger the average cell size of a species. Screening publications on studies with monoculture experiments, Tanioka and Matsumoto (2020) found a negative correlation between nutrient availability and C:P and C:N ratios of phytoplankton in their meta-analysis. Ultimately, the responses of individual phytoplankton

populations to changing environmental conditions determine if and how the structure of communities are altered.

Studies of phytoplankton communities have been conducted either by means of experiments or models to assess the influence of global change drivers, including increases in temperature, pCO_2, or changes in dissolved nutrient concentrations, on taxonomic community composition and the diversity or evenness of communities. These studies have shown, for example, that phytoplankton community composition depends not only on nutrient ratios but also on the total nutrient load of the oceans, with diatoms being more abundant when N or P is limited, while smaller green algae may have an advantage at high nutrient levels when large biomass leads to light limitation (Burson *et al.*, 2018). Eggers *et al.* (2014) found, however, that initial community composition has a greater impact on phytoplankton biomass than elevated pCO_2, but also that elevated pCO_2 can select for larger diatoms depending on initial community composition. Besides taxonomic approaches, trait-based ecological studies provide a mechanistic understanding on the impact of global change on phytoplankton. Indeed, traits like cell size are important characteristics describing community structure, and are strongly influenced by changes in environmental parameters. Multiple studies have shown that seawater warming tends to be favorable to small-sized phytoplankton, and a meta-analysis of data from the eastern and western temperate North Atlantic Ocean identified that independent of dissolved nutrient concentrations, temperature explains 73% of the variance in the relative contribution of small cells to total phytoplankton biomass (Morán *et al.*, 2010). Another important abiotic parameter that can affect the size structure of phytoplankton communities is the concentration of dissolved inorganic nutrients. More regular and intense river discharge leading to high nutrient inputs in coastal areas may favor large phytoplankton. Indeed, larger cells may have a competitive advantage because of their high vacuole nutrient storage capacity (Grover, 1991, Litchman *et al.*, 2009, Stolte & Riegman, 1996), whereas small sizes are advantageous under nutrient-limiting conditions because of the high surface area to volume ratio which increases nutrient uptake efficiency (Chisholm, 1992). But not only do nutrient concentrations play an important role, but also the ratio of available nutrients can have great effects on the compositions of phytoplankton communities. In an experiment with North Sea phytoplankton communities, Burson et al. (2018) showed that a community dominated by diatoms can shift toward the dominance of green algae at high N concentrations and towards cyanobacteria under

high P concentrations. Furthermore, the few studies addressing the combined effects of multiple drivers on phytoplankton communities showed, for example, shifts in phytoplankton organismal size (Sommer *et al.*, 2015, Alvarez-Fernandez et al., 2018, Sett *et al.*, 2018).

Despite the urgent need to understand and predict how global change will influence phytoplankton, there is still a striking paucity of information on the integrated impact of multiple drivers (Finkel et al., 2010, Häder & Gao, 2015). Within phytoplankton communities, individual species differ in their maximum growth rate and associated nutrient uptake and storage capacities. Long-term environmental changes, as well as extreme weather events, favor certain species over others, with species sorting being primarily determined by the characteristics of the different species, which could result in large shifts in community structure. However, these processes are still largely unknown. In this thesis, I aim to contribute to filling that knowledge gap by linking population and community responses to altered growth rates resulting from extreme weather events.

Aims of the thesis

The overall aim of my thesis is to investigate the long-term effects of global change, as well as the impact of extreme weather events, on phytoplankton functional traits at different scales, from single cells to natural phytoplankton communities. For this purpose, I focused in multi-driver experiments on simultaneous changes in temperature, pCO_2, and dissolved inorganic nitrogen:phosphorus (N:P) ratios, predicted by the intergovernmental panel on climate change (IPCC) and their impact on single phytoplankton strains and populations (**chapter two** and **three**). To investigate the impact of extreme weather events on phytoplankton, I conducted a heatwave experiment with a single phytoplankton population (**chapter four**) and subjected natural North Sea communities to pulses of nutrient-rich freshwater, simulating increased river discharge after heavy precipitation events (**chapter five**). The specific aims of the thesis were:

In **chapter two**, I focus on single-cell variation within one strain of the diatom species *Thalassiosira weissflogii* when growing under two different future scenarios. In a multiple driver experiment, temperature, pCO_2, and dissolved N:P ratios were manipulated simultaneously to reveal the link between growth rate, cell size, and biochemical composition of the cells. I hypothesized that not only between species and population but also within a single strain, cell-to-cell variability of phytoplankton decreases with increasing growth rate.

Chapter three focuses on carbon fluxes and stress responses of the diatom species *Phaeodactylum tricornutum* when growing under elevated temperature and pCO_2 and two dissolved N:P ratios, as expected in long-term future scenarios. Among other parameters, primary production, respiration, dissolved organic carbon production, and cellular carbon content of *P. tricornutum* cells were investigated to determine how multiple environmental drivers can alter the physiological processes of phytoplankton cells.

Chapter four focuses on the response of the diatom *P. tricornutum* to a marine heatwave, considering the ratio of dissolved N:P in the environment. Changes in cell properties were

measured both immediately after the temperature increase and after an acclimation period to test for cellular stress responses. In addition, links between the growth rate of *P. tricornutum*, cell size, and biochemical composition were investigated. To test whether short-term temperature increases and an elevated N:P ratio lead to cellular stress, the contribution of alternative oxidase (AOX) to cellular respiration was measured before and after acclimation to elevated temperature. In addition, changes in growth rate and cell size of *P. tricornutum*, which are considered master traits, were assessed. Furthermore, it was tested whether cellular lipid content increased when phytoplankton cells were potentially stressed by warmer water temperatures or increased dissolved N:P ratios.

In **chapter five**, I focus on the responses of natural phytoplankton communities from three different stations in the North Sea when exposed to pulses of nutrient-rich freshwater simulating heavy precipitation events. I examined the influence that initial community structure can have on the response of phytoplankton communities to abrupt changes in dissolved nutrients and salinity and whether nearshore phytoplankton communities, because they are more frequently exposed to changes in abiotic conditions, are affected differently than offshore phytoplankton communities. In addition, I examined the effects of a simultaneous increase in nutrients and decrease in salinity on community cell size and elemental stoichiometry.

Publications and manuscripts

The thesis is based on the following papers:

Paper I (Chapter 2)	**Groß E**, Boersma M, Meunier CL (2021) Environmental impacts on single-cell variation within a ubiquitous diatom: The role of growth rate. PLoS ONE 16(5): e0251213.
Paper II (Chapter 3)	Moreno HD, Rokitta S, Tremblay N, Boersma M, **Groß E**, Klip H, Wiltshire KH, Meunier CL. Global change induces oxidative stress and alters the carbon metabolism of phytoplankton. *Manuscript.*
Paper III (Chapter 4)	**Groß E**, Rijsdijk N, Tremblay N, Boersma M, Meunier CL. The impact of heat waves on the physiology of the diatom *Phaeodactylum tricornutum*. *Manuscript.*
Paper IV (Chapter 5)	**Groß E**, Di Pane J, Boersma M, Meunier CL. Extreme weather events: potential consequences of abrupt increases in river discharge on North Sea phytoplankton communities: an experimental study. *Under review in Journal of Plankton Research.*

My contributions to the papers:

Paper I and **Paper IV**: I developed the scientific concepts with the help of CLM and MB. I conducted the experiments, analyzed the samples, and evaluated the data. In **paper IV**, JDP contributed to data analysis. I wrote the manuscripts, which were commented on and improved by the co-authors.

Paper II: The scientific concept was developed by HM, SR, NT, MB, CLM, and me. HM, HK, and I conducted the experiment. HM analyzed the samples, evaluated the data, and wrote the manuscript. Together with the other co-authors, I commented on and improved the manuscript.

Paper III: I developed the scientific concept with NR. NR and I conducted the experiment. NR analyzed the samples. I evaluated the data with NR. I wrote the manuscript with the help of NR, which was commented on and improved by the co-authors.

Chapter 2

Environmental impacts on single-cell variation within a ubiquitous diatom: the role of growth rate

Elisabeth Groß[1*], Maarten Boersma[1,2], Cédric L. Meunier[1]

[1] Alfred-Wegener-Institut Helmholtz-Zentrum für Polar- und Meeresforschung, Biologische Anstalt Helgoland, Helgoland, Germany

[2] University of Bremen, FB2, Bremen, Germany

Published in PLoS ONE 16(5): e0251213

https://doi.org/10.1371/journal.pone.0251213

Abstract

Morphological and physiological characteristics of phytoplankton cells are highly sensitive to changes in environmental conditions and, in turn, influence the dynamics of phytoplankton populations and communities. To cope with environmental change, trait variability and phenotypic plasticity may play an important role. Since global change comprises simultaneous changes in abiotic parameters, we assessed the impact of multiple drivers on functional traits of the diatom *Thalassiosira (Conticribra) weissflogii* by manipulating concurrently temperature, pCO_2, and dissolved nitrogen:phosphorus (N:P) ratio. We tested three scenarios: ambient (ambient temperature and atmospheric pCO_2; 16 N:P ratio), moderate future scenario (+1.5°C and 800 ppm CO_2; 25 N:P ratio), and more severe future scenario (+3°C and 1000 ppm CO_2; 25 N:P ratio). We applied flow cytometry to measure on single-cell levels to investigate trait variability and phenotypic plasticity within one strain of diatoms. Growth rates differed significantly between the treatments and were strongly correlated with cell size and cellular chlorophyll *a* content. We observed a negative correlation of growth rate with chlorophyll *a* variability among single strain populations and a negative correlation with the phenotypic plasticity of cell size, i.e. when growth rates were higher, the cell size cell-to-cell variability within cultures was lower. Additionally, the phenotypic plasticity in cell size was lower under the global change scenarios. Overall, our study shows that multiple traits are interlinked and driven by growth rate and that this interconnection may partly be shaped by environmental factors.

2.1. Introduction

Phytoplankton are responsible for about 50 % of Earth's primary production (Field *et al.*, 1998), with diatoms accounting for about half of this (Nelson *et al.*, 1995, Smetacek, 1999). As primary producers, phytoplankton form the basis of most marine food webs. In addition, diatoms and phytoplankton in general can serve as indicators of ecosystem change since they are particularly sensitive to shifts in environmental conditions. This is also important in the context of regional and global change, since human activities and associated increases in greenhouse gas emissions have led to simultaneous changes in a number of aquatic abiotic parameters. Consequently, phytoplankton are exposed to the simultaneous effects of multiple anthropogenic stressors, such as increasing temperature and pCO_2, as well as shifts in dissolved nutrient concentrations and stoichiometry.

Phytoplankton can respond to changes in environmental conditions at different levels. At the first level, the phenotypic plasticity of individual phytoplankton cells largely determines whether the cells can subsist under changing abiotic conditions. How well a single strain copes with changing environmental conditions depends on the tolerance range of individual cells (Collins et al., 2013, Sett et al., 2014). At the second level, the plasticity of different strains within a population is the critical factor. High plasticity of individual strains has the potential to buffer negative effects of environmental change, while low plasticity of these strains can lead to shifts in population structure (Godhe & Rynearson, 2017). At this level, the sum of the tolerance ranges of different strains within a population determines whether the population can cope with environmental change. The third level of phytoplankton response results in a change in community composition when altered abiotic conditions lead to species selection. Despite the importance of all three levels of response (within strains, between strains, between species), many studies have focused on the response of community (Weithoff & Beisner, 2019, Marañón, 2015, Litchman *et al.*, 2007), populations (Fontana *et al.*, 2019, Hofmann *et al.*, 2019), and strains (Godhe & Rynearson, 2017, Wolf *et al.*, 2018, Kremp et al., 2012), while much less attention has been paid to the phenotypic plasticity of individual cells within a strain.

One of the most important characteristics or traits of individual phytoplankton cells that determine their ecological success is cell size (reviewed by Weithoff & Beisner, 2019), as it is

directly correlated with many other traits and is influenced by a range of environmental factors. Smaller cells have lower sinking rates (Smayda, 1970), better nutrient uptake due to a higher surface-to-volume ratio, and a smaller diffusive boundary layer (Ploug *et al.*, 1999, Sherwood *et al.*, 1975). On the other hand, smaller cells are often more susceptible to grazing (Thingstad *et al.*, 2005). Thus, cellular characteristics not only affect the ecological role of plankton but are also shaped in part by environmental conditions. Changing temperature and pCO_2 regimes could, therefore, have an impact on cellular traits, with consequences for trophic and system processes. So far, most studies of phytoplankton traits and their response to environmental drivers have been conducted using bulk measurements. For example, Hillebrand *et al.* (2013) observed that phytoplankton exhibit large variability in cellular nutrient content at low growth rates and that cellular nitrogen to phosphorus (N:P) ratios converge with increasing growth rate. Hence, faster growth causes cultures to become more similar and their variability to decrease. This phenomenon was first observed by Goldman (1986). However, the study by Hillebrand et al. (2013) compared different populations and different species, and although the authors conclude that this should be the case, it remains unclear whether the above-mentioned patterns also apply within individual strains. Given the importance of phenotypic plasticity in coping with altered environmental conditions, a proper evaluation of the response of phytoplankton to global change cannot be made without studying their phenotypic plasticity and cell-to-cell variability within individual strains. Flow cytometry, which measures traits of individual cells, is a well-established method to investigate the variability of cellular characteristics such as cell size, pigments, and biochemical components (Moreira-Turcq & Martin, 1998, Markina, 2019, Jochem, 2000).

Since current CO_2 concentrations are not saturating for Rubisco, the enzyme that catalyzes primary fixation of inorganic carbon (Badger et al., 1998), higher pCO_2 resulting from anthropogenic emissions can potentially favor photosynthesis and phytoplankton growth (Riebesell, 2004, Finkel et al., 2010, Giordano *et al.*, 2005). Furthermore, rising water temperatures caused by increased atmospheric CO_2 can affect physiological processes, including growth, resource acquisition, and photosynthesis (Eppley, 1972, Raven & Geider, 1988). Additionally, human activities influence the concentrations and ratios of dissolved nutrients such as nitrogen (N) and phosphorus (P), which are essential for phytoplankton growth. Legal restrictions on nutrient inputs to the environment have resulted in increasing N:P

ratios, which are predicted to rise even further in the future, as atmospheric N deposition is likely to continue to increase (Grizzetti et al., 2012), and P reserves on Earth could be depleted in 50 to 200 years if current levels of use are maintained or increased (Ober, 2016, Herrera-Estrella & López-Arredondo, 2016). However, as environmental conditions change, the elemental stoichiometry of phytoplankton species and their biochemical requirements will also be affected (Finkel et al., 2010). Given the influence of these global change drivers on phytoplankton growth rate and the strong correlation of growth rate with other traits such as cell size (Finkel et al., 2010), it is crucial to investigate the phenotypic plasticity of multiple phytoplankton traits, and how the traits are correlated.

Considering that changes in pCO_2, temperature, and nutrient concentrations do not happen separately, but rather simultaneously, we conducted a multi-driver experiment with realistic future conditions based on predictions from the Intergovernmental Panel on Climate Change (IPCC). We tested the RCP 6.0 and 8.5 scenarios by simulating a temperature increase of 1.5 and 3°C combined with increasing pCO_2 up to 800 and 1000 ppm, respectively, and we combined these scenarios with an increase in dissolved N:P ratios from 16 to 25. Using a single-cell approach, we analyzed the response of a single strain of the diatom species *Thalassiosira weissflogii*, currently also named *Conticribra weissflogii*. Since we acquired the strain we worked with from an algal culture bank under the name *T. weissflogii*, we will retain the generic name *Thalassiosira* in this paper. *T. weissflogii* is mostly found in temperate brackish waters, but it has also been isolated all around the globe in areas ranging from the Long Island Sound, New York, USA, to Jakarta Harbor, Indonesia, to the German Bight (North Sea), as well as in the middle of the Pacific Ocean (Donald *et al.*, 1997, Von Dassow *et al.*, 2006, Kaeppel *et al.*, 2012) and can, therefore, be considered as a cosmopolitan species. Furthermore, *T. weissflogii* is known to react in a number of ways to altered abiotic conditions (Montagnes & Franklin, 2001, Passow & Laws, 2015). Sugie and Yoshimura (2016) reported a decrease in cell size of *T. weissflogii* under increased pCO_2 and Wu *et al.* (2014) identified a slight increase of growth rate at higher pCO_2. Nevertheless, the single-cell plasticity of multiple traits of *T. weissflogii* has never been investigated. Since measurements on a single-cell level require certain criteria regarding cell size and chain-formation, we used this well-studied diatom species to analyze the link between growth rate, cell size, and biochemical composition of cells growing under different future global change conditions. More specifically, we tested the hypothesis that not

only between species and populations (Hillebrand et al., 2013) but also within one single strain, cell-to-cell variability of phytoplankton decreases with increasing growth rate. Using flow cytometry, we are able to analyze both, the reaction of single strain populations to different environmental conditions by studying the variation between cultures, as well as the variability within one replicate at a distinct growth rate. The former, we describe in the following as among-strain population variability and the latter as cell-to-cell variability within a single strain population. Both concepts can be used to assess phenotypic plasticity which plays an important role when addressing the question of the effect of global change on phytoplankton.

2.2. Materials and methods

Experimental setup

A single strain stock culture of *T. weissflogii* (Grunow) Fryxell & Hasle (obtained from the Culture Collection of Algae at Göttingen University, SAG, strain number 122.79) was grown in semi-continuous dilute-batch culture. This stock culture was diluted by 95% every 4-5 days with f/2 medium (Guillard & Ryther, 1962) prepared with artificial seawater. The inoculation stock culture was maintained under a 14:10 day:night cycle at 14°C and irradiance of 95µmol photons m^{-2} s^{-1} (GHL Mitras Lightbar 2 Daylight, 6500K, dimmed to 80%). All bottles were gently homogenized manually several times a day, which prevented sedimentation of the cells.

In a multi-driver experiment, we tested six scenarios based on IPCC predictions for the end of the 21st century. It is important to note that our main interest was not to investigate the effects of the different stressors individually, but rather to create the complete scenarios, since temperature is not going to change without CO_2 concentrations and vice versa. These combinations were crossed with two different nutrient scenarios, as the direction of change in nutrient stoichiometry is less well established in the current literature. Since the strain used in our experiment was maintained at 14°C for many months, which is within the optimal growth temperature range of *T. weissflogii* (Chen *et al.*, 2020), we used this temperature as a reference for the "ambient" scenario. Hence, temperature and pCO_2 levels were chosen to represent ambient conditions (amb = 14°C and 450ppm CO_2), a moderate global change scenario based

on RCP 6.0 (rcp6.0 = 15.5°C and 800ppm CO_2), and a more severe global change scenario based on RCP 8.5 (rcp8.5 = 17°C and 1000ppm CO_2). Since dissolved phosphorus concentrations are expected to decrease relative to nitrogen concentrations in the future, resulting in increased N:P ratio (Grizzetti et al., 2012), these three treatments were crossed with **N**:**P** = 16 (Redfield ratio) and **N**:p = 25 (increased N:P ratio). We used batch cultures, as we were also interested in the dynamics of cellular traits over different growth phases. This enabled us to study the impact of global change scenarios on the one hand and the effects of shifts from exponential growth to stationary phase and from nutrient-replete to nutrient-depleted conditions on the other.

The experiment was initiated by inoculating 1L glass bottles with the stock culture at a starting cell density of 1000 cells ml^{-1} in six biological replicates for each treatment, yielding a total of 6 times 6 = 36 bottles. Each culture can be seen as a single strain population. We prepared the culture medium with artificial seawater based on f/2 medium (Guillard & Ryther, 1962). The N concentration was 880 µmol L^{-1} and the P concentrations were 54 and 35 µmol L^{-1} for the **N**:**P** 16 and **N**:p 25 treatments, respectively. To maintain constant temperatures, the experiment was conducted in temperature-controlled rooms at 14.0, 15.5, and 17.0°C. To reach the desired pCO_2, we aerated the culture medium with a mixture of air stripped of CO_2 by soda lime and pure CO_2 for 24 h before inoculation. At early and late stationary phase, we took samples for total alkalinity. Due to the high volume required for this analysis, we used two of the six replicates for both analyses. For each alkalinity sample, 125ml from the culture were filtered with a 0.45µm nylon filter (Sartorius) and stored airtight in borosilicate bottles at 4°C. We used the software CO2calc v4.0.9 to calculate the initial pCO_2 in our treatments based on the measured alkalinity and the corresponding pH (amb_i = 412 ppm, $rcp6.0_i$ = 776 ppm, $rcp8.5_i$ = 922 ppm) as well as at early stationary phase at day 5 (amb_5 = 76 ppm, $rcp6.0_5$ = 64 ppm, $rcp8.5_5$ = 17 ppm) and the late stationary phase at day 10 (amb_{10} = 1 ppm, $rcp6.0_{10}$ = 1 ppm, $rcp8.5_{10}$ = 1 ppm). Macronutrients were measured at the same time points (Suppl. Table 2.1).

After inoculation, *T. weissflogii* was grown in batch cultures for 10 days under the same light conditions as the stock culture. We sampled two milliliters of each biological replicate daily one hour after artificial sunrise and analyzed them directly via flow cytometry to evaluate how different traits are linked during different growth phases. Immediately after each

measurement, we fixed the samples with acidic Lugol's iodine solution at a final concentration of 2%, since Lugol is less hazardous than aldehyde-based or more toxic fixatives and does not cause cellular damage due to intracellular freezing. These samples were stored in the dark for subsequent flow cytometric analyses of cellular lipid and protein content.

Flow cytometry

Fresh samples were analyzed daily using a flow cytometer (BD Bioscience Accuri C6) to determine the cell density of each culture. We processed the samples by running the flow cytometer at a medium flow rate (35 µl min^{-1}). Volumes of 102 and 68 µl were measured for samples taken during exponential growth and stationary phase, respectively. This procedure ensured that at least 200 diatom cells of each sample were counted. The cell density was used to calculate growth rates for each replicate by the following equation:

$$\mu = \ln(N_t/N_0) \cdot \Delta t^{-1}$$

whereby N_0 and N_t describe cell concentrations at t0 and t and Δt is 1 since we measured every day.

To analyze correlations between growth rate and other functional traits, we used flow cytometric measurements of the same samples to detect changes in the cell size of *T. weissflogii* based on the forward scatter (FSC) and the chlorophyll *a* cell content using the FL3 (670+ nm) and FL4 (675/25 nm) fluorescence detectors. The fluorescence detectors FL3 and FL4 differ in their selective transmission of the fluorescence signals. Whereas FL3 (670 nm) is a longpass optical filter, the FL4 (675/25 nm) is a bandpass filter. The main Chl a fluorescence band of diatoms is at 685/695 nm of the photosystem II, which means that both detectors cover the Chl a signal but FL3 is more distinct with a coverage between 650 and 700 nm whereas FL4 also includes the fluorescence signal of the photosystem I at 720/740 nm of the cells (Lamb *et al.*, 2018). While the different detectors do not give absolute values of size and chlorophyll *a*, here, we were interested in the variation between and within treatments rather than absolute changes in parameters. Consequently, we measured cell characteristics with arbitrary units, which is a well-established way to deal with flow cytometric measurements, with forward scatter correlating with cell size and the 670 nm fluorescence signal correlating closely with the cellular chlorophyll *a* content (reviewed by Hyka *et al.*, 2013). Since the natural fluorescence of cells

is sensitive to light and temperature, we took samples of 2 ml each from six cultures at a time, followed by immediate measurement and fixation. The side scatter (SSC) detects granularity of cells. Every cell is measured individually using flow cytometry. Therefore, with each measurement, not only the mean value of each parameter of a sample was recorded, but also the coefficient of variation ($CV = (SD/mean) \cdot 100$) of the sample to determine the cell-to-cell variability. We used the flow cytometric results to analyze the variability among single strain populations as well as cell-to-cell variability within a single strain population. For the former, we used the mean values of each parameter from the different flow cytometry detectors and analyzed the variance of each trait among cultures, and for the latter, we used the coefficient of variation (CV) of cellular parameters.

Staining

Samples from days 1, 3, 5, 6, and 10 were used for cellular lipid and protein analysis, representing exponential growth and early and late stationary phase. To analyze cellular lipid and protein contents, we used the stains Nile Red (Thermo Fisher Scientific) and Fluorescein-5-Maleimide (FITC, Thermo Fisher Scientific) (Hutter & Eipel, 1978, Paau *et al.*, 1978), respectively. Nile Red can be used to detect both polar (membrane) lipids, stained in red, and non-polar lipids, which are present in lipid droplets and stained in yellow (Diaz *et al.*, 2008). The Nile Red working solution was prepared each day by diluting an initial stock solution (10mg ml^{-1}) with acetone to a concentration of 2.5 µg ml^{-1}. The FITC working solution for protein staining was prepared fresh each day from the stock solution by dissolving and diluting with ethanol to a concentration of 5 µg ml^{-1}. For each of the stains, we used 225 µl of the Lugol-fixed samples. The color of the iodide was removed by adding 12.5 µl of sodium thiosulfate solution (Pomroy, 1984) directly before staining. Afterward, 25 µl of the working solution of either Nile Red or FITC was added to the sample. The incubation of the stains was performed in black Eppendorf tubes for 30min, as both the optimal incubation time and stain quantity were determined in a preliminary experiment. Samples were measured by flow cytometry at a low flow rate (14µl min^{-1}) and a sample volume of 41µl was measured. Since the cell concentration was still quite low at day 1 and fewer cells were detected with staining than in fresh samples, the measured sample size ranged from 70 to 100. The staining signal of Nile Red was detected using FL2 (585/40 nm) and FL3 (670+ nm) fluorescence detectors for the non-polar and polar

lipids. The signal from FITC was detected with the fluorescence detector FL1 (533/30 nm). A control was measured from each sample to correct the staining signals of Nile Red and FITC with the natural fluorescence signal of the diatom cells.

Data analysis

The software R (R Core Team, 2013) was used for all statistical analyses. Differences between the treatments were tested using analysis of variance (two-way ANOVA) and Tukey's (HSD) *post-hoc* comparisons, with IPCC scenario (ambient, 6.0, and 8.5) and nutrient scenario as independent factors. For all statistical comparisons, normality (Shapiro) and variance homogeneity (Barlett) tests were performed. Data were transformed (square root) if criteria of a normal distribution or variance homogeneity were not met. If a transformation of data did not allow the use of ANOVA, the non-parametric Kruskal-Wallis test was performed. In that case, a multi comparison test from the package pgirmess was used for *post*-hoc comparison. A principal component analysis (PCA) was used to test for the correlations between cellular parameters of *T. weissflogii* by using the results from the flow cytometric measurements. To investigate the effect of growth rate on the strain variance, we grouped the observations in equal numbers of observations starting at the low growth rates and plotted the variance of the parameters in these different groups. For this, all negative growth rates were set to zero. We used the libraries *mltools*, *data.table*, and *reshape* to group the growth rate for equal numbers of observations and extracted the values of the variance of each group. Analyzing the linear correlation between growth rate and the cell size variability, we used the libraries *lsmeans*, *psych*, and *data.table* to test for differences between the slopes and to calculate the Pearson correlation coefficient R^2 of the six treatments. The significance level of all comparisons was fixed at 95% ($p = 0.05$).

2.3. Results

Growth rate and cellular parameters

All cultures of *T. weissflogii* reached a similar maximum cell density of approximately 51,000 cells ml^{-1} (Suppl. Fig. 2.1). The higher temperature and pCO_2 in the RCP 6.0 and

RCP 8.5 scenarios resulted in higher maximum growth rates in the exponential growth phase, and the RCP 6.0 and RCP 8.5 cultures reached the stationary phase one and two days earlier than the ambient cultures, respectively. To identify the effect of the treatments, we plotted the average growth rate during the exponential growth phase. Within the exponential growth phase, the growth rate of *T. weissflogii* increased with increasing temperature and pCO_2 (Fig. 2.1 A). Overall, the global change scenarios significantly influenced growth rates during the exponential growth phase (two-way ANOVA, $F_{2, 98} = 20.99$, $p < 0.001$), with significantly higher growth rates in the RCP 8.5 scenarios than in the ambient scenarios (Tukey's post-hoc test, $p < 0.001$). The N:P treatment did not influence growth rates (Tukey's post-hoc test, $p = 0.21$). During the exponential growth phase, average cell size was also significantly affected by the global change scenarios (two-way ANOVA, $F_{2, 98} = 52.59$, $p < 0.001$), with significantly larger cell size in the RCP 8.5 scenarios than in the ambient and the RCP 6.0 scenarios (Tukey's post-hoc test, $p < 0.001$), but no effect of the two N:P ratios (Tukey's post-hoc test, $p = 0.91$) (Fig. 2.1 B). The global change scenarios also affected the average chlorophyll *a* content during the exponential growth phase of the cultures (Fig. 2.1 C) (two-way ANOVA, $F_{2, 98} = 11.69$, $p = 0.003$), with significantly lower cellular chlorophyll *a* content at the RCP 8.5 scenarios and the amb **N**:**P** scenario than in the other scenarios (Tukey's post-hoc test, $p < 0.001$).

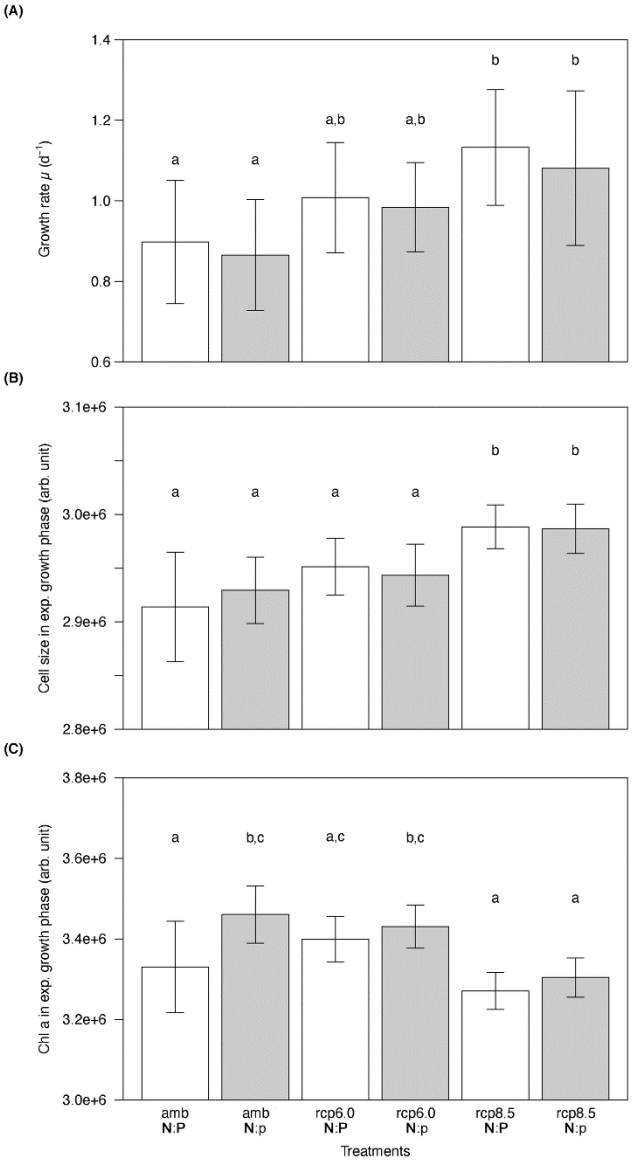

Figure 2.1: Growth rates (A), cell size (B), and chlorophyll *a* content (C) of *T. weissflogii* during the exponential growth phase under three different temperature and pCO_2 treatments (amb = 14°C, 450ppm; rcp6.0 = 15.5°C, 800ppm; rcp8.5 = 17°C, 1000ppm) crossed with two N:P ratios (N:P = 16; N:p = 25). Data presented are means and standard deviations of six replicates. Different letters (a, b, c) indicate significant differences (two-way ANOVA, $p < 0.05$). A notation with more than one letter (a,b) means that there is no significant difference with either (a) or (b), but there is a statistically significant difference with (c).

Using a principal component analysis (PCA), we tested whether the exponential growth and stationary phase of batch cultures can be distinguished by cellular characteristics of *T. weissflogii*, and if so, which cellular traits are correlated with the growth phases (Fig. 2.2). The PCA included the mean value of each cellular trait for each sample measured by flow

cytometry: cell concentration, forward scatter (FSC, representing cell size), side scatter (SSC, representing the shape and internal complexity or granularity of the cells), as well as signals from the fluorescence detectors (FL3 and FL4) for chlorophyll *a* emission of the diatom cells, and from lipid and protein staining. Along with the first principal component (PC1, 73.1%), two clusters can be identified within the data set. The two clusters characterize the exponential growth phase and the stationary growth phase, respectively, and thus describe growth-related characteristics of *T. weissflogii*. The PCA indicates several correlations between cellular traits and growth phases. Cell concentration, SSC, FL3, and FL4 were positive correlated, whereas a negative correlation was detected between these parameters and the FSC as well as cellular lipid content. In contrast, the protein content of the cells did not correlate with growth phases and mainly described PC2 (11.2 %). An analysis testing for the effect of the treatments on these parameters, combining exponential growth and stationary phase, showed no or only a marginal significant differences (Kruskal-Wallis $_{FSC,}$ $H_5 = 7.79$, $p = 0.17$; Kruskal-Wallis $_{FL3}$, $H_5 = 11.79$, $p = 0.037$, Kruskal-Wallis $_{FL4}$, $H_5 = 6.60$, $p = 0.25$, , Kruskal-Wallis $_{lipids}$, $H_5 = 13.98$, $p = 0.014$). A *post-hoc* comparison identified the marginal significant difference in FL3 between the scenarios amb, **N**:**P** and RCP 6.0, **N**:p, but no significant differences in cellular lipid content between any treatment. Compared with the cellular parameters describing PC1, the differences in cellular protein content were not caused by different growth phases but by the experimental treatments. Indeed, the protein content was significantly higher in both RCP 6.0 **N**:**P** and RCP 6.0 **N**:p scenarios than in the ambient and RCP 8.5 scenarios (Fig. 2.3, two-way ANOVA, $F_{2,84} = 21.18$, $p < 0.001$), with no influence of N:P treatments (Tukey's post-hoc test, $p = 0.28$).

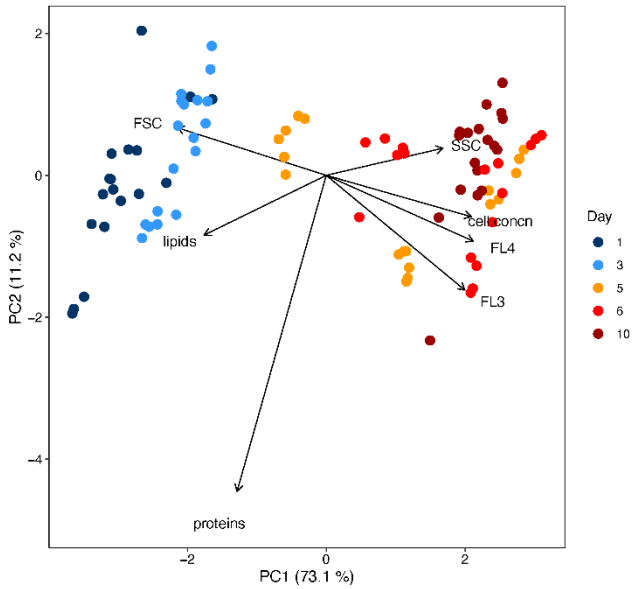

Figure 2.2: Results of the principal component analysis (PCA) of the two dominant components produced by parameters measured by flow cytometry: Cell concentration, FSC (cell size), SSC (granularity), FL3 and FL4 (chlorophyll *a*), and the staining signal of lipids and proteins. The PCA includes measurements from days 1, 3, 5, 6, 10. The first two days cover the exponential growth phase and the last two the stationary phase of the *T. weissflogii* cultures. At day 5 the cultures were in between these two phases. The PCA includes 90 samples.

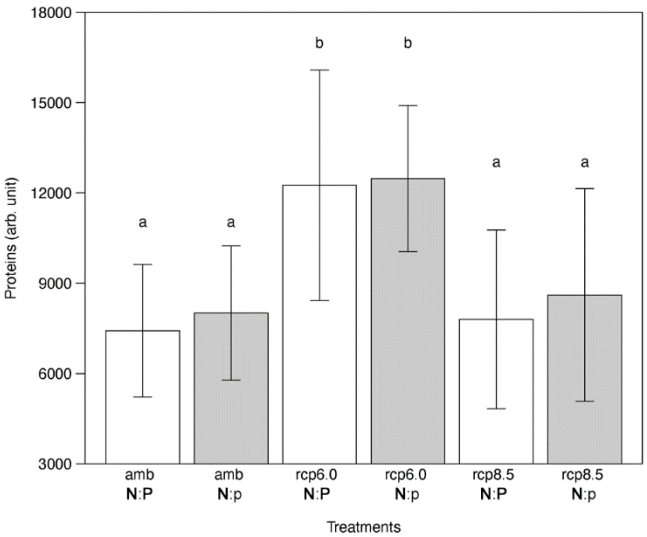

Figure 2.3: Cellular protein content measured through Fluorescein-5-Maleimide (FITC) staining (detected by FL1) of *T. weissflogii* under three different temperature and pCO_2 treatments (amb = 14°C, 450ppm; rcp6.0 = 15.5°C, 800ppm; rcp8.5 = 17°C, 1000ppm) crossed with two N:P ratios (N:P = 16; N:p = 25). Data presented are means and standard deviations of three replicates. Different letters (a, b) indicate significant differences (two-way ANOVA, $p < 0.05$). A notation with more than one letter (a,b) means that there is no significant difference with either (a) or (b), but there is a statistically significant difference with (c).

Among-strain population and cell-to-cell variability

While the above-described results represent the effect of different abiotic conditions on cellular traits of *T. weissflogii*, the following describe the dynamics of cellular traits over different growth phases. We focused on growth rate, including both growth phases of the batch culture, as a master trait of phytoplankton (Litchman & Klausmeier, 2008), and linked it to the biochemical composition of *T. weissflogii* cells by examining changes in size, chlorophyll *a*, lipid, and protein content of the cells.

The response of the FSC, representative of cell size, to increasing growth rates followed a sigmoidal shape with larger cell size at higher growth rates (Fig. 2.4 A), whereas the cellular chlorophyll *a* content, as detected by FL3 and FL4, decreased with increasing growth rate (Fig. 2.4 C and E). Since phytoplankton populations naturally transition quite fast from exponential growth phase to stationary phase, the number of observations was higher at low and high growth rates around 0 and 1 d^{-1} than at intermediate growth rates between 0.2 and 0.6 d^{-1}. Therefore, we created bins of an equal number of observations to test for changes in variability as a function of growth rates. While the among-strain population variability, i.e., the variation between cultures, of the FSC signal did not vary with growth rate (Fig. 2.4 B), the variability in cellular chlorophyll *a* content decreased with increasing growth rate (Fig. 2.4 D and E). The variance of cellular protein contents, detected by FITC stain, showed no clear trend over a range of growth rates (Suppl. Fig. 2.2 B and D). The variance of cellular lipid content, in contrast to the other measured parameters, was higher in the exponential growth phase than in the stationary phase (Suppl. Fig. 2.2 C).

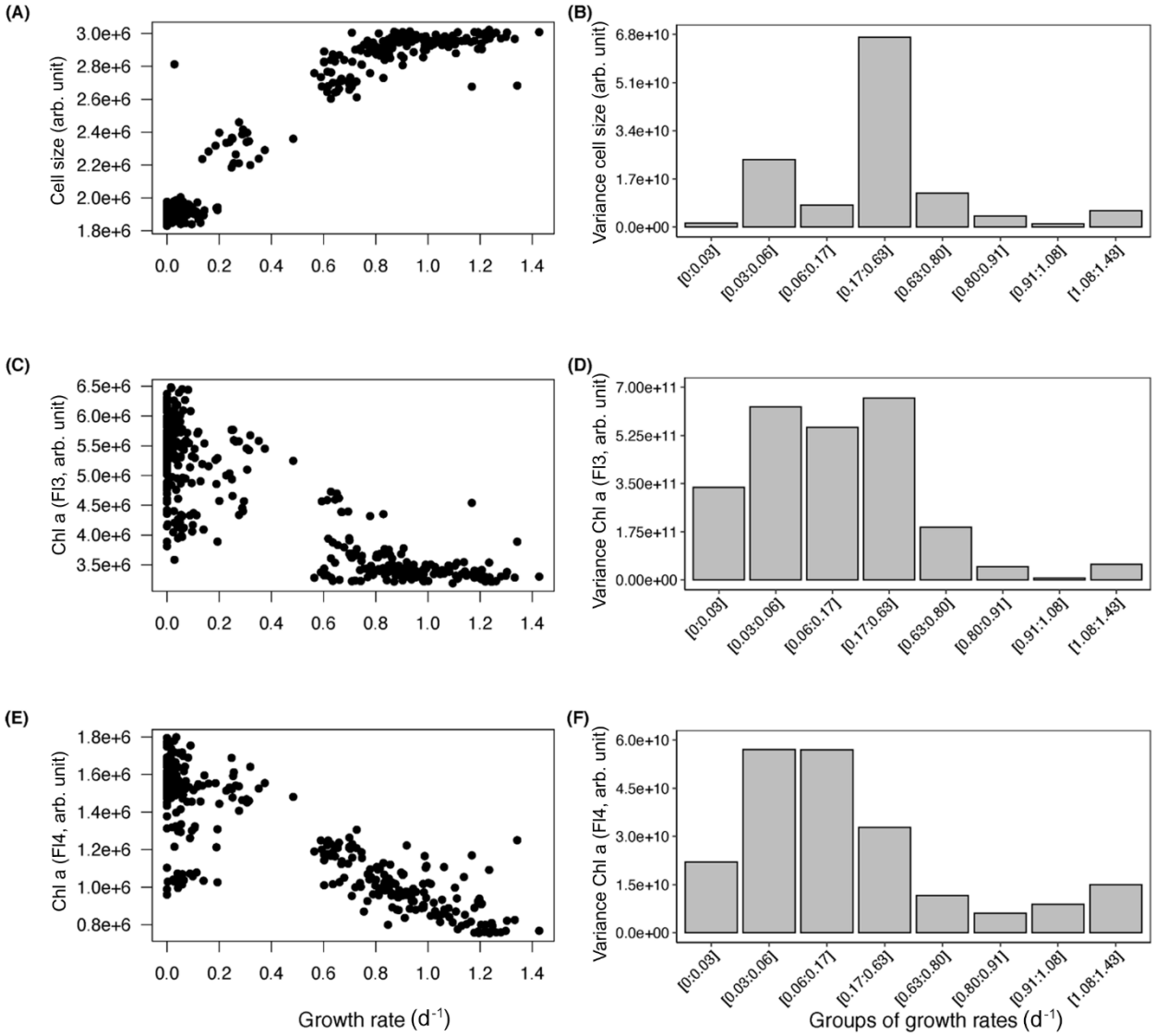

Figure 2.4: Cell size represented by FSC (A) and chlorophyll *a* content represented by FL3 and FL4 fluorescence (C, E) of *T. weissflogii* over growth rates from exponential growth and stationary phase. The variance of these parameters (B, D, F) in growth rates grouped by equal numbers of observations. Data represent the mean values of each triplicate sample measured via flow cytometry at five days.

To assess the impact of concurrent changes in abiotic parameters on the phenotypic plasticity of *T. weissflogii*, we further tested for a correlation between cell-to-cell variability within strain populations, i.e., differences between single cells within a culture as captured by the coefficient of variation (CV), and growth rate. Differences in cell-to-cell variability were observed only for cell size (FSC). Growth rate and CV of FSC were negatively correlated and followed a linear model (Fig. 2.5). When comparing the regression lines of the six treatments with a pairwise comparison test, we observed an increase in the strength of the correlation

between growth rate and CV of FSC with treatment intensity, indicated by an increase in Pearson correlation coefficient R^2 from 0.76 in both ambient scenarios to 0.92 in the future scenarios RCP 6.0 and RCP 8.5 with **N**:p= 25 (Fig. 5). Additionally, we observed a significant interaction in the relationship between growth rate and CV of FSC (two-way ANOVA, $F_{5,348}$ = 9.27, $p < 0.001$), and a pairwise comparison of the slopes identified significantly higher cell size cell-to-cell variability within single strain populations in the ambient scenarios than in the global change scenarios RCP 6.0 and RCP 8.5 ($p \leq 0.029$).

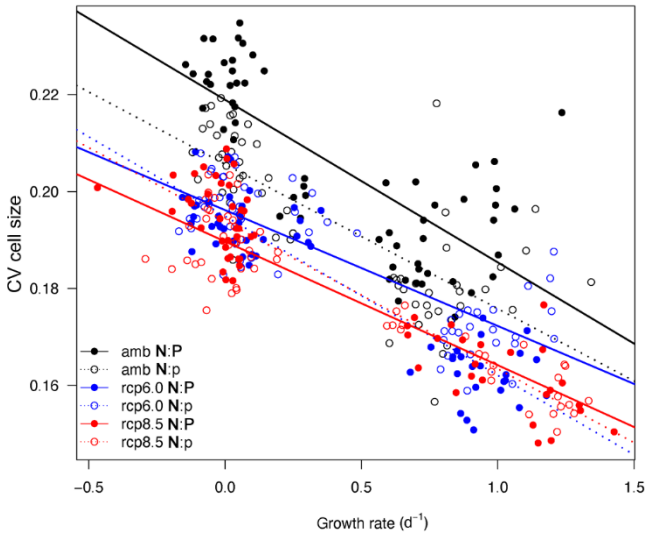

Figure 2.5: Linear regression model of cell size variability (CV FSC) over growth rate of *T. weissflogii* from exponential growth and stationary phase; data represented for each treatment are mean values of six replicates. The R^2 (Pearson correlation coefficient), representing the fit of the model, indicated an increase in linear correlation between cell size variability and growth rate with increasing treatment intensity: From ambient ($R^2_{amb;N:P}$ = 0.76, $R^2_{amb;N:p}$ = 0.76) to RCP 6.0 ($R^2_{rcp6.0;N:P}$ = 0.83, $R^2_{rcp6.0;N:p}$ = 0.92) and to RCP 8.5 ($R^2_{rcp8.5;N:P}$ = 0.91, $R^2_{rcp8.5;N:p}$ = 0.92). Regression lines of the ambient treatments are significantly different from the RCP 6.0 and RCP 8.5 treatments ($p<0.01$)

2.4. Discussion

Growth rate and cellular parameters

Future increases in surface water temperature and pCO_2 may lead to increased metabolic activity and growth of phytoplankton (reviewed by Finkel et al., 2010). The results of our study are in line with these predictions, and we observed that an increase in temperature combined with higher pCO_2 can enhance the growth of *T. weissflogii*. Testing realistic scenarios with

temperature increases of +1.5 and +3°C enabled us to identify that phytoplankton respond to even relatively small changes in the environment. Moreover, an association between growth and other functional traits can often be found (Litchman et al., 2007). These phytoplankton traits may be affected not only directly by changes in temperature and pCO_2, but also indirectly by increasing growth rates. The absence of significant differences between the two N:P ratios may be due to a relatively short incubation time, as the batch culture approach used in this study did not leave much time for the phytoplankton cells to acclimate to culture conditions. Additionally, the absence of differences between the N:P scenarios may indicate that the supply of N and P may have been sufficient for growth in both treatments. However, our results show that growth rate is a master trait, which is significantly correlated with multiple other traits. For instance, we identified a positive correlation between growth rate and cell size of *T. weissflogii*. In the exponential growth phase, both growth rate and cell size increased with increasing temperature and pCO_2. As the diatom populations grew slower during the transition from exponential growth to stationary phase, cells became smaller, too. The correlation between cell size and growth rate has been investigated before and seems to be species dependent (Marañón et al., 2013, Montagnes & Franklin, 2001). Additionally, during asexual reproduction, cell division produces progressively smaller diatom cells until a certain threshold at which sexual reproduction takes place, allowing cells to regain a larger size. Amato *et al.* (2005) as well as Chisholm and Costello (1980) reported that cell size in *Coscinodiscus pavillardii* and *Pseudo-nitzschia delicatissima* decreases significantly with increasing growth rate. Our results are also supported by other studies on *T. weissflogii,* which observed a strong positive relationship between growth rate and cell size when different subclones of the same isolate were compared (Von Dassow et al., 2006, Chisholm & Costello, 1980). To calculate the percentage of decrease in cell size, we used the FSC signal from the flow cytometer and observed a 33-36% decrease in size from exponential growth to stationary phase. According to Olenina *et al.* (2006), *T. weissflogii* can be found in three size classes (12-15 µm, 15-18 µm, 18-22 µm), covering the same range of variation as the one we recorded. Thus, the relationship between growth rate and cell size appears to be species-specific and has been shown to be a function of the balance between sexual and asexual reproduction (Von Dassow et al., 2006). Moreover, smaller cells have a higher surface area to volume ratios, which enhances nutrient transport capacity under low dissolved nutrient conditions (Meunier et al., 2017, Irwin *et al.*, 2006). Therefore, it is possible that the decrease in cell size from exponential growth to stationary phase we recorded

is a strategy by *T. weissflogii* to increase its nutrient uptake efficiency and competitive ability under decreasing nutrient concentrations.

We also observed a negative correlation between growth rate and cellular chlorophyll *a* content. At higher growth rates, the chlorophyll *a* content of *T. weissflogii* decreased slightly in the RCP 8.5 scenario. This result contradicts phytoplankton ecophysiology studies conducted in chemostats that report generally higher chlorophyll *a* content in faster-growing phytoplankton populations (Liu *et al.*, 1999, Wen *et al.*, 2014). However, in our experiment, we used batch cultures and the populations transitioned from exponential growth to stationary phase. Cell densities increased while growth rates decreased. At high cell densities, phytoplankton cells can increase their chlorophyll *a* content to compensate for self-shading (Falkowski & LaRoche, 1991). Therefore, cellular chlorophyll *a* content should be related not only to growth rate but also to cell density.

Interestingly, the cellular protein content of *T. weissflogii* was not correlated with its growth rate. Instead of an increase or decrease of cellular protein content with increasing growth rate, we recorded an overall higher cellular protein content in the RCP 6.0 scenario than in the ambient, but not in the RCP 8.5 scenario. Toseland *et al.* (2013) found a similar dependence of cellular protein content to temperature, with increased protein synthesis as temperature increased, and suggested the temperature dependence of ribosomal translation as a likely explanation. However, it is unclear why the cellular protein content of *T. weissflogii* was higher in the RCP 6.0 scenario than in the RCP 8.5 scenario. The lipid content of T. *weissflogii* was higher at the beginning of the experiment and decreased from the exponential growth phase to the stationary phase. Other studies have reported relatively low lipid content under optimal growth conditions (reviewed by Sharma *et al.*, 2012) or an accumulation of lipids when diatom cultures are nutrient limited, especially under N-limitation (McGinnis *et al.*, 1997, Yodsuwan *et al.*, 2017). As mentioned above, the absence of differences between the N:P scenarios may indicate that the supply of N and P may have been sufficient for growth, which explains the patterns of cellular lipid content of *T. weissflogii* we observed here.

Among-strain populations and cell-to-cell variability

In a meta-analysis conducted with 55 data sets, Hillebrand et al. (2013) assessed the correlation between stoichiometry and growth rate of several phytoplankton species and observed that higher growth rates constrained the N:P stoichiometry of phytoplankton cells. Here, we hypothesized that among-strain population variability in functional traits, which describes the variation within one strain growing at different environmental conditions, as well as cell-to-cell variability within a single strain population of phytoplankton, representing the phenotypic variability of one culture, decrease with increasing growth rate, not only between species (Hillebrand et al., 2013) but also within one strain. Our results partially support this hypothesis. While the variability in cellular protein content was not affected by growth rate, neither on the single strain population level nor on the cell-to-cell level, the among-strain population variability in cellular lipid content was higher at higher growth rates. However, the higher variability was most likely caused by the overall higher cellular lipid content at high growth rates compared with the lipid content at low growth rates. In contrast, the among-strain population variability in cellular chlorophyll *a* content decreased significantly with increasing growth rates, as well as the cell-to-cell variability in cell size. Whereas the among-strain population variability indicates that faster growth channels the chlorophyll *a* content to an optimal budget, as stated by Hillebrand et al. (2013), growth rate did not influence the chlorophyll *a* cell-to-cell variability within a single strain population, which was constant overall. A possible explanation for this could be that not only in our experiment but also in nature phytoplankton cells experience slightly different light conditions, since light is supplied from an angle that does not allow homogenous irradiation, causing some degree of phenotypic plasticity in cellular chlorophyll *a*. On the other hand, the constant strain variability in cell size suggests that cell size is linked only to growth rate and not to environmental parameters, supporting the idea that changes in cell size with growth rates are caused by the reproduction of diatom cells. We also observed a decrease in cell-to-cell variability in cell size with increasing growth rates, i.e., at higher growth rate, cells within a single strain culture become more similar in cell size. Additionally, the global change scenarios RCP 6.0 and 8.5 resulted in an overall lower cell-to-cell variability in cell size, which did not only hold true during the exponential growth phase but was also maintained during the stationary phase. Hence, it seems that the degree of variability in cell size within a single strain population develops at fast growth

and is maintained as the growth rate decreases. This second type of variability, the cell-to-cell variability, can only be explained through phenotypic plasticity. High phenotypic plasticity in cell size can be advantageous to cope with shifts in environmental conditions, whether abiotic parameters or predation pressure, and it is indeed a key aspect determining the ability of phytoplankton to respond to environmental changes (reviewed by Godhe & Rynearson, 2017). Since it is directly correlated to nutrient uptake efficiency and resistance to grazers (Meunier et al., 2017), cell size is an important trait of phytoplankton. However, phenotypic plasticity responses have received little focus from global change studies, and, as far as we know, our study is the first to investigate not only the variability among single strain populations but also the cell-to-cell variability of phytoplankton functional traits in a global change context.

2.5. Conclusion

In this study, we observed that realistic future global change scenarios significantly influence the growth rate of the diatom species *T. weissflogii*. We also identified strong correlations between growth rate and cellular traits. Growth rate was positively correlated with cell size and cellular lipid content, and negatively correlated with cellular chlorophyll *a* content. We have shown that trait variability among single strain populations as well as cell-to-cell variability within a single strain population decrease as growth rate increases. Independent of growth rate, higher temperature and pCO_2 also caused an overall decrease in cell size cell-to-cell variability. Future studies should therefore focus on the interaction between abiotic conditions, growth rate, and phenotypic trait plasticity of other phytoplankton species to evaluate the impact of global change.

Acknowledgments

We would like to thank Julia Haafke and Ursula Ecker for the technical assistance and Julien di Pane for his help with the statistical analysis. We are grateful to Nelly Tremblay for many helpful discussions throughout the development of this manuscript. We thank two anonymous reviewers for their valuable recommendations that improved our manuscript.

Supplementary material

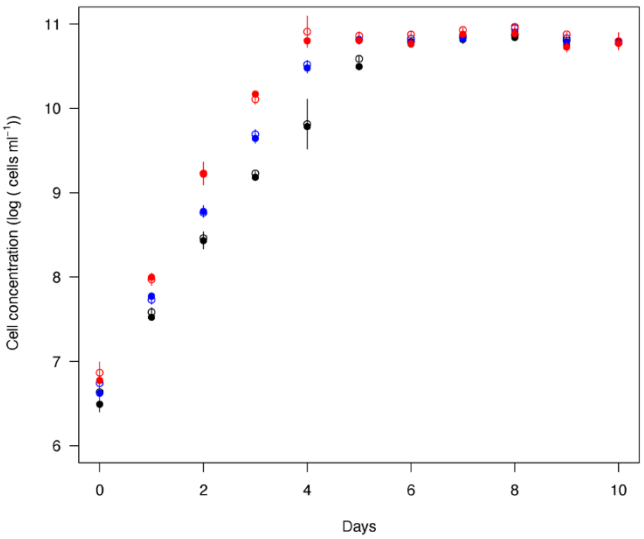

Suppl. Figure 2.1: Growth curve of *T. weissflogii* under three different temperature and pCO_2 treatments: ambient = 14°C, 450ppm (black); RCP 6.0 = 15.5°C, 800ppm (blue); RCP 8.5 = 17°C, 1000ppm (red) crossed with two N:P ratios: N:P = 16 (filled circles); N:p = 25(open circles). Data presented are means and standard deviations of six replicates.

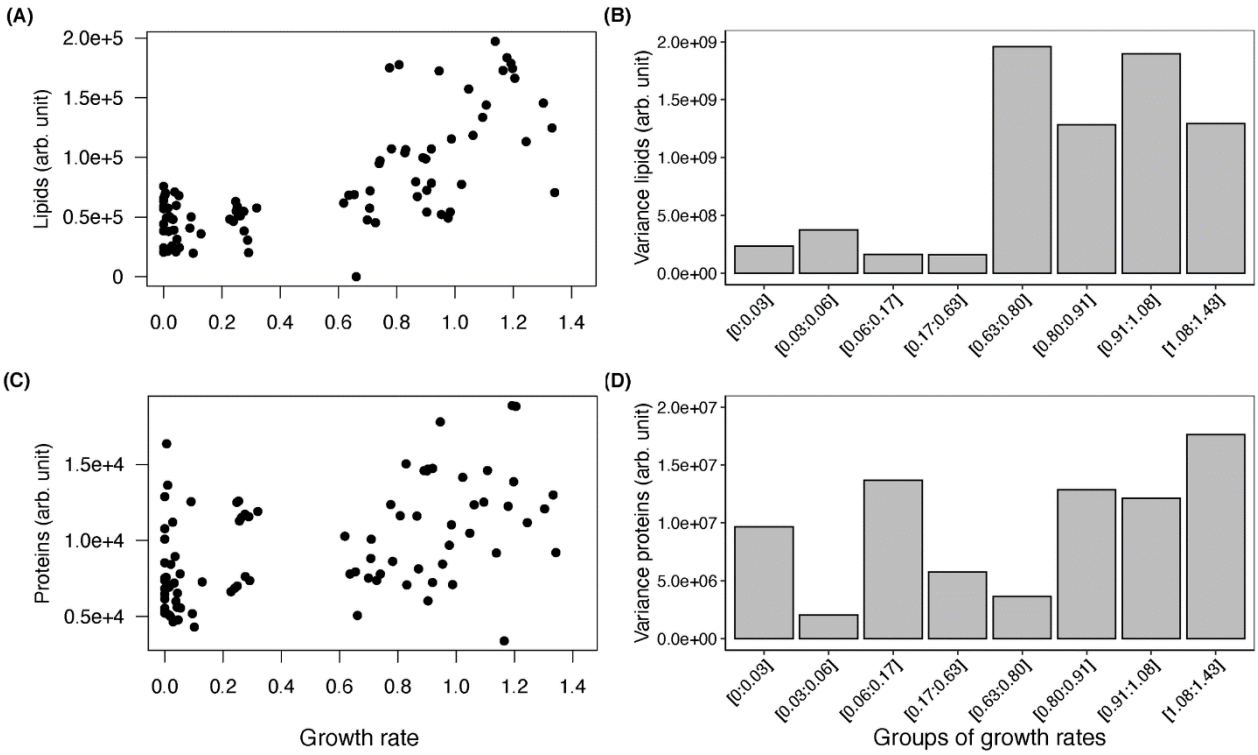

Suppl. Figure 2.0.2: Lipid content, measured through NILE RED staining (detected by FL2 and FL3), (A) and protein content, measured through Fluorescein-5-Maleimide (FITC) staining (detected by FL1),

(C) of *T. weissflogii* over growth rate, and variance of these parameters (B, D) in growth rates grouped by equal numbers of observations. Data represent the mean values of each triplicate sample measured via flow cytometry at five days.

Suppl. Table 2.1: Dissolved inorganic nitrogen (DIN) and phosphorus (DIP) concentration in µmol L^{-1} sampled at day 5 (early stationary phase) and day 10 (late stationary phase) of the batch culture experiment.

DIN (µmol L^{-1})	amb N:P	amb N:p	rcp6.0 N:P	rcp6.0 N:p	rcp8.5 N:P	rcp8.5 N:p
Day 5	379.10	338.45	402.30	418.40	388.05	302.90
Day 10	250.80	270.80	285.05	226.65	386.95	312.55
DIP (µmol/L)	amb N:P	amb N:p	rcp6.0 N:P	rcp6.0 N:p	rcp8.5 N:P	rcp8.5 N:p
Day 5	29.30	14.95	27.65	16.20	29.65	17.25
Day 10	21.20	16.45	17.95	15.70	11.95	12.65

Chapter 3

Global change induces oxidative stress and alters the carbon metabolism of phytoplankton

Hugo Duarte Moreno[1], Sebastian Rokitta[2], Nelly Tremblay[1,3], Maarten Boersma[1,4], Elisabeth Groß[1], Helena Klip[1], Karen H. Wiltshire[5], Cédric L. Meunier[1]

[1]Alfred-Wegener-Institut, Helmholtz-Zentrum für Polar- und Meeresforschung, Biologische Anstalt Helgoland, Germany

[2]Alfred-Wegener-Institut, Helmholtz-Zentrum für Polar- und Meeresforschung, Bremerhaven, Germany

[3]Pêches et Océans Canada, 850 Route de la Mer, Mont-Joli, QC, Canada

[4]University of Bremen, Bremen, Germany

[5]Alfred-Wegener-Institut, Helmholtz-Zentrum für Polar- und Meeresforschung, Wattenmeerstation, List auf Sylt, Germany

Manuscript

Abstract

Phytoplankton are responsible for about 90% of the oceanic primary production, largely supporting marine food webs and actively contributing to the carbon biogeochemical cycle. Increasing temperature and pCO_2, along with higher dissolved nitrogen:phosphorus ratios in coastal waters, can impact phytoplankton physiology. Here, we conducted a full-factorial experiment to identify the individual and combined effects of temperature, pCO_2, and N:P ratios on the antioxidant capacity and carbon metabolism of the diatom *Phaeodactylum tricornutum*. Our results demonstrate that, among these three drivers, temperature is the most influential factor on phytoplankton physiology, with warming causing oxidative stress and lower activity of antioxidant enzymes. Furthermore, the photosynthetic rate was higher under warmer conditions and higher pCO_2 and, together with lower dark respiration rate and higher dissolved organic carbon exudation, generated cells with lower carbon content. An enhanced oceanic CO_2 uptake and an overall stimulated microbial loop benefiting from higher dissolved organic carbon exudation may be the longer-term consequences of rising temperatures, elevated pCO_2 as well as shifted dissolved N:P ratios.

3.1. Introduction

Phytoplankton species are responsible for about 90% of the total oceanic primary production (Duarte & Cebrián, 1996), making these organisms major contributors to the biogeochemical cycling of carbon (Buesseler, 1998, Bowler *et al.*, 2010). Two distinct marine carbon pools derive directly from the biological activity of photosynthetic organisms: particulate organic carbon (POC), bound in cell biomass, and dissolved organic carbon (DOC), released by living phytoplankton or decaying cells through sloppy feeding of grazers, consumption and excretion by higher trophic levels or viral lysis (Jiao *et al.*, 2010). Once fixed as phytoplankton biomass, carbon can be transferred via trophic processes through the food web or sink to the deep sea (Honjo & Manganini, 1993). These fluxes are essential components of biogeochemical cycling and the 'marine organic carbon pump' and are influenced by phytoplankton cellular physiological processes.

After inorganic carbon is assimilated into carbohydrates through photosynthesis, it can take different pathways in a phytoplankton cell: The carbon can be used for storage and growth; it can be remineralized for mitochondrial energy generation and fuel cellular processes; or it can be exuded in the form of organic molecules (Marra & Barber, 2004, Tortell *et al.*, 2008, Thornton, 2014). The relative proportions of these intracellular carbon fluxes are directly influenced by environmental conditions, such as temperature, partial pressure of carbon dioxide (pCO_2), and concentrations of dissolved nutrients (Neori & Holm-Hansen, 1982, Alipanah *et al.*, 2015, Padfield *et al.*, 2016) all of which experience large perturbations due to human activities. Indeed, anthropogenic CO_2 emissions and the resulting increase in atmospheric CO_2 partial pressures contribute to the greenhouse effect, i.e., global warming. In addition, part of this CO_2 dissolves into the ocean and lowers seawater pH, leading to ocean acidification (Doney *et al.*, 2009, Anderson *et al.*, 2016). Human activities also alter dissolved nutrient concentrations through nutrient runoffs, leading to a general increase of dissolved nitrogen:phosphorus (N:P) ratios in European coastal waters (Grizzetti et al., 2012) and increasing the potential of P limitation for phytoplankton. Hence, there is an urgent need to study the individual and combined effects of these environmental drivers on the cellular carbon fluxes of phytoplankton to ultimately understand and predict potential changes in the marine carbon cycle.

Coupled with temperature rise, aqueous CO_2 concentrations increase could positively affect primary producers that profit from the higher availability of CO_2 (Bach *et al.*, 2019). However, other studies have shown that phytoplankton responses to increasing oceanic pCO_2 may be complex (Beardall & Raven, 2004, Taucher *et al.*, 2015, Alvarez-Fernandez et al., 2018), and the consequences for photosynthesis and wider phytoplankton ecophysiology are still to be clarified. Studies have found different effects of warming and ocean acidification on various physiological processes related to carbon metabolism in phytoplankton, including an increase in photosynthesis and respiration rates (Wu *et al.*, 2010, Goldman *et al.*, 2017), higher DOC production (Engel *et al.*, 2011), and down-regulation of carbon-concentrating mechanisms (Rokitta *et al.*, in press, Thangaraj & Sun, 2021). Environmental ratios of dissolved inorganic N:P are also known to influence cellular quotas of particulate organic carbon (POC), photosynthetic and growth rate in phytoplankton (Rasdi & Qin, 2015, Li & Sun, 2016), as well as DOC exudation (Obernosterer & Herndl, 1995). The uncertainties about the interactivity of environmental drivers and the co-dependency of cellular carbon pathways make the responses of phytoplankton cells to future environmental change even more difficult to predict (Gao & Campbell, 2014, Wolf *et al.*, 2019).

Changing environmental conditions modulate the rates of respiration and photosynthesis in phytoplankton (Hancke *et al.*, 2008, Padfield et al., 2016), and the associated electron transport rates which determine the degree of reduction of the electron transport chains (ETC) in chloroplasts and mitochondria (Mittler *et al.*, 2004, Janknegt *et al.*, 2008). When ETCs are overreduced, electrons can 'leak' and react with free O_2, extensively generated as a photosynthesis by-product, creating superoxide radicals ($O_2^{-\bullet}$) (Gechev *et al.*, 2006). This primary reactive oxygen species (ROS) is further converted into other oxidative compounds, such as hydrogen peroxide (H_2O_2) and the highly reactive hydroxyl radical ($HO^{\bullet}$), which can cause oxidative damage to lipids, proteins, and DNA (Halliwell, 1987). Oxidative damage can lead to loss of photosynthetic capacity due to membrane lipid peroxidation (Rajagopal *et al.*, 2000, Juan *et al.*, 2004), to lower growth rates as well as decreased chlorophyll *a* content (Mallick *et al.*, 2002). Phytoplankton can apply different strategies to prevent the formation of ROS and combat such compounds when their formation cannot be avoided. In the chloroplast, excess light absorbed by the antenna complex can be quenched as thermal energy by activating the xanthophyll cycle (Janknegt et al., 2008), while the proportions of photoprotective versus

light-harvesting pigments can be rearranged to better tune energy flow to the photosystems (Dubinsky & Stambler, 2009). Activation of the Alternative Oxidase (AOX) pathway within the mitochondria can relieve electron flow through the ETC to prevent leakages, yet at lower energy yield by dark respiration (Day & Wiskich, 1995, Allen *et al.*, 2008). Antioxidant enzymes also play an important role in scavenging ROS. Superoxide dismutases (SODs) are potent antioxidants widely utilized to catalyse the dismutation of $O_2^{-\bullet}$ into O_2 and H_2O_2 (Janknegt et al., 2008). Once formed, H_2O_2 can be further decomposed into harmless O_2 and H_2O by other enzymes, such as Catalase and Glutathione Peroxidase (Barros *et al.*, 2003, Vega-López *et al.*, 2013). While several studies have reported modulation of antioxidant response and oxidative stress by temperature, pCO_2, and dissolved nutrient concentrations in different classes of photosynthetic organisms (Lesser, 1997, Choo *et al.*, 2004, Yakovleva *et al.*, 2009, Gillespie *et al.*, 2011, Brutemark *et al.*, 2015, Kvernvik *et al.*, 2020), the potential interactions between these environmental factors remain poorly understood.

In this study, we tested the influence of temperature, pCO_2, and dissolved N:P ratios on the cellular antioxidant response and carbon fluxes of the phytoplankton *Phaeodactylum tricornutum*. As a possible consequence of oxidative stress on metabolic pathways of carbon, we also quantified carbon fluxes by measuring rates of primary production, dark respiration, net dissolved organic carbon production and cellular organic carbon content. Overall, our work assesses how multiple global change drivers may act individually and together to influence physiological processes related to antioxidant capacity and carbon metabolism in phytoplankton.

3.2. Materials and methods

A full factorial design was applied to test the influence of two CO_2 partial pressures (400 and 1000 µatm), temperatures (18 and 21 °C), and N:P ratios of dissolved inorganic nutrients (16 and 25 molar), forming eight independent treatments in quadruplicates. The pCO_2 levels were chosen to represent the contemporary and the RCP 8.5 scenario atmospheric pCO_2 based on predictions of CO_2 emissions by the Intergovernmental Panel on Climate Change for the end of the 21st century (IPCC, 2021). The temperature of 18 °C is the mean value for summer (July-August) at the Helgoland roads time-series station (North Sea) and 21 °C

represents the + 3.0 °C increase expected according to the RCP 8.5 scenario. We included different nutrient regimes in this experiment as well. Thus, an N:P of 16 represents the balanced Redfield ratio while an N:P of 25, achieved by lowering the concentrations of dissolved P, resembles the increasing P-limitation predicted for the future (Grizzetti et al., 2012). The model diatom *Phaeodactylum tricornutum* was chosen as it is native to the North Sea and does not form chains, which allowed us to precisely determine cellular concentrations by flow cytometry. Further, it has been used in other experiments (Tong *et al.*, 2021), which allow comparisons between studies.

Culture conditions

Cultures of *Phaeodactylum tricornutum* (Strain CCAP 1052/1A) were grown at 18°C in a temperature-controlled room in 2 L glass bottles (Duran, Mainz, Germany) closed with airtight lids. The cultures were grown in F/20 medium (Guillard, 1975) prepared with artificial seawater according to the protocol of Harrison *et al.* (1980) modified by Berges *et al.* (2001), and sterile filtered (0.2 µm) to avoid contamination. Total alkalinity (TA) was adjusted by adding NaOH until it reached natural seawater levels (~ 2350 µmol kg SW^{-1}). To yield N:P ratios of 16 and 25, nitrate was added to reach a concentration of 88 µmol NO_3 L^{-1}, and phosphate concentrations in the growth medium were set to 5.5 µmol PO_4 L^{-1} and 3.5 µmol PO_4 L^{-1}, respectively (suppl. Fig. 3.1). The pCO_2 of the medium was adjusted by bubbling it for 24 hours with air mixtures containing either 400 or 1000 µatm CO_2, which were obtained from a CO_2-mixing system (GDZ 401, Denkendorf, Germany, Schoo et al., 2013). Cultures were irradiated with 100 µmol photons m^{-2} s^{-1} by LED light bars (Mitras 2 Daylight, GHL, Germany) under a 14:10 hours light:dark cycle. The culture bottles were continuously rotated on a roller table to prevent cell sedimentation. The diatom cultures were pre-acclimated to every treatment for at least 20 generations. The experiment was subdivided into two periods. In the first period of four days, we concentrated on the measuring of dissolved carbon production, whereas the second period was focused on the measurements of ROS. Samples for production rates of dissolved organic carbon (DOC) and particulate organic carbon (POC) were collected over a four-day incubation period following the acclimation period. Initial cell concentration was always ~400 cells mL^{-1}. After the incubation of four days, cells were diluted back to 400 cell

mL^{-1} with described media and grown for a second incubation period to acquire more biomass for further measurements. From the second incubation period, cells were harvested for assessments of dark respiration, primary production, AOX activity, antioxidant enzyme assays and MDA concentration, as well as for the analyses of photosynthetic/photoprotective pigments. Cultures were kept dilute to avoid self-shading and drifts in carbonate chemistry and were harvested during the exponential growth phase before ~ 10 % of the dissolved inorganic carbon (DIC) in the culture was consumed. This limit was ascertained through a model of the carbonate system by the CO_2SYS Excel Macro (Pierrot *et al.*, 2006) to minimize fluctuations in pH during the experiment.

Seawater carbonate system and dissolved macronutrients

The seawater carbonate system was calculated based on determined DIC, pH, temperature, and salinity using the CO_2SYS Excel Macro (Pierrot et al., 2006) with acidity constants defined by Mehrbach *et al.* (1973) refitted by Dickson and Millero (1987). Salinity was measured with a salinometer (WTW Cond 3110 SET 1, Weilheim, Germany) directly from total alkalinity samples. An aliquot of each culture was taken daily to measure pH with a WTW Tetracon® 925 probe. Total alkalinity samples were taken by filling an airtight 100 mL transparent glass bottle, avoiding air bubbles, with filtered culture medium (GF/F filter 0.45 µm, Whatman, Buckinghamshire, UK). The samples were stored at 4°C before analysis through linear Gran-titration (Dickson, 1981) using a TitroLine alpha plus (Schott, Mainz, Germany). Samples for DIC samples were filtered through 0.45 µm polytetrafluoroethylene (PTFE) filters and kept in 5 mL brown glass bottles, free of air bubbles, at 4 °C prior to analysis with the colorimetric method of Stoll *et al.* (2001). Samples for dissolved inorganic nutrients, salinity, TA and DIC were taken from the medium prior to cell inoculation, and on the last day of the incubation period. Dissolved inorganic nutrients (DIP = PO_4^{3-} and DIN = NO_x) samples were kept frozen at – 20 °C until being measured with a continuous-flow analyzer (QuAAtro39, Seal Analytical, Norderstedt, Germany) according to Strickland and Parsons (1972). Results of dissolved inorganic nutrient analyses and seawater carbonate chemistry are available as suppl. Fig. 3.1 and suppl. Table 3.1, respectively.

Enzyme assays and pigment detection

Alternative Oxidase activity (AOX) was determined using Substrate-uncoupler-inhibitor titration (SUIT, 022 www.bioblast.at/index.php/SUIT-022_O2_ce_D051 and 023 www.bioblast.at/index.php/SUIT-023_O2_ce_D053) protocols specifically developed to distinguish between oxygen consumption derived from mitochondrial AOX and from respiratory complex IV (CIV) using a high-resolution O2k-FluoRespirometer (Oroboros Instruments, Innsbruck, Austria) calibrated with each treatment medium. The 2 mL incubation chambers of the respirometer are airtight, temperature-controlled, and equipped with magnet stirrers to gently homogenize the cell suspension. To have enough cells to reach rates within the equipment resolution, cells were concentrated by gently filtering 100-200 mL of each culture on a polycarbonate filter (0.45 µm pore size) with suction pressure lower than 200 mbar. The volume used depended on cell concentration in the culture. Phytoplankton cells were resuspended in 5 mL of 30 µmol L^{-1} 4-(2-hydroxyethyl)-1-piperazineethanesulfonic acid (HEPES) buffered culture medium to maintain constant pH during the measurements. As a first step, routine dark respiration was measured for both chambers. Then, one of the chambers was used to quantify AOX dependent respiration after inhibition of CIV with 1 mM potassium cyanide (KCN), while the other was used for CIV dependent respiration after inhibition of AOX with 1 mM salicylhydroxamic acid (SHAM). We expressed AOX as the ratio between SHAM inhibited respiration rate and routine respiration (AOX:Resp). The AOX:Resp ratio indicates the proportion of electrons that ends up in the alternative oxidase pathway from all electrons used during the dark respiration process.

Bacterial cell concentration was determined from each aliquot in the respirometer to ensure that bacterial biomass accounted for less than 10% of the total carbon biomass. These samples were fixed with glutaraldehyde (0.1% final concentration) and frozen at – 80 °C until analysis. The samples were thawed in a water bath (20 °C) and stained with SYBR Green (Invitrogen) as described in Marie et al. (2005). Bacterial cells were quantified by processing the samples through flow cytometry (BD AccuriTM C6 Plus, BD Biosciences) at a flow rate of 12 µL min^{-1} for 1-2 minutes. Samples were diluted with sterile filtered seawater (0.2 µm) when flow cytometry events were higher than 400 events s^{-1}. Bacteria cell counts were converted into carbon using the 20 fg C $cell^{-1}$ factor defined by Lee and Fuhrman (1987).

Samples for assessing antioxidant enzyme activities and MDA as an oxidative stress marker were collected by filtering 200-250 mL of the culture through a polycarbonate membrane filter (3 µm pore size, Millipore, USA) to concentrate cells. The cells caught on the filter were resuspended in culture medium, transferred into a 1.5 mL assay reaction tube (Eppendorf, Hamburg, Germany) and centrifuged at 15,000 rpm for 3 minutes at treatment temperature to form a cell pellet. Then, the supernatant was removed and the phytoplankton cells were immediately frozen in liquid N_2 and kept at – 80 °C until analysis. To determine malondialdehyde (MDA), the samples were thawed and homogenized in 250 µL of 1.1% H_3PO_4 (Mixer Mill MM301, Retsch, Haan, Germany) for 1 minute with the frequency of 30 rotations s^{-1}. Measurements of MDA content were done in triplicate according to Uchiyama and Mihara (1978).

To quantify the antioxidant enzyme activities and soluble proteins, samples were homogenized with 125 µL of phosphate buffer solution [50 mmol L^{-1} potassium phosphate dibasic and monobasic mixture (K_2HPO_4/KH_2PO_4), 50 mmol L^{-1} Ethylenediaminetetraacetic acid (EDTA), 1 mmol L^{-1} Phenylmethylsulfonyl fluoride (PMSF; $C_7H_7FO_2S$), pH 7.5] and centrifuged at 15,000 rpm for 5 minutes at 4 °C. The same supernatant extract was measured in technical triplicates for Catalase (CAT) following Aebi (1984), Manganese Superoxide Dismutase (SOD-Mn) following Taniguchi and Gutteridge (2000), Glutathione Peroxidase (GPx) following Ahmad and Pardini (1988), and Glutathione S-transferase (GST) following the protocol from Habig and Jakoby (1981). Soluble protein contents were determined following Bradford (1976) to report enzymatic activity in activity unit (U) mg $protein^{-1}$. All assays were conducted at room temperature (20 °C) and measured with a spectrophotometer (Thermo Scientific Multiskan® Spectrum, Bremen, Germany). Activities of antioxidant enzymes and MDA contents are shown in a star plot and were analyzed using the Integrated Biomarker Response (IBR) method suggested by Beliaeff and Burgeot (2002), which merges the results into one index. The IBR method allows clear visualization (using radar plots) of biological effects of treatments and simplifies the interpretation as all data is normalized to the same scale with arbitrary units. Individual results of antioxidant enzymatic activity and MDA concentration are shown in suppl. Fig. 2 and 3.

Samples for chlorophyll *a* (Chl-*a*) and photosynthetic pigments were taken by filtering 250 mL of the culture onto a polycarbonate filter (0.45 µm pore size, Millipore, USA) protected from direct irradiance. The filter was conserved in 2 mL of 100% acetone at – 80 °C until analysis. Pigments were extracted and subsequently analyzed by high performance liquid chromatography (HPLC, Waters Alliance 2695, Agilent, California, USA), following methods described in Wiltshire *et al.* (2000). Prior to analysis, we ran a standard containing more than 20 different pigments (Mixed Pigments, DHI, Germany). Pigments quantified in the analysis were chlorophyll *a*, fucoxanthin, diadinoxanthin, β-carotene and violaxanthin. Pigments were divided into 'photosynthetic pigments' (PSP, including chlorophyll *a* and fucoxanthin) and 'photoprotective carotenoids' (PPC, including diadinoxanthin, violaxanthin and β-carotene). Individual results of carotenoids content are shown in suppl. Fig. 3.2.

Photosynthesis and dark respiration rate

A concentrated phytoplankton aliquot (obtained as described above) was incubated in the two chambers O2k-FluoRespirometer at treatment temperature, and net O_2 evolution rates of photosynthesis and dark respiration were measured. This aliquot was dark acclimated in the instrument for 10 minutes at the respective experimental temperatures before applying a rapid light curve (RLC), where the aliquot was exposed for 10 minutes to irradiance of 50, 100, 150 and 300 µmol photons m^{-2} s^{-1} provided by LEDs. A last light intensity step of 600 µmol photons m^{-2} s^{-1} was provided by a Zeiss / Schott CL 1500 ECO lamp (Colombes, France). Each light step was followed by 10 minutes of darkness to account for variation in dark respiration due to a higher photosynthetic rate. Dark respiration was calculated as the mean of all respiration measurements taken during every dark period. To quantify carbon fluxes, O_2 fluxes were converted into CO_2 fluxes using a photosynthetic quotient of 1.56 and a respiratory quotient of 0.6 determined for *P. tricornutum* (Wagner *et al.*, 2006). We used least-squares fitting on the obtained data to derive physiological photosynthesis parameters, such as compensation point, as well as photochemical efficiency (α), light acclimation index (I_k) and maximum net photosynthesis rate (V_{max}), following equations from Rokitta and Rost (2012). The compensation point represents the point in the rapid light curve where the respiration rate is equal to the photosynthesis rate, α is the initial slope of the RLC and indicates the efficiency of light energy conversion into chemical energy via photosynthesis, I_k represents the highest light

irradiance that the phytoplankton is acclimated to and V_{max} shows the highest electron transport rate attained during the RLC.

Bacterial cell concentration was determined from each aliquot in the respirometer to ensure that bacterial biomass accounted for less than 10% of the total carbon biomass (see flow cytometry protocol above).

Determination of growth rates, elemental quotas, and DOC production

Cell concentrations were measured by flow cytometry (BD Accuri C6 Plus, BD Biosciences) with 100 µL samples processed at a flow rate of 35 µL min^{-1}. Specific growth rate (μ) was calculated as:

$$\mu = (ln_{C1} - ln_{C0}) * \Delta t^{-1}$$

where c_0 and c_1 are the initial and final cell concentrations and Δt is the time interval in days. The growth rate was calculated based on cell concentrations on the initial and final day of each incubation and computed as mean of both incubations, generating one growth rate value per replicate.

Samples for particulate organic carbon were taken by filtering 200 mL of each phytoplankton culture on precombusted (12h, 500°C) GF/F filters (0.45 µm, Whatman, Buckinghamshire, UK), with suction pressure of -200 mbar. The filters were then soaked with 200 µL of 0.2 mol L^{-1} HCl to remove any calcite contaminants and dried in an oven at 60 °C. Carbon content on the filters was determined with an elemental analyzer (Vario Micro Cube, Elementar, Hanau, Germany). To quantify dissolved organic carbon, samples of 20 mL were collected from the artificial seawater batch produced to prepare the medium prior to cells' incubation (initial) and from every culture bottle on the last and fourth day of incubation. Samples were collected with a sterile plastic syringe and filtered through a 0.45 µm PTFE filter. The first 2 mL of the sample were used to rinse the filter and were discarded. The samples were collected in technical duplicates and stored in HCl washed and precombusted glass vials. Samples were acidified with HCl and kept at – 20 °C until analysis. Dissolved organic carbon was determined by high temperature catalytic oxidation and subsequent nondispersive infrared spectroscopy and chemiluminescence detection, automatically conducted in a TOC-$L_{CPH/CPN}$

analyzer (Shimadzu, Kyoto, Japan). Net dissolved organic carbon production per cell (*D*) was calculated based on the following formula derived from the integral of total DOC production in the culture and cell growth:

$$D = \frac{DOC_p}{C_0} \cdot \frac{\mu}{\left(\frac{C_1}{C_0} - 1\right)}$$

where DOC_p is the total DOC production in the culture over the whole incubation period (pmol mL^{-1}), C_0 and C_1 are the initial and final cell concentrations (cells mL^{-1}), and μ is the specific growth rate (d^{-1}; see suppl. Information 3.1 for the integral resolution). To account for bacterial DOC consumption, 200 mL of each culture were filtered through a polycarbonate filter (3 µm pore size, Millipore, USA) to remove phytoplankton cells and subsequently filtered through a polycarbonate filter (0.45 µm pore size). The bacterial cells captured on the 0.45 µm filter were resuspended and incubated in an O2k-FluoRespirometer to measure their respiration rate for the phytoplankton cells (see below). This procedure ensured enough bacterial cell biomass for accurate measurements. The aliquots of each respirometric incubation were subsequently preserved to determine bacterial cell concentrations. Bacterial respiration rate (pmol O_2 $cell^{-1}$ d^{-1}) was as well converted to C consumption using an average respiratory quotient of 1.55 (Allesson *et al.*, 2016), and the bacterial carbon consumption was added to the phytoplankton DOC production since DOC is the carbon source for bacteria in the culture. Bacterial DOC consumption (DOC_c) was calculated using the formula:

$$DOC_c = \frac{C_{0\,.\,\left({}^{C_1}/_{C_0} - 1\right)\,.\,c}}{\mu}$$

where *c* is the bacterial respiration rate (pmol C $cell^{-1}$ d^{-1}), C_0 and C_1 are the bacterial cell initial and final concentrations in the cultures (cells mL^{-1}), and µ is the specific bacteria growth rate (d^{-1}) based on the initial and final bacterial cell concentration in the culture and calculated as for phytoplankton.

Statistical analyses

Statistical analyses were performed using R 3.4.3 software (R Core Team, 2021). For all analyses, the threshold of significance was set to 0.05. Effects of different temperatures, pCO_2, and N:P were assessed through a three-way Analysis of Variance (3-way ANOVA) followed by a pairwise Tukey PostHoc test. Data were log-transformed when normality and homoscedasticity of residuals were not met. Principal Component Analysis (PCA) was applied to assess the multivariate response of the experimental treatments on the dependent variables using Temperature, pCO_2 and N:P ratio as supplementary variables.

3.3. Results

Antioxidant response

The integrated biomarker response index (IBR) was on average 4.48 under 18 °C and higher than at 21 °C ($F_{1,16}$ 19.41, $p < 0.001$, Fig. 1 A, B), showing that temperature is the main driver for antioxidant responses. We observed no statistically significant effect of pCO_2, dissolved N:P ratios, or any driver combination on the IBR. The temperature-driven decrease in IBR was mainly caused by the lower activity of antioxidant enzymes, especially GPx, GST and SOD-Mn (Fig. 1 A, B and suppl. Fig. 3.3). Cellular MDA concentrations were stimulated by temperature in all treatments ($F_{1,16}$ 18.06, $p < 0.001$). In all low-temperature treatments, MDA concentrations were highest under high pCO_2 and high N:P (Fig. 1 A). The ratio of AOX to dark respiration was significantly stimulated by high temperatures in all driver constellations, going from 0.20 to 0.40, except under low pCO_2 and low N:P (Fig. 2 A). The ratio of photoprotective carotenoids (violaxanthin, diadinoxanthin, β-carotene) to photosynthetic pigments (chl-*a*, fucoxanthin; PPC:PSP) decreased under high temperatures in all treatments (MS 0.012, $F_{1,24}$ 208.3, $p < 0.001$, Fig. 2 B). Since photosynthetic pigments were not different across treatments, the reduction of this ratio was primarily driven by the decrease in photoprotective carotenoids (suppl. Fig. 3.4, Table 3.1).

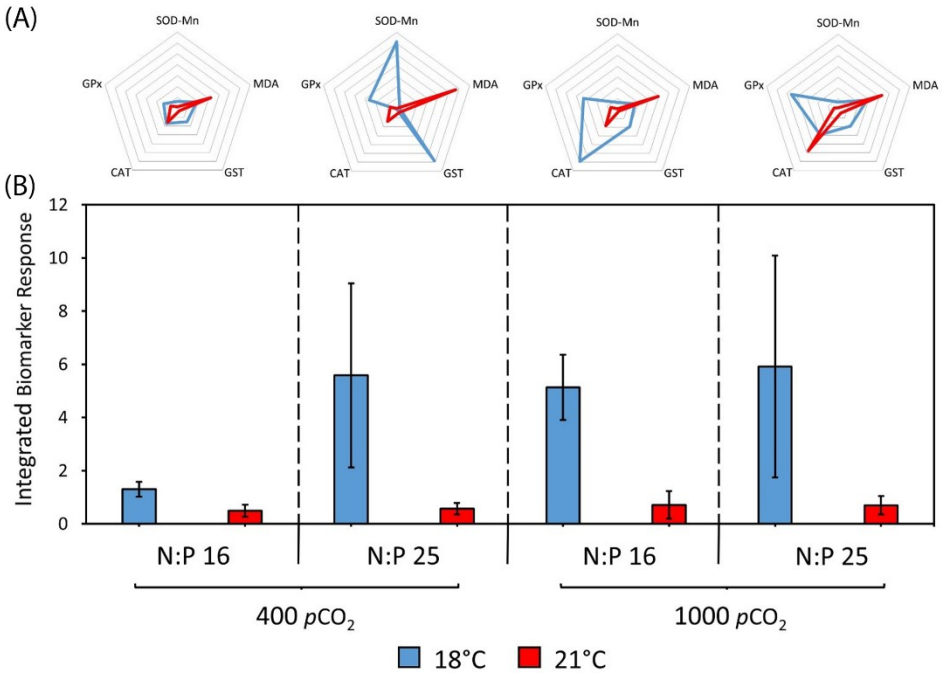

Figure 3.1: Antioxidant enzymatic response and oxidative stress. (A) Normalized radar plots of antioxidant enzyme activities and MDA as a biomarker for oxidative stress. MDA = Malondialdehyde, SOD-Mn = Managanese Superoxide Dismutase, GST = Glutathione S-transferase, CAT = Catalase, GPx = Glutathione Peroxidase. All radar plots are to the same scale. (B) Integrated Biomarker Response. X-axis represents N:P ratios and pCO_2. Colours represent temperature (blue = 18°C, red = 21°C). Data as mean ± standard deviation.

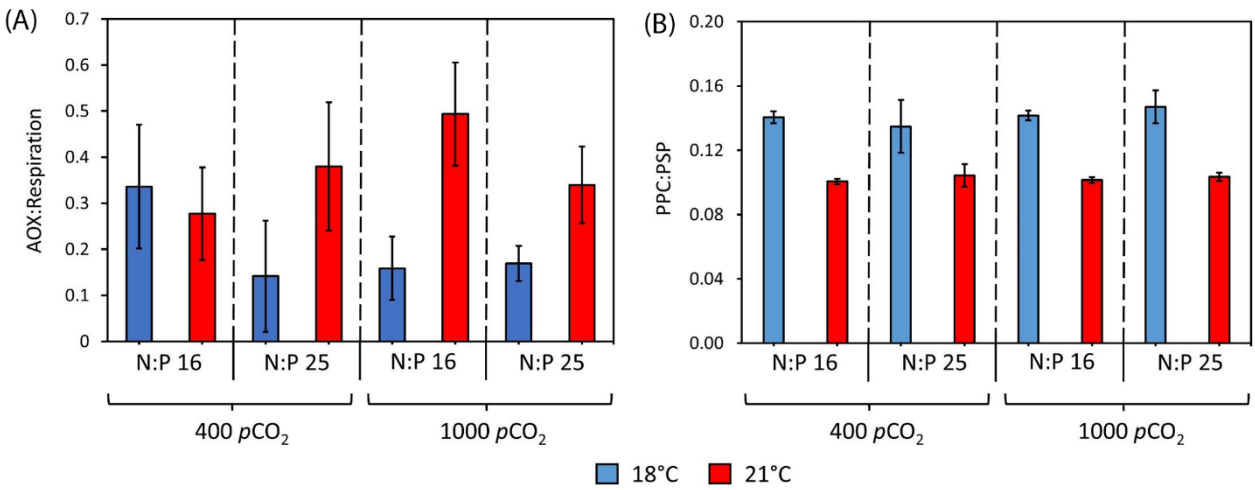

Figure 3.2: Alternative oxidase activity and carotenoids. (A) Ratio of Alternative oxidase (AOX) activity relative to dark respiration rate, (B) Ratio of Photoprotective Carotenoids (PPC, Diadinoxanthin, Violaxanthin and β-Carotene) relative to Photosynthetic Pigments (PSP, Chlorophyll *a* and Fucoxanthin). X-axis represents N:P ratios and pCO_2. Colors represent temperature (blue = 18°C, red = 21°C). Data as mean ± standard deviation.

Table 3.1: The rapid light curve fitted parameters under different treatments. Apparent photochemical efficiency (α), light compensation point (cp), maximum electron transport rate (V_{max}), light saturation point (I_k) based on the rates of µmol O_2 µg Chl-a^{-1} h^{-1}. Chl-a content as pg cell^{-1}. Data as mean ± standard deviation.

	18°C				21°C			
Variable	**400 pCO_2**		**1000 pCO_2**		**400 pCO_2**		**1000 pCO_2**	
	N:P 16	**N:P 25**	**N:P 16**	**N:P 25**	**N:P 16**	**N:P 25**	**N:P 16**	**N:P 25**
α	0.015 (±0.003)	0.015 (±0.005)	0.016 (±0.003)	0.020 (±0.004)	0.015 (±0.003)	0.014 (±0.004)	0.019 (±0.004)	0.015 (±0.003)
cp (µmol photons m^{-2} s^{-1})	8.20 (±1.07)	8.21 (±0.28)	10.86 (±0.93)	9.99 (±0.73)	8.41 (±0.28)	8.17 (±0.93)	6.55 (±0.69)	6.17 (±0.49)
V_{max} (µmol O_2 µg Chl-a^{-1} h^{-1})	1.14 (±0.18)	1.09 (±0.35)	1.18 (±0.19)	1.57 (±0.43)	1.55 (±0.21)	1.38 (±0.37)	1.59 (±0.09)	1.33 (±0.12)
I_k (µmol photons m^{-2} s^{-1})	86.3 (±6.2)	82.1 (±1.7)	86.7 (±3.1)	86.1 (±8.1)	109.4 (±9.8)	110.9 (±20.4)	94.6 (±17.1)	96.4 (±11.5)
Chl-a content (pg cell^{-1})	0.15 (±0.01)	0.15 (±0.03)	0.15 (±0.02)	0.12 (±0.02)	0.15 (±0.01)	0.16 (±0.03)	0.15 (±0.01)	0.16 (±0.01)

Carbon fluxes and cellular carbon content

Primary production, which represents the major share of organic carbon flow into the cell, was significantly affected by temperature as well as by pCO_2, but not by N:P ratios or by any of the driver combinations. The primary production of *P. tricornutum* was 2.06 pmol C cell^{-1} d^{-1} at 18 °C and was higher at 21 °C (2.38 pmol C cell^{-1} d^{-1}, $F_{1,24}$ 9.918, p = 0.004, Fig. 3). Primary production was also higher at 1000 µatm pCO_2 than at 400 µatm pCO_2 (2.33 pmol C cell^{-1} d^{-1} vs. 2.11 pmol C cell^{-1} d^{-1}, $F_{1,24}$ 4.854, p = 0.037). Dark respiration rate did not differ between temperatures at pCO_2 of 400 µatm, but it was negatively affected by higher temperature when pCO_2 was 1000 µatm ($F_{1,24}$ 30.86, p < 0.001, Fig. 3.3). Dark respiration rates were unaffected by dissolved N:P ratios. Concerning DOC production, we observed a significant stimulation by pCO_2 under 21 °C but not under 18 °C (0.36 vs. 0.25 pmol cell^{-1} d^{-1}, $F_{1,24}$ 9.542, p = 0.005, Fig. 3.3). In addition, DOC production was also significantly stimulated by higher N:P ratios, higher by about 0.13 pmol cell^{-1} d^{-1} ($F_{1,24}$ 7.023, p = 0.014). In all 21 °C treatments, DOC production rates were positive, indicating exudation rates of 0.31 pmol C cell^{-1} d^{-1} on average, while under 18 °C, values of DOC production were negative, indicating uptake rates

of 0.65 pmol C cell^{-1} d^{-1} ($F_{1,24}$ 400.2, $p < 0.001$). Cellular carbon contents were significantly influenced by temperature, being higher at 18 °C than at 21 °C (1.26 pmol C cell^{-1} vs. 0.89 pmol C cell^{-1}, $F_{1,24}$ 272.8, $p < 0.001$, Fig. 3.4 A).

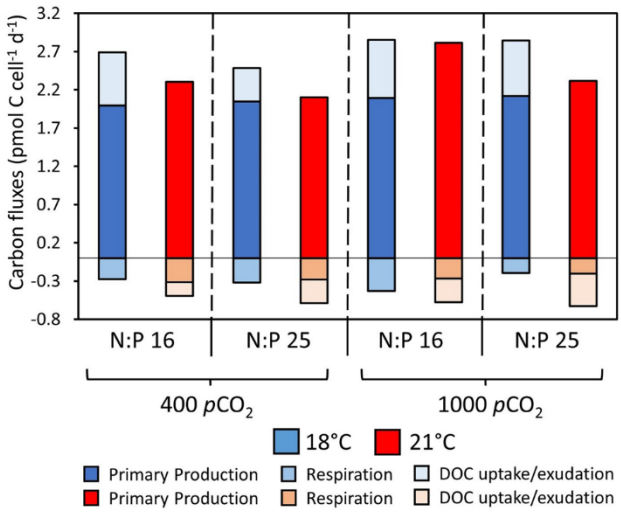

Figure 3.3: Carbon fluxes in the *Phaeodactylum tricornutum* cell under different treatments. Carbon production (primary production) and carbon consumption (net DOC production and dark respiration). Positive DOC production represents DOC uptake by the cell, while negative DOC production represents DOC exudation by the cell. X-axis represents N:P ratios and pCO_2. Colors represent temperature (blue = 18°C, red = 21°C). Different shades represent Primary Production, Respiration, and Net DOC production. Data as mean.

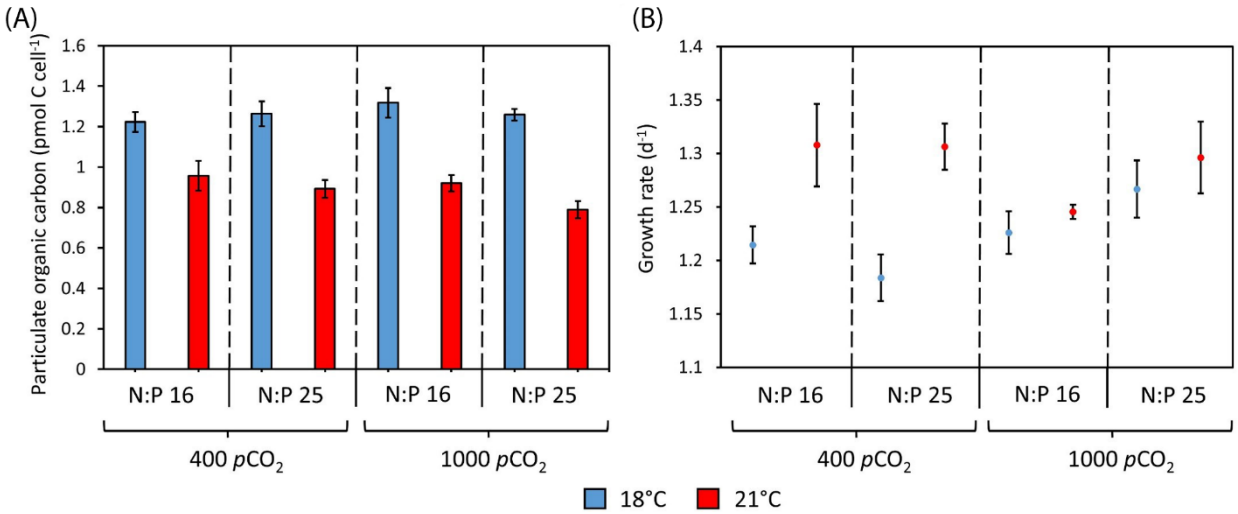

Figure 3.4: Cellular carbon content and *Phaeodactylum tricornutum* specific growth rate. (A) Particulate organic matter. (B) P. tricornutum specific growth rate. X-axis represents N:P ratios and pCO_2. Colors represent temperature (blue = 18°C, red = 21°C). Data as mean ± standard deviation.

Growth rate

Growth rates of *P. tricornutum* were positively affected by higher temperature at 400 µatm pCO_2, but the increase was lower at 1000 µatm pCO_2 (MS 0.014, $F_{1,24}$ 15.39, p = 0.008, Fig. 3.4 B). Furthermore, pCO_2 and N:P ratios in isolation did not significantly influence growth rates, but in combination, a significantly higher growth rate was achieved under 1000 µatm pCO_2 and an N:P of 25, indicating an interactive effect of these drivers. The combination of temperature and N:P ratios, as well as all three drivers, did not significantly influence growth rates.

Photochemical performance and Chl-*a* content

Photochemical efficiency (α) was 0.016 on average in all treatments and was neither affected by temperature nor by pCO_2 or N:P ratio (p > 0.05). The compensation point (cp) was significantly lower under 21 °C and high pCO_2 (10.49 ±1.04 vs. 6.51 ±0.76 µmol photons m^{-2} s^{-1}) but no temperature effect could be detected under low pCO_2, showing the interactivity of these drivers ($F_{1,24}$ 48.31, p < 0.001; Table 3.1). Maximum rates of net photosynthesis (V_{max}) were positively affected by higher temperature ($F_{1,24}$ 4.885, p = 0.037), increasing from 1.25 ±0.36 to 1.46 ±0.25 µmol O_2 µg Chl-a^{-1} h^{-1}. No effects of pCO_2 and N:P were detected. The light saturation point (I_k) was higher under high temperature (~ 85 vs. ~ 100 µmol photons m^{-2} s^{-1} ; ($F_{1,24}$ 14.03, p < 0.001, Table 3.1), irrespective of the applied pCO_2 levels and N:P ratios. None of the above-mentioned photochemical parameters was affected by N:P ratio (p > 0.05, Table 3.1). Chlorophyll *a* content was on average 0.15 ±0.02 pg $cell^{-1}$ and was not affected by temperature, pCO_2 or N:P ratio (p > 0.05, Table 3.1).

Synthesis of cellular responses

Results from the PCA identified temperature as the most influential driver of changes in the measured variables, followed by pCO_2 and, to a lower degree, N:P ratio (Fig. 3.5). The first two principal component axes of the PCA explained 60.2 % of variance within all observations (Fig. 3.5). Higher DOC production, growth rate, and MDA concentration were related to higher temperature (21 °C), while higher POC, dark respiration rate, and antioxidant response were positively correlated to the lower temperature we tested (18 °C). On the other

hand, primary production and maximum net photosynthesis rates (V_{max}) were rather influenced by pCO_2 than temperature. In contrast, contents of photosynthetic pigments, Chl-*a* and Fucoxanthin contents, were the least influenced variable by the environmental drivers.

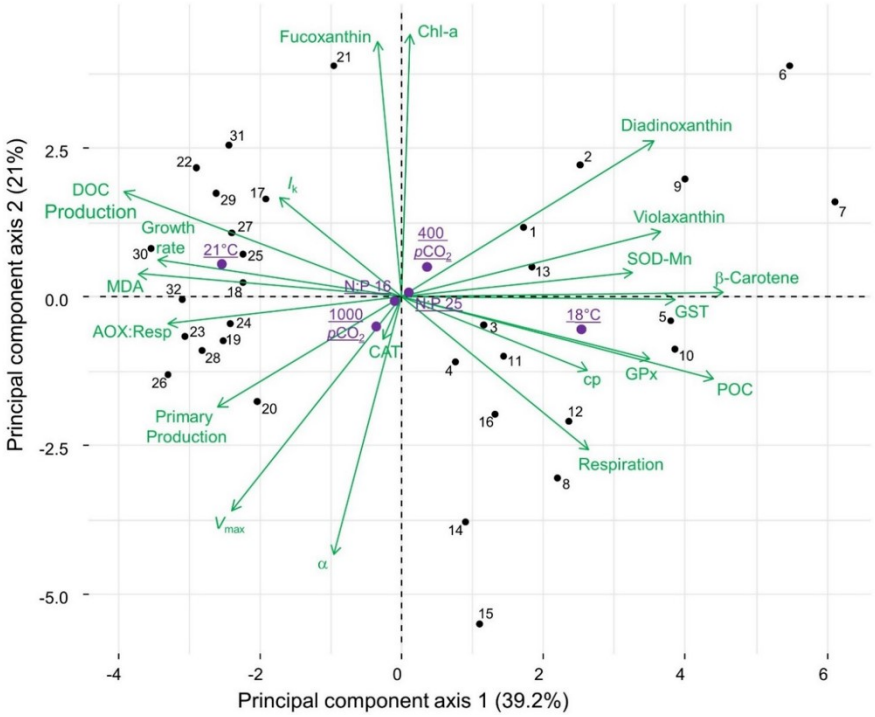

Figure 3.5: Principal Component Analysis (PCA) of the *Phaeodactylum tricornutum* response to climate change factors. Dependent variables are displayed in green, supplementary variables are displayed in purple, and black dots represent the individual observations (replicates). The two first principal component axes explain 60.2% of all variation within observations. Location of dependent variables near to supplementary variables indicates positive correlation of that experimental factor on the dependent variable. The position of the supplementary variables (drivers) relative to the point 0 show the intensity of the drivers on the dependent variables. The further the drivers are from point 0, the stronger their effect is. Black dots represent individual replicates: 1-4 (T: 18°C, pCO_2 400 µatm, N:P 16), 5-8 (T: 18°C, pCO_2 400 µatm, N:P 25), 9-12 (T: 18°C, pCO_2 1000 µatm, N:P 16), 12-16 (T: 18°C, pCO_2 1000 µatm, N:P 25), 17-20 (T: 21°C, pCO_2 400 µatm, N:P 16), 21-24 (T: 21°C, pCO_2 400 µatm, N:P 25), 25-28 (T: 21°C, pCO_2 1000 µatm, N:P 16) and 29-32 (T: 21°C, pCO_2 1000 µatm, N:P 25).

3.4. Discussion

The full-factorial design of our experiment enabled us to identify that temperature has a stronger influence than pCO_2 and dissolved N:P ratios on the antioxidant capacity and carbon metabolism of *Phaeodactylum tricornutum*. Higher temperatures influenced photosynthesis,

DOC exudation, growth rate, and respiration, overall yielding a decrease in net C fluxes and cells with lower carbon content. We also observed synergy between temperature and pCO_2 and, to a lesser extent between temperature and N:P. The cells were mostly unaffected by pCO_2 and N:P ratio at 18 °C, and only under increased temperatures cells became prone to these environmental drivers. At 21 °C, the phytoplankton cells had higher oxidative stress and lower antioxidant enzymatic activity, indicating a reduced capacity for dealing with ROS generated under warmer conditions.

We observed higher cellular contents of MDA and an increased electron flow through the AOX pathway coincided at 21 °C than at 18 °C, which was exacerbated under the combined influence of warming and elevated pCO_2. Both are indicators of oxidative stress because the cells reroute electrons through the AOX pathway to alleviate flow through the inner mitochondrial membrane and because MDA arises from harmful oxidation reactions in lipid membranes (Uchiyama & Mihara, 1978). The chloroplast and mitochondrion constantly exchange compounds such as ADP/ATP and electron carriers, whereby the mitochondrion can serve as an electron sink under photosynthetic overproduction by activating the AOX pathway. This generates less energy but allows a more rapid supply of ADP and electron carriers to the chloroplast, avoiding photoinhibition due to the lack of these compounds in the chloroplast (Bailleul *et al.*, 2015, Launay *et al.*, 2020). The increase of AOX:Respiration in cells we observed under elevated temperature, despite lower dark respiration and higher photosynthetic rates, suggests that the mitochondrion was acting as an electron sink as a stress response mechanism (Allen et al., 2008, Prihoda *et al.*, 2012). Regarding the detoxification of oxidative stress, we observed an overall lower activity of most antioxidant enzymes under high temperatures (GPx, GST, SOD-Mn; CAT under low N:P) which is counterintuitive since higher contents of these enzymes could reduce oxidative stress. However, these results are supported by another study which also observed decreased amounts of antioxidant enzymes in phytoplankton after high temperature acclimation (Perelman *et al.*, 2006). We hypothesized that these lower enzyme abundances reflect an inability of the mitochondria to maintain the respective gene expression, suggesting that 21 °C past the optimum temperature of *P. tricornutum*, which was observed by other studies as well (Bitaubé Pérez *et al.*, 2008, Tong et al., 2021). Our findings suggest not only that oxidative stress is a mediator of physiological

responses but also that pCO_2 as an additional driver, synergistically imposes additional oxidative pressure on cells under high temperatures (Fig. 3.1, 3.2 A, 3.3).

We observed a higher photosynthetic rate at 21 °C than at 18 °C, which may be related to the enhanced activity of Rubisco under higher temperatures, causing a higher I_k (Table 3.2, Ras *et al.*, 2013). In addition to warming, elevated pCO_2 further increased photosynthetic activity, likely as a result of higher C availability, which may enable a reallocation of energy possible due to a lower demand for the carbon concentration mechanism activity (Young *et al.*, 2015). Light harvesting pigments (chl-*a*, fucoxanthin) were not affected by any of the drivers, indicating that the light-harvesting portion of the antenna complex was not affected by temperature, pCO_2, or dissolved nutrient ratios. However, the concentration of protective carotenoids (especially diadinoxanthin and violaxanthin; Arbones *et al.* (2000), Wagner et al. (2006), Janknegt et al. (2008)) and of their precursor, β-carotene (Kuczynska *et al.*, 2015), decreased under high temperature. This likely enhanced the overall photosynthetic activity because relatively more captured photons were directed to the light dependent reactions of photosynthesis. Protective carotenoids compete for light energy trapping in the photosystem and dissipate it as thermal energy before it reaches the reaction center, a useful photoprotection mechanism when light irradiance is higher than needed (Arbones et al., 2000, Wagner et al., 2006, Janknegt et al., 2008). On the one hand, the lower concentration of carotenoids can increase photosynthetic rates, on the other hand, this reduction decreases photoprotection, the main short-term response against the formation of ROS in the chloroplast (Kuczynska et al., 2015).

High pCO_2 increased the photosynthetic compensation points (Table 3.2), meaning that cells needed more light to reach positive net primary production at 18 °C, whereas at 21 °C, high pCO_2 lowered the photosynthetic compensation point. We hypothesize that the overall mitochondrial function was negatively affected by increasing temperature, which was exacerbated under high pCO_2. In other words, respiration had the opposite reaction to temperature and pCO_2 as photosynthesis. This is unexpected since, typically, the dark respiration is positively correlated with photosynthesis, acting as a sink for organic carbon (Yoshida *et al.*, 2007) and also for the reduction equivalents (Bailleul et al., 2015). This disparity of chloroplast and mitochondrial activity reveals an imbalance under high

temperature, which has been observed previously in this species, for instance, by Tong et al. (2021), who found that respiration peaked at 18 °C while photosynthesis had an optimum around 20 °C. The negative effect of high pCO_2 on dark respiration has also been observed in diatoms before (Shi *et al.*, 2019). This imbalance causes high photosynthetic organic carbon production, as well as a reduced respiration, which should lead to higher organic carbon retention, i.e., both processes should support the POC production of the cells. However, phytoplankton cells did not accumulate C, rather, we observed an increasing DOC exudation (especially under high N:P ratio), which may be used as mechanism to regulate cellular POC production rates. DOC exudation has previously been shown to range from 1 to 55 % of the total carbon fixation in different phytoplankton taxa. In line with our data, DOC production was found to be stimulated by high temperatures, as well as by higher pCO_2 (Zlotnik & Dubinsky, 1989, Baines & Pace, 1991, Riebesell *et al.*, 2007, Wetz & Wheeler, 2007, Engel et al., 2011, Torstensson *et al.*, 2015). The stimulating effect of high N:P ratios on DOC production has been found before in phytoplankton (Li & Sun, 2016) and seems to be an additional supporting mechanism to balance cellular elemental stoichiometry (Thornton, 2014) since RuBisCO activity is more sensitive to low supplies of nitrogen than of phosphorus (Geider *et al.*, 1993). Although *P. tricornutum* and other phytoplankton species are known to take up DOC (Villanova *et al.*, 2017), the net cellular flows of DOC were sensitive to the environmental drivers tested here. We measured DOC uptake at 18 °C and exudation at 21 °C, with a synergistic influence of warming, elevated pCO_2, and elevated N:P ratios on the degree of DOC exudation. These results are supported by another study which found higher DOC exudation by phytoplankton under oxidative stress (Mohamed, 2008). While the stimulated photosynthetic POC production and the lower consumption by mitochondrial respiration under high temperature were compensated by DOC exudation (Fig. 2), other temperature effects could not be compensated, for instance, the stimulation of growth rates that typically derives from enhanced nutrient uptake, more rapid DNA duplication, etc. Consequently, given the steady net POC production, the increased division rates resulted in cells with overall lower carbon content (Fig. 3.3 A, B).

If the results obtained for this single strain of one species are indicative of what would happen with other species as well, an expected scenario for 2100 corresponding to RCP 8.5 with higher temperature and pCO_2 combined with increasing N:P ratio can significantly alter metabolic fluxes of microalgae and have the potential to alter the biogeochemical cycling of

carbon in the oceans: An increased photosynthesis, as well as a decreased respiration, might lower the overall CO_2 concentrations in surface waters and could thus both enhance the air-sea gas exchange, i.e., the uptake of atmospheric CO_2. The fact that organic carbon is not channeled into biomass and fed to higher trophic levels but rather exuded suggests an enhanced carbon input into the microbial loop (Azam *et al.*, 1983). This is supported by a recent study in which a mesocosm experiment was subjecting plankton communities to simultaneous changes in temperature, pCO_2, and N:P ratios identified an intensification of the microbial loop (Moreno *et al.*, 2022). These results highlight the sensitivity of microalgal physiology to the combined effects of multiple drivers. Remarkably, the manifestation of further effects of pCO_2 and N:P were enabled by elevated temperatures, underlining that temperature functions as a 'master variable' for phototrophic phytoplankton. An enhanced oceanic CO_2 uptake and an overall stimulated microbial loop may be the longer-term consequences of rising temperatures, elevated pCO_2 as well as shifted dissolved N:P ratios.

Acknowledgments

HDM, EG, and CLM were supported by the German Federal Ministry of Education and Research (BMBF grant no. 01LN1702A). We thank the colleagues from Alfred-Wegener-Institut for their technical and scientific support during the experiment, especially Julia Haafke, Marcel Machnik, and Kristine Carstens. Sincere thanks to the colleagues who supported us in analyzing some of the samples, including Bernhard Fuchs (bacteria), Claudia Burau (DOC) and Johanna Strauß (total alkalinity). Special thanks to Dr. Mathias Wegner for lending us the flow cytometer and Ivan de Palma for supporting us with calculations for DOC production.

Supplementary material

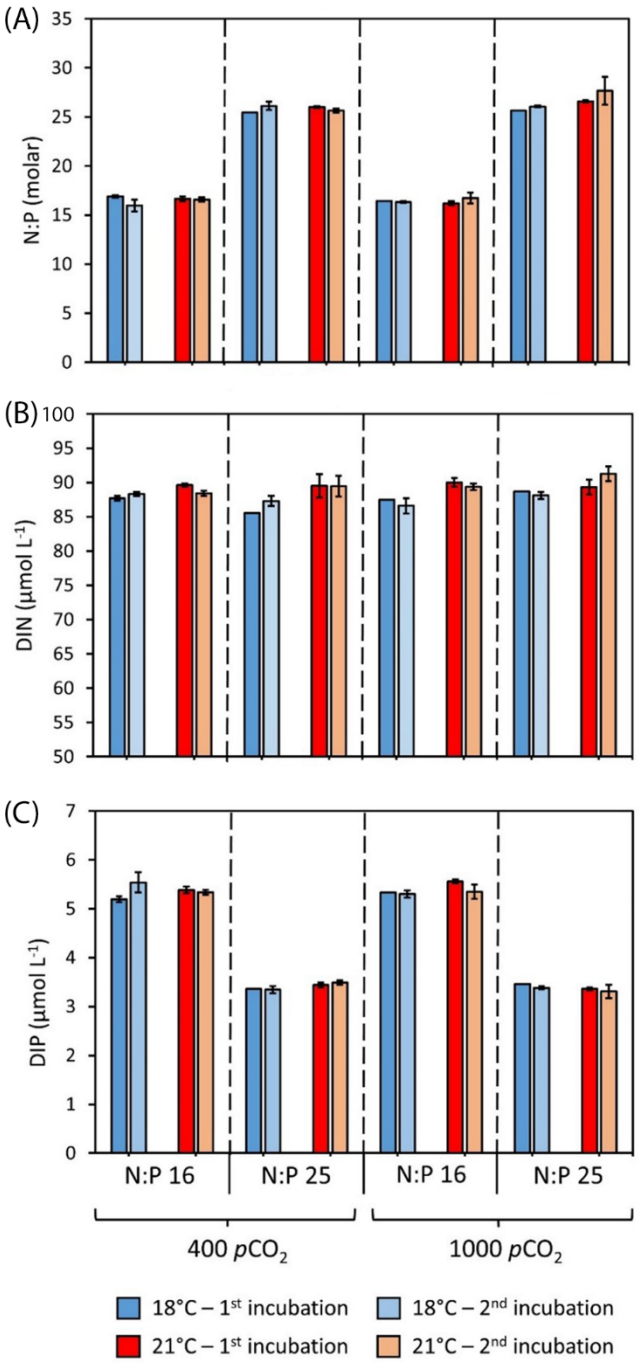

Suppl. Figure 3.1: Dissolved inorganic nutrients. Initial nutrient concentrations and N:P ratios across treatments. Incubation refers to first or second incubation. (A) N:P ratio (molar). (B) Dissolved inorganic nitrogen (DIN = NO_x). (C) Dissolved inorganic phosphorus (DIP = PO_4^{3-}). Data as mean ± standard deviation.

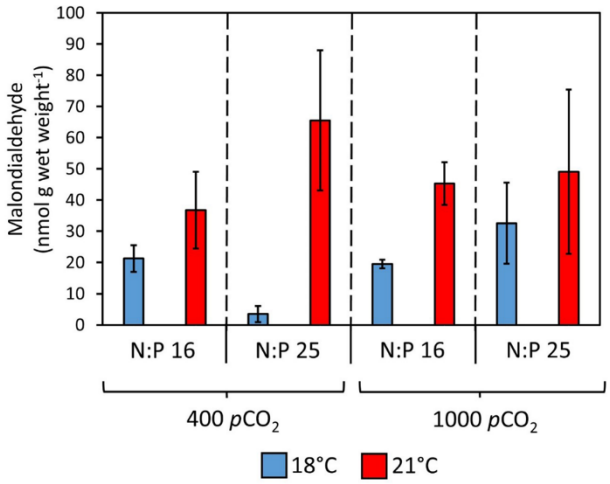

Suppl. Figure 3.2: Biomarker of oxidative stress. Malondialdehyde (MDA) cellular concentration. X-axis represents N:P ratios and pCO_2. Colors represent temperature (blue = 18°C, red = 21°C). Data as mean ± standard deviation.

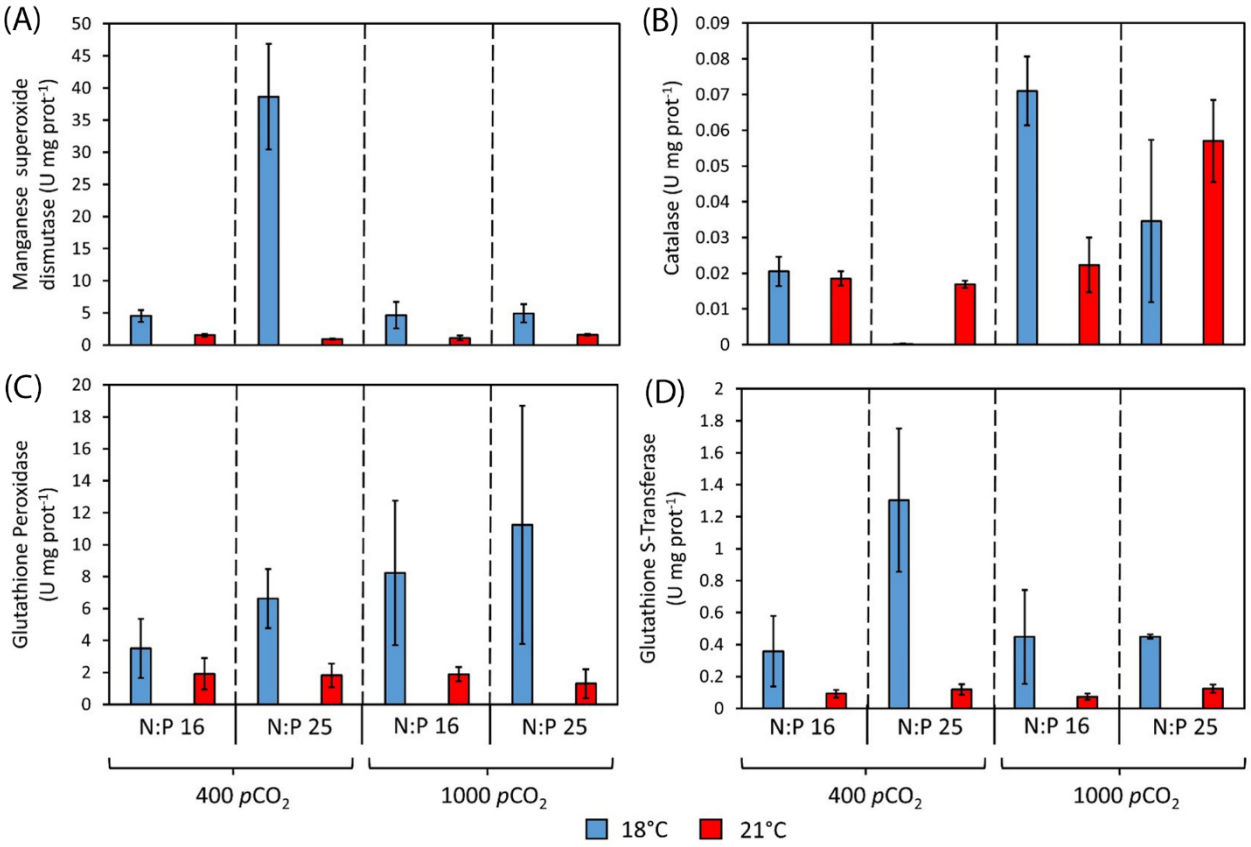

Suppl. Figure 3.3: Biomarkers of enzymatic antioxidant response. (A) Manganese Superoxide Dismutase (SOD-Mn) activity. (B) Catalase (CAT) activity. (C) Glutathione Peroxidase (GPx) activity. (D) Glutathione S-transferase (GST) activity. X-axis represents N:P ratios and pCO_2. Colors represent temperature (blue = 18°C, red = 21°C). Data as mean ± standard deviation.

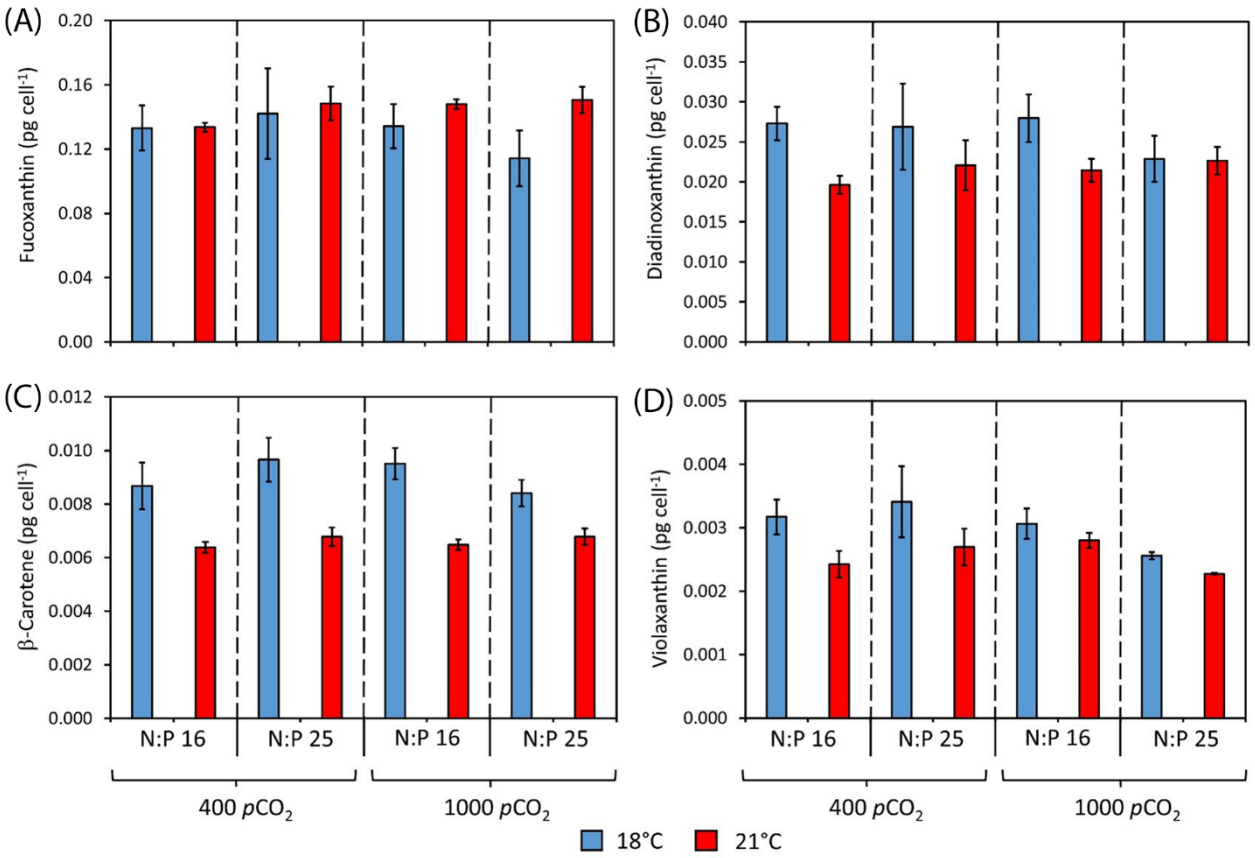

Suppl. Figure 3.4: Cellular carotenoids concentration. (A) Fucoxanthin, (B) Diadinoxanthin, (C) β-Carotene, (D) Violaxanthin. X-axis represents N:P ratios and pCO_2. Colors represent temperature (blue = 18°C, red = 21°C). Data as mean ± standard deviation.

try. Final and initial seawater carb
final. Total alkalinity (TA), dissol
Carbon dioxide (CO_2) were calcu
deviation.

Incubation and day	Temperature (°C)	Target pCO_2 (µatm)	N:P	pH	TA (µmol KgSW^{-1})	DIC (µmol KgSW^{-1})	Attained pCO_2 (µatm)	HCO_3^- (µmol KgSW^{-1})	CO_3^{2-} (µmol KgSW^{-1})	CO_2 (µmol KgSW^{-1})
1 d_0	18	400	16	8.13 (±0.01)	2424.16 (±3.74)	2118.68 (±10.95)	456.80 (±18.44)	1946.68 (±13.85)	156.14 (±4.49)	15.85 (±0.64)
1 d_0	18	400	25	8.11 (±0.01)	2404.52 (±2.16)	2111.08 (±2.24)	484.79 (±5.10)	1946.19 (±2.21)	148.09 (±1.41)	16.78 (±0.18)
1 d_0	18	1000	16	7.79 (±0.01)	2411.68 (±2.98)	2229.64 (±4.31)	1084.99 (±27.18)	2114.48 (±3.62)	77.52 (±2.05)	37.65 (±0.94)
1 d_0	18	1000	25	7.79 (±0.01)	2391.67 (±0.94)	2233.07 (±8.80)	1083.20 (±25.50)	2117.11 (±9.06)	78.46 (±1.28)	37.50 (±0.88)
1 d_4	18	400	16	8.15 (±0.01)	2428.01 (±2.63)	2128.58 (±8.74)	436.62 (±6.81)	1949.73 (±9.23)	163.69 (±1.33)	15.15 (±0.24)
1 d_4	18	400	25	8.18 (±0.05)	2421.96 (±4.24)	2111.16 (±7.47)	413.28 (±9.83)	1926.57 (±9.28)	170.28 (±2.50)	14.31 (±0.34)
1 d_4	18	1000	16	7.86 (±0.03)	2433.69 (±5.13)	2226.87 (±5.40)	920.82 (±63.83)	2104.11 (±4.01)	90.81 (±6.07)	31.95 (±2.21)
1 d_4	18	1000	25	7.86 (±0.01)	2424.46 (±1.77)	2222.93 (±3.69)	930.79 (±22.71)	2100.78 (±2.82)	89.92 (±2.32)	32.23 (±0.79)
2 d_0	18	400	16	8.16 (±0.01)	2424.53 (±3.74)	2141.28 (±3.80)	434.0 (±13.77)	1959.73 (±6.71)	166.49 (±4.13)	15.06 (±0.48)
2 d_0	18	400	25	8.14 (±0.02)	2438.33 (±16.73)	2108.68 (±29.13)	443.71 (±21.70)	1934.32 (±23.26)	158.96 (±9.14)	15.40 (±0.75)
2 d_0	18	1000	16	7.78 (±0.01)	2411.56 (±2.94)	2259.87 (±1.87)	1119.04 (±20.84)	2143.81 (±1.22)	77.24 (±1.51)	38.83 (±0.72)
2 d_0	18	1000	25	7.78 (±0.01)	2442.33 (±0.01)	2233.74 (±3.62)	1113.38 (±13.89)	2119.39 (±3.63)	75.70 (±0.81)	38.65 (±0.48)
2 d_4	18	400	16	8.12 (±0.01)	2427.64 (±9.00)	2157.40 (±15.10)	476.57 (±15.67)	1985.29 (±16.43)	155.58 (±3.07)	16.53 (±0.54)
2 d_4	18	400	25	8.18 (±0.05)	2418.60 (±2.71)	2139.85 (±20.06)	423.80 (±53.44)	1953.54 (±35.87)	171.60 (±17.93)	14.70 (±1.85)
2 d_4	18	1000	16	7.81 (±0.01)	2421.16 (±1.55)	2235.12 (±3.46)	1037.85 (±28.49)	2117.81 (±4.16)	81.30 (±1.96)	36.01 (±0.99)
2 d_4	18	1000	25	7.80 (±0.01)	2418.97 (±1.91)	2235.36 (±4.12)	1069.99 (±38.38)	2119.36 (±4.65)	78.85 (±2.56)	37.15 (±1.33)

Incubation and day	Temperature (°C)	Target pCO_2 (µatm)	N:P	pH	TA (µmol $KgSW^{-1}$)	DIC (µmol $KgSW^{-1}$)	Attained pCO_2 (µatm)	HCO_3^- (µmol $KgSW^{-1}$)	CO_3^{2-} (µmol $KgSW^{-1}$)	CO_2 (µmol $KgSW^{-1}$)
1 d_0	21	400	16	8.17	2407.67	2080.62	423.32	1885.48	181.66	13.47
				(±0.01)	(±4.99)	(±6.50)	(±7.69)	(±4.05)	(±3.66)	(±0.24)
1 d_0	21	400	25	8.18	2432.33	2041.79	402.28	1845.11	183.85	12.82
				(±0.00)	(±0.47)	(±9.12)	(±6.11)	(±9.70)	(±0.95)	(±0.19)
1 d_0	21	1000	16	7.80	2451.28	2195.87	1081.54	2074.37	87.18	34.32
				(±0.02)	(±7.48)	(±8.55)	(±40.73)	(±8.41)	(±3.09)	(±1.29)
1 d_0	21	1000	25	7.79	2453.33	2169.63	1087.59	2050.3	84.70	34.51
				(±0.02)	(±11.90)	(±9.92)	(±38.88)	(±9.53)	(±2.82)	(±1.23)
1 d_4	21	400	16	8.18	2422.63	2083.10	406.12	1881.33	188.84	12.93
				(±0.02)	(±2.03)	(±11.89)	(±21.96)	(±14.13)	(±7.91)	(±0.69)
1 d_4	21	400	25	8.20	2448.89	2085.88	390.34	1876.16	197.2	12.40
				(±0.02)	(±8.04)	(±19.49)	(±23.55)	(±23.89)	(±7.65)	(±0.75)
1 d_4	21	1000	16	7.87	2435.82	2185.69	923.02	2056.05	100.35	29.29
				(±0.02)	(±7.96)	(±8.31)	(±35.59)	(±10.02)	(±3.05)	(±1.13)
1 d_4	21	1000	25	7.83	2434.82	2206.42	1032.24	2080.65	93.03	32.75
				(±0.06)	(±4.09)	(±28.23)	(±138.88)	(±32.49)	(±9.19)	(±4.41)
2 d_0	21	400	16	8.12	2447.67	2071.18	469.40	1890.29	165.97	14.91
				(±0.01)	(±2.62)	(±3.42)	(±9.79)	(±4.37)	(±2.89)	(±0.31)
2 d_0	21	400	25	8.17	2450.33	2057.60	419.68	1863.79	180.48	13.33
				(±0.01)	(±13.22)	(±9.85)	(±9.03)	(±9.23)	(±3.51)	(±0.29)
2 d_0	21	1000	16	7.82	2424.41	2183.45	1032.82	2060.99	89.65	32.81
				(±0.01)	(±6.53)	(±15.50)	(±13.68)	(±14.71)	(±1.01)	(±0.43)
2 d_0	21	1000	25	7.83	2427.80	2191.87	1005.99	2067.14	92.79	31.94
				(±0.01)	(±4.90)	(±9.26)	(±20.99)	(±9.65)	(±1.08)	(±0.66)
2 d_4	21	400	16	8.17	2442.09	2142.30	437.20	1940.9	187.92	13.88
				(±0.01)	(±12.07)	(±16.16)	(±12.64)	(±15.37)	(±4.59)	(±0.40)
2 d_4	21	400	25	8.17	2424.01	2119.16	421.83	1915.88	189.88	13.40
				(±0.02)	(±8.43)	(±9.20)	(±17.42)	(±12.69)	(±5.43)	(±0.55)
2 d_4	21	1000	16	7.85	2433.41	2227.99	965.02	2097.80	99.54	30.65
				(±0.02)	(±9.02)	(±4.31)	(±39.09)	(±5.52)	(±3.58)	(±1.24)
2 d_4	21	1000	25	7.89	2423.34	2236.95	902.24	2101.17	107.14	28.64
				(±0.03)	(±8.98)	(±13.99)	(±53.18)	(±16.66)	(±4.48)	(±1.69)

Suppl. Information 3.1: Net DOC Production Integral resolution. Step-by-step resolution of integral explaining the formula for Net DOC Production.

DOC_p = Total DOC production (ΔDOC pmol mL^{-1})

$DOC_p' = \frac{dQ}{dt}$

D = DOC production cell^{-1} d^{-1}

C_1 = final cells concentration

$D = \frac{Q'}{C_1}$

G = cells growth

t = time

$C_1(t)$ = Cell concentration in the function of time

C_0 = Initial cells concentration

Cells growth: $C_1(t) = C_0.e^{Gt}$

DOC production d^{-1}: $\frac{dDOCp}{dt} = D.C1(t)$

DOC production:

$$DOCp = \int_{to}^{t} \frac{dDOCp}{dt} dt = \int_{to}^{t} D.C1(t).dt$$

$$\int_{to}^{t} D.C1(t).dt = \int_{to}^{t} D.C0.e^{Gt}.dt$$

$$\int_{to}^{t} D.C0.e^{Gt}.dt = D.C0.\left[\frac{e^{Gt}}{G}\right]_{to}^{t}$$

$$D.C0.\left[\frac{e^{Gt}}{G}\right]_{to}^{t} = D.C0.\left(\frac{e^{Gt}}{G} - \frac{e^{Gto}}{G}\right)$$

$$DOCp = D.C0.\left(\frac{e^{Gt}}{G} - \frac{e^{Gto}}{G}\right)$$

$$DOCp = D.C0.\left(\frac{e^{G.4}}{G} - \frac{e^{G.0}}{G}\right)$$

$$(I)\ DOCp = D.C0.\left(\frac{e^{G.4}}{G} - \frac{1}{G}\right)$$

Determining G = $C1(t) = C0.e^{\mu t}$

$$C1(t) = C0.e^{Gt}$$

$$\frac{C1(t)}{C0} = e^{Gt}$$

$$ln\left(\frac{C1(t)}{C0}\right) = \ln\left(e^{Gt}\right)$$

$$ln\left(\frac{C1(t)}{C0}\right) = Gt$$

$$\frac{\ln C1(t) - lnC0}{t} = G$$

Applying *C1*, *C0* and *t* measured during the experiment to determine *G*.

$$G = \frac{ln81290 - ln320}{4}$$

$$G = \frac{ln\,{}^{81290}/_{320}}{4}$$

$$G = \frac{ln256}{4} = \frac{ln4^4}{4} = \frac{4}{4} ln4$$

$$G = ln4\ (II)$$

Replacing II in I

$$DOCp = D.C0.\left(\frac{e^{ln4.4}}{ln4} - \frac{1}{ln4}\right)$$

$$\frac{DOCp}{C0.\left(\frac{e^{ln4.4}}{ln4} - \frac{1}{ln4}\right)} = D$$

$$\frac{DOCp}{C0.\left(\frac{e^{G.4}}{G} - \frac{1}{G}\right)} = D$$

Replacing *G* by the specific growth rate (μ)

$$D = \frac{DOCp}{C0}.\frac{\mu}{\left(\frac{C1}{C0} - 1\right)}$$

Chapter 4

The impact of marine heatwaves under two dissolved N:P ratios on the physiology of the diatom *Phaeodactylum tricornutum*

Elisabeth Groß[1*], Nadine Rijsdijk[1,2*], Nelly Tremblay[1,3], Maarten Boersma[1,4], Cédric Leo Meunier[1]

*** Shared first authorship**

[1] Alfred-Wegener-Institut Helmholtz-Zentrum für Polar- und Meeresforschung, Biologische Anstalt Helgoland, Helgoland, Germany

[2] Protistology and Aquatic Ecology, Department of Biology, Ghent University, Krijgslaan 281 S8, 9000 Ghent, Belgium

[3] Pêches et Océans Canada, 850 Route de la Mer, Mont-Joli, QC, Canada

[4] University of Bremen, FB2, Bremen, Germany

Manuscript

Abstract

Future climate change scenarios indicate that both the frequency and intensity of marine heatwaves will increase, affecting a large proportion of marine organisms, including phytoplankton. As primary producers, phytoplankton are directly affected by both an increase in temperature and changes in dissolved nutrient concentrations. Therefore, we conducted a study to investigate the effects of marine heatwaves on the well-studied diatom *Phaeodactylum tricornutum* at two different dissolved N:P ratios (N:P = 16 and N:P = 25). Cells were exposed to a temperature increase from 15 to 20 °C for five days and an additional acclimation period of five days at elevated temperature. To determine if the cells were stressed, we measured alternative oxidase (AOX)-dependent respiration. In addition, we quantified changes in growth rate and cell size, as well as particulate organic carbon (POC) and lipid content of the cells. We did not find that the increase in temperature led to increased AOX activity. Also, the increased N:P ratio only led to a decrease in total respiration but did not affect other cellular properties. However, the growth rate and POC content of *P. tricornutum* increased after the acclimation period at higher temperatures, while cell size and cellular lipid content decreased. Interestingly, significant changes in the measured traits occurred in most cases after the acclimation phase of five days but not directly after the temperature increase in the heatwave treatment. Hence, our study demonstrates that phytoplankton cells might have the potential to buffer environmental fluctuations but also that marine heatwaves can lead to significant changes in phytoplankton traits.

4.1. Introduction

Phytoplankton form the foundation of most marine ecosystems, as they fix inorganic carbon to produce glucose and oxygen in photosynthetic processes. Diatoms are the most speciose group of phytoplankton and play ecologically important roles. They tend to be the dominant group in phytoplankton communities in coastal and upwelling regions and are at the basis of most marine food webs (Armbrust, 2009). Diatoms also contribute up to 40% of the marine primary production and play a large role in carbon sequestration to the deep ocean (Smetacek, 1999). However, diatoms, and phytoplankton in general, are highly sensitive to changes in environmental conditions and can respond quickly because of their high reproduction rates (Paerl *et al.*, 2007, Schindler, 1987).

Future climate change scenarios indicate that marine heatwaves defined as discrete anomalously warm water events that occur in a particular location for at least five days, will increase in intensity and occur more frequently in the 21st century (Hobday *et al.*, 2016, IPCC, 2019). This rapid increase in seawater temperature can drastically impact marine organisms, for instance, by causing loss of genetic diversity (Gurgel et al., 2020) or by promoting local extinction of species (Thomsen et al., 2019). At the same time, nutrient availability will also be affected by climate change and anthropogenic activities, leading to shifts in dissolved nutrient ratios. Legal restrictions on riverine nutrient loads have led to increased nitrogen:phosphorus (N:P) ratios, as observed, for example, in the North Sea (Burson *et al.*, 2016) and estuaries in North Carolina (Paerl *et al.*, 2014). Two important drivers of these changes are that nitrogen comes from sources that are not immediately limited, which may lead to further increases in atmospheric nitrogen deposition (Grizzetti et al., 2012) and, at the same time, the potential depletion of global P reserves in 50 to 200 years if current levels of use are maintained or increased (Ober, 2016, Herrera-Estrella & López-Arredondo, 2016).

The simultaneous increase in frequency and intensity of marine heatwaves in combination with shifts in dissolved nutrient concentrations can have profound influences on the physiological processes of phytoplankton cells. Temperature, as well as nutrient concentrations, have a strong effect on cell metabolism and mitochondrial respiration (Laws & Caperon, 1976, Martinez, 1992), which can, in turn, affect growth rate (Eppley, 1972, Raven

& Geider, 1988) and the macromolecular content of the cell (Liefer *et al.*, 2019). In aerobic organisms, most cellular respiration is the electron transport chain by the cytochrome pathway (CIII-CIV). However, studies have found that biotic or abiotic stress can increase the use of another terminal electron acceptor: the alternative oxidase (AOX) in higher plants, protists, fungi, and some phytoplankton species (reviewed by Vanlerberghe, 2013). For instance, thermal stress (both a decrease from 26 to 18 °C and an increase from 26 to 32 °C) in the coral symbiont dinoflagellate *Symbiodinium* spp. resulted in a significant increase in the contribution of the AOX pathway to total respiration (Oakley *et al.*, 2014). Although less energy efficient, the AOX respiration pathway is expected to be beneficial to organisms exposed to biotic or abiotic stress as it reduces the overproduction of reactive oxygen species formed in cells that can damage vital structures such as lipid membranes, proteins and DNA (Møller, 2001). Therefore, assessing the respiration rate of the AOX pathway compared to the total respiration rate can provide information on the degree of stress when phytoplankton are exposed to sudden changes in temperature, such as in marine heatwaves. Additionally, lipids, which are important for functions such as structuring the cell membrane and internal energy storage, are accumulated when phytoplankton cells experience stress caused by warmer water (Sharma et al., 2012, Thangaraj & Sun, 2020) or by lower concentrations of nutrients such as P (Feng *et al.*, 2015, Siron *et al.*, 1989). Increased metabolic rates due to elevated temperatures could also lead to a higher demand for dissolved inorganic P since photosynthetic processes require large amounts of proteins synthesized by P-rich ribosomes (Ågren, 2004). Another important cellular trait that is influenced by temperature and dissolved nutrient concentrations is cell size as it is linked to nutrient uptake capacities, growth and metabolic rates as well as storage capacities of phytoplankton cells (Finkel et al., 2010). A negative correlation between growth rate and cell size has been observed (Finkel et al., 2010). Under suboptimal nutrient conditions, smaller cells are advantageous as their higher surface-to-volume ratio enhances nutrient transport capacities (Irwin & Finkel, 2008). However, smaller cells have fewer storage capacities than larger cells (Sommer, 1984), which can be of a disadvantage when abrupt changes in the environment lead to abiotic stress.

The physiological changes phytoplankton experience due to climate change and anthropogenic activities might lead to altered seasonal dynamics, community composition, and phytoplankton productivity (Winder & Sommer, 2012). Understanding how phytoplankton will

respond to heatwaves and shifts in dissolved nutrient concentrations is thus essential in understanding how ecosystems will change in the future. The influence of heatwaves on phytoplankton physiology remains poorly studied and to our knowledge, was never studied in conjunction with different dissolved nutrient ratios. In this study, we aimed to assess the influence of a heatwave on the physiology of the marine diatom *Phaeodactylum tricornutum* (Bohlin, 1897), a coastal species that has been widely used as a model system to study diatom physiology (e.g., De Martino *et al.*, 2011). Because increasing water temperatures and shifts in dissolved nutrient concentrations will likely occur simultaneously, we studied the effect of a heatwave combined under two N:P ratios, 16 (Redfield) and 25 (representing an increase predicted for future decades (Peñuelas et al., 2013)). We postulate the following three hypotheses: 1) the combination of a heatwave with an elevated N:P ratio would lead to cellular stress and an increase in AOX activity, especially directly after the temperature increase; 2) higher temperatures would lead to an increase in metabolic activity, resulting in an increase in total respiration, growth rate, as well as POC and cellular lipid content; and 3) since phytoplankton growth rate and cell size have been shown to be negatively correlated, cell size would decrease at a higher growth rate under elevated temperatures.

4.2. Materials and methods

Experimental setup and culture conditions

The diatom *Phaeodactylum tricornutum* (strain CCAP 1052/1A) was grown in semi-continuous dilute batch cultures at 15 °C with a 16:8 light:dark cycle and irradiance of 100-120 µmol photons m^{-2} s^{-1} (GHL Mitras Lightbar 2 Daylight). This stock culture was diluted every five days to maintain cells in the exponential growth phase (with concentrations below 1.10^5 cells mL^{-1}) and avoid nutrient depletion, light-limitation, and the accumulation of toxic by-products of metabolism (Fogg, 1957). Initial cell concentration was always approximately 400 cells mL^{-1}. The medium cultures were diluted with f/20 medium (Guillard & Ryther, 1962, Guillard, 1975) prepared with 0.2 µm sterile filtered seawater. Cultures were placed on a roller table to keep the cells in suspension. Before starting the experiment, inoculation stock cultures were prepared, adding the nutrient solution NaH_2PO_4 to adjust the dissolved N:P ratio of the medium to N:P = 16 and N:P = 25. Exact nutrient concentrations can be found in suppl. Table

4.1. The inoculation stock cultures were acclimated in 1L Schott glass bottles to these nutrient conditions for seven days in the same growth conditions as the stock cultures.

To test the effect of a marine heatwave, we subjected the cultures to either heatwave (Heat) or control (Ctrl) conditions in combination with the two dissolved N:P ratios (NP16 and NP25) in a factorial design. This resulted in four treatment combinations (Heat-NP16, Heat-NP25, Ctrl-NP16, and Ctrl-NP25). The cultures were grown in 1L glass bottles with four replicates per treatment, yielding a total of 16 bottles (Fig. 4.1). To simulate the heatwave conditions, a temperature-controlled room was heated up from 15 to 20 °C with an increase of 1 °C day^{-1}. Then, the temperature was kept constant at 20 °C for five days. The control cultures were kept in a separate temperature-controlled room under a constant temperature of 15 °C. Three sampling points were defined: After initial acclimation (day 0), after the temperature increase of 5°C in the heatwave treatments (day 5), and after the acclimation at 20°C in the heatwave treatments (day 10). The three sampling points will be described in the following as d0 (day 0), d5 (day 5), and d10 (day 10). Since we expected the strongest response after temperature fluctuations and were particularly interested in rapid physiological changes immediately after the temperature rise, we focused on the immediate (day 5) and longer-term (day 10) responses to a heat wave. In addition, it should be mentioned that we did not want to exceed the thermal window to study only the response to a sharp temperature rise and not the effects of lethal temperatures. During the experiment, the light conditions and dilution patterns were the same as those used during the acclimation phase.

Temperature and pH were measured daily. Dissolved inorganic nutrients were analyzed at d0, d5, and d10. Samples were filtered with a 0.45 µm Nylon membrane filter and stored in 50 mL CELLSTAR® tubes at -20 °C before measuring with an autoanalyzer (Evolution III, Alliance Instruments GmbH), according to the methods of Grasshoff (1976).

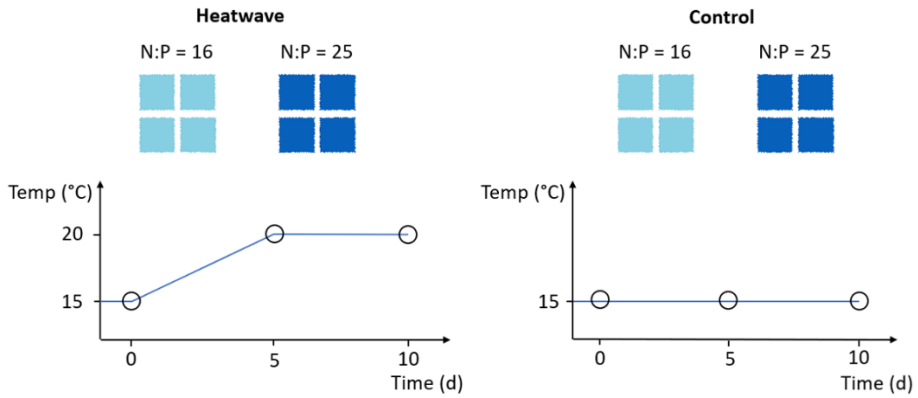

Figure 4.1: Schematic overview of the experimental setup. Using a full factorial design, *Phaeodactylum tricornutum* cultures were subjected to either heatwave or control conditions, in either N:P = 16 or N:P = 25 medium. Each treatment consisted of four replicates. The three measurement points (day 0, day 5, and day 10) at which samples were taken are indicated by the circles.

Respiration and AOX

To quantify the respiration rate and the AOX activity of *P. tricornutum*, cells were collected at d0, d5, and d10 by gentle filtration on a 0.45 µm Nylon membrane filter (approximately 3.10^6 to 4.10^6 per replicate) and resuspension in 5 mL medium followed by a direct measurement through high-resolution respirometry with Oroboros O2k (Oroboros Instruments GmbH, Innsbruck, Austria). Oxygen fluxes were monitored at 15 °C or 20 °C, depending on the treatment, excluding any light in the chambers. Routine respiration and AOX activity were measured by using substrate-uncoupler-inhibitor titration (SUIT, 022 www.bioblast.at/index.php/SUIT-022_O2_ce_D051 and 023 www.bioblast.at/index.php/SUIT-023_O2_ce_D053) protocols specifically developed to distinguish between oxygen consumption derived from mitochondrial AOX and respiratory complex III-IV (CIII-IV). Briefly, in a first step, routine respiration was measured for both chambers. Then, one of the chambers was used to quantify AOX-dependent respiration after inhibition of the CIII-IV with 1 mM potassium cyanide (KCN), while the other was used for CIII-IV-dependent respiration after inhibition of AOX with 1 mM salicylhydroxamic acid (SHAM). To determine AOX activity, we used the ratio between SHAM-inhibited respiration and routine respiration.

Growth rate and cell size

To determine growth rates of *P. tricornutum*, cell density was measured daily by flow cytometry (BD Accuri™ C6, Belgium) at medium flow rate (35 µL min^{-1}). Detectors used were the forward scatter (FSC) and the fluorescence detector FL3 (670 nm) which detects the autofluorescence of chlorophyll *a* pigments in phytoplankton. The FL3 fluorescence detector was used to select only living cells for the detection signal and remove debris signals. Growth rate μ (d^{-1}) was calculated daily with the formula:

$$\mu = \ln(N_t/N_0) \cdot \Delta t^{-1}$$

whereby N_0 and N_t describe cell concentrations at t0 and t and Δt is 1 since we measured every day.

For growth rate analysis, we calculated growth rates for d0, d5, and d10, where d0 describes the growth rate from the last day of acclimation to day 0, d5 was calculated using cell numbers from day 4 to 5, and d10 was calculated from day 9 to 10. Additionally, we used flow cytometric measurements of the samples at d0, d5, and d10 to detect changes in the cell size of *P. tricornutum* based on the FSC.

POC and total lipids

Particulate organic carbon (POC) and total lipids of *P. tricornutum* were determined at d0, d5, and d10. Cells were sampled by filtering 200 mL on pre-combusted (500 °C for 4 h) Whatman® GF/F filters (25 mm). For POC analyses, filters were dried for at least 48 h at 60 °C in a drying chamber before being wrapped in tin foil and analyzed with an elemental analyzer (Vario Micro cube CHN analyzer, Elementar). Samples for total lipid determination were stored at -80 °C before extraction with dichloromethane (CH_2Cl_2). Sulfuric acid was added to react with the unsaturated lipids to form a carbonium ion (Knight *et al.*, 1972). Phosphor-vanillin solution was added, which reacts with the carbonium ion to form a colored compound. This compound was measured with a photometer at 540 nm (Multiskan Spectrum, ThermoFisher Scientific™). To determine total lipid content of each sample, the absorbance values measured were compared against a calibration curve made with cholesterol.

Statistical analysis

Statistical analyses were performed using R 4.0.0 (R Core Team, 2021). We used the 'drop1' function starting with a three-way ANOVA including interactions, to choose the best statistical model to test for the effect of both treatments and the three sampling points. Residuals were tested for normal distribution and homogeneity, followed by a pairwise *post-hoc* test (Tukey's HSD). The threshold of significance was set at 5 % for all analyses.

4.3. Results

The diatom *P. tricornutum* was grown in semi-continuous cultures to test the effect of a marine heatwave under two different dissolved N:P ratios (N:P = 16, N:P = 25). In the heatwave treatment, the temperature was gradually elevated from 15 to 20 °C over five days and kept constant for another five days. Samples were taken after initial acclimation (day 0), after the temperature increase (day 5), and after the acclimation at 20 °C (day 10).

Respiration and AOX activity

To investigate if the increase in temperature during a heatwave leads to stress responses within the cells of *P. tricornutum*, we measured the contribution of the AOX pathway to total cellular respiration (Fig. 4.2). The total routine respiration varied between 1.24 and 4.80 pmol O_2 s^{-1} million $cells^{-1}$ and was significantly affected by all three factors (temperature, nutrients, and time; three-way ANOVA, Table 1). Overall, the heatwave treatments led to significantly higher respiration rates of *P. tricornutum* in comparison to the control (Tukey's post-hoc test, $p < 0.001$). Total respiration was significantly lower in NP25 than in NP16 (Tukey's post-hoc test, $p < 0.001$). Whereas we did not observe a significant difference between Heat and Ctrl at d0 and d5, the respiration rate of *P. tricornutum* was in the heatwave treatment at d10 significantly higher than in the control at d10 treatment (Tukey's post-hoc test, $p < 0.001$).

The AOX activity, which describes the ratio between AOX-dependent respiration (AOX pathway inhibited by SHAM) and routine respiration of *P. tricornutum,* varied between 0.0065 and 0.35 and was significantly affected by N:P treatments as well as by the three different

sampling points (three-way ANOVA, Table 4.1). Overall, AOX activity was significantly lower in NP25 than in NP16 (Tukey's post-hoc test, $p = 0.0041$) and in both NP treatments significantly higher at d10 than at d5 (Tukey's post-hoc test, $p \leq 0.026$). In NP25, almost no AOX activity could be detected at d5.

Table 4.1: ANOVA results of best-fit model of total respiration and AOX activity of *P. tricornutum* in two temperature treatments (Ctrl, Heat) and N:P treatments (NP16, NP25) as well as by the three different sampling points (d0, d5, d10). Significant differences ($p < 0.05$) are highlighted in bold.

Variable	Factor 1	Factor 2	Factor 3	MS	F	p-value
Routine respiration rate (pmol O_2 (sec * mio cells)$^{-1}$)	Treatment	-	-	8.90	14.29	**<0.001*****
	-	Day	-	9.95	15.98	**<0.001*****
	-	-	N:P	18.62	29.90	**<0.001*****
	Treatment	Day	-	6.00	9.64	**<0.001*****
	-	Day	N:P	6.76	10.86	**<0.001*****
AOX activity	-	Day	-	0.11	13.69	**<0.001*****
	-	-	N:P	0.077	9.50	**0.0041****
	-	Day	N:P	0.041	5.02	**0.013***

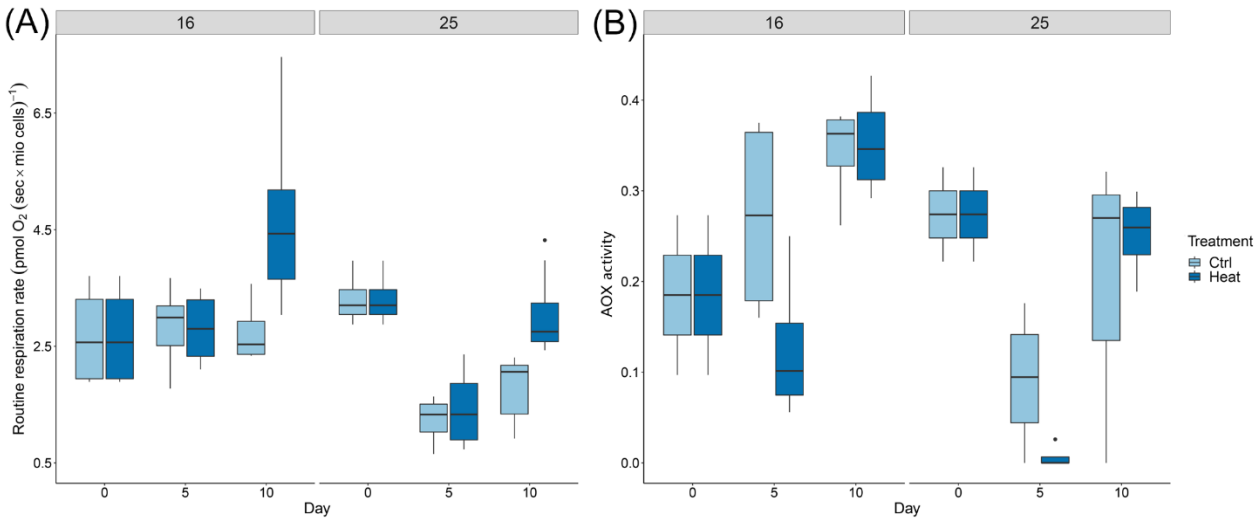

Figure 4.2: Routine rate (A) in pmol O_2 s^{-1} million $cells^{-1}$ and AOX activity (B) of *P. tricornutum* in semi-continuous cultures. Cultures were grown in two temperature treatments (Ctrl, Heat) and two dissolved nutrient treatments (NP16, NP25). Samples were taken at three points (d0, d5, d10). Each treatment consisted of four replicates. Boxes represent 50 % of the central data and the median. Lower and upper whiskers represent minimum and maximum values, respectively, without outliers, which are represented as dots.

Growth rate and cell size

Growth rates of *P. tricornutum* varied from 0.86 day^{-1} to 1.28 day^{-1} across treatments (Fig. 4.3). Growth rates were not significantly affected by the two dissolved nutrient treatments but were significantly different between the two temperature treatments (MS 0.13, $F_{1,36}$ 4.14, p = 0.050) and three sampling points (MS 0.15, $F_{2,36}$ 4.76, p = 0.015). Overall, growth rates of *P. tricornutum* were positively correlated with temperature and were significantly higher in the heatwave treatment than in the control (Tukey's post-hoc test, p = 0.050), as well as at d10 compared to d5 (Tukey's post-hoc test, p = 0.022).

Changes in cell size of *P. tricornutum* were detected by flow cytometry using the forward scatter signal (Fig. 4.4). Cell size of *P. tricornutum* was significantly affected by the three sampling points (MS < 0.001, $F_{2,34}$ 5.39, p = 0.00092) and by the interaction of temperature treatments and sampling points (MS < 0.001, $F_{2,34}$ 10.61, p < 0.001). Only after acclimation at 20 °C at d10 cell size was significantly lower in the heatwave treatments than in the control d5 (Tukey's post-hoc test, p = 0.0040).

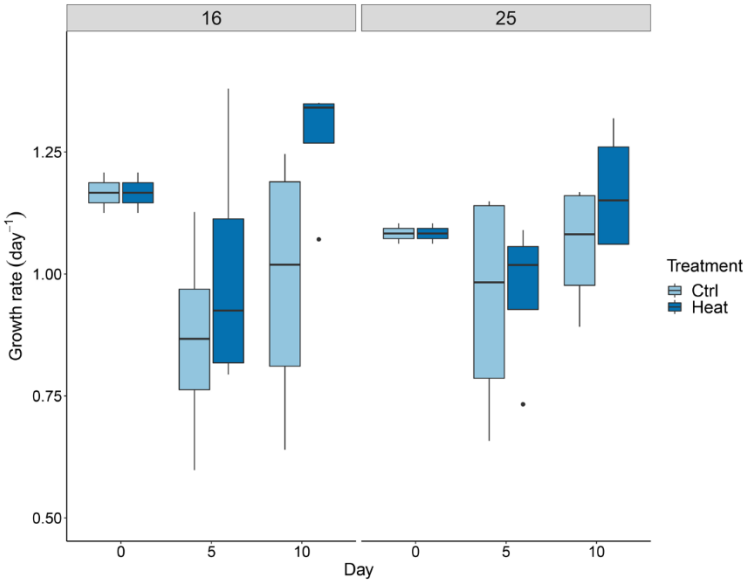

Figure 4.3: Growth rate (day^{-1}) of *P. tricornutum* in semi-continuous cultures. Cultures were grown in two temperature treatments (Ctrl, Heat) and two dissolved nutrient treatments (NP16, NP25). Samples were taken at three points (d0, d5, d10). Each treatment consisted of four replicates. Boxes represent 50 % of the central data and the median. Lower and upper whiskers represent minimum and maximum values, respectively, without outliers, which are represented as dots.

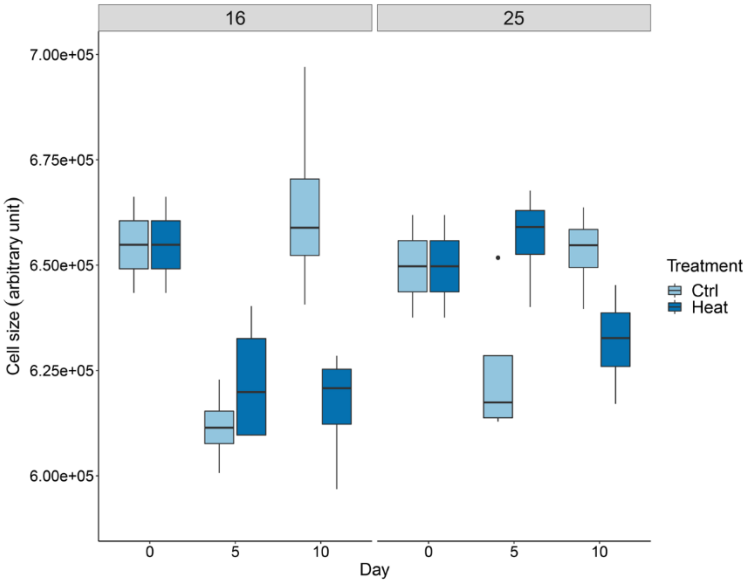

Figure 4.4: Cell size (forward scatter, arbitrary unit) of *P. tricornutum* in semi-continuous cultures. Cultures were grown in two temperature treatments (Ctrl, Heat) and two dissolved nutrient treatments (NP16, NP25). Samples were taken at three points (d0, d5, d10). Each treatment consisted of four replicates. Boxes represent 50 % of the central data and the median. Lower and upper whiskers represent minimum and maximum values, respectively, without outliers, which are represented as dots.

POC and total lipids

Particulate organic carbon (POC) of *P. tricornutum* varied between 8.27 and 11.40 pg cell^{-1} (Fig. 4.5). POC was not significantly affected by the two temperature treatments or the dissolved nutrient treatments. However, we observed a significant difference between the sampling points (MS = 3.65, $F_{2,36}$ 4.06, p = 0.026), where POC of *P. tricornutum* was significantly higher after acclimation at d10 compared to d5 (Tukey's post-hoc test, p = 0.043).

Cellular lipid content of *P. tricornutum* varied between 0.33 and 0.52 pg cell^{-1} (Fig. 4.6). Neither the two dissolved nutrient treatments nor the sampling points led to significant differences in the cellular lipid content. However, we observed a significant effect of the heatwave treatment (MS = 0.032, $F_{2,36}$ 5,68, p = 0.022). Overall, the cellular lipid content of *P. tricornutum* was in the heatwave treatment significantly lower than in the control (Tukey's post-hoc test, p = 0.022).

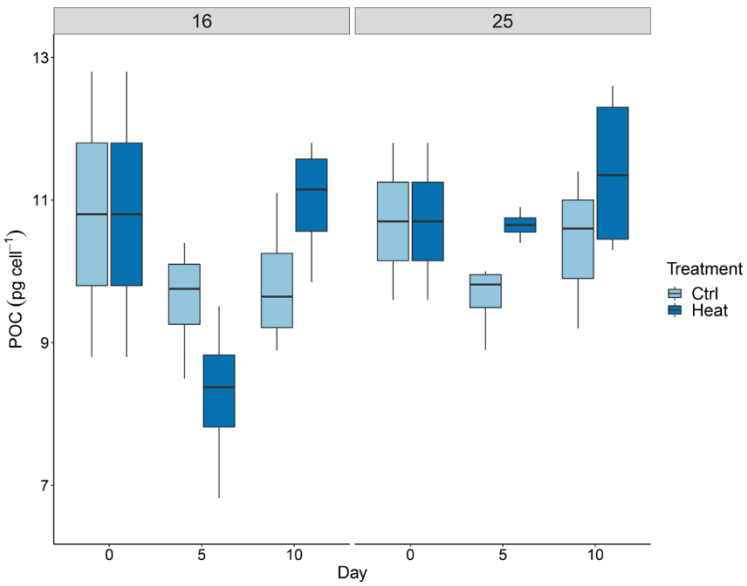

Figure 4.5: POC (pg cell^{-1}) of *P. tricornutum* in semi-continuous cultures. Cultures were grown in two temperature treatments (Ctrl, Heat) and two dissolved nutrient treatments (NP16, NP25). Samples were taken at three points (d0, d5, d10). Each treatment consisted of four replicates. Boxes represent 50 % of the central data and the median. Lower and upper whiskers represent minimum and maximum values, respectively, without outliers, which are represented as dots.

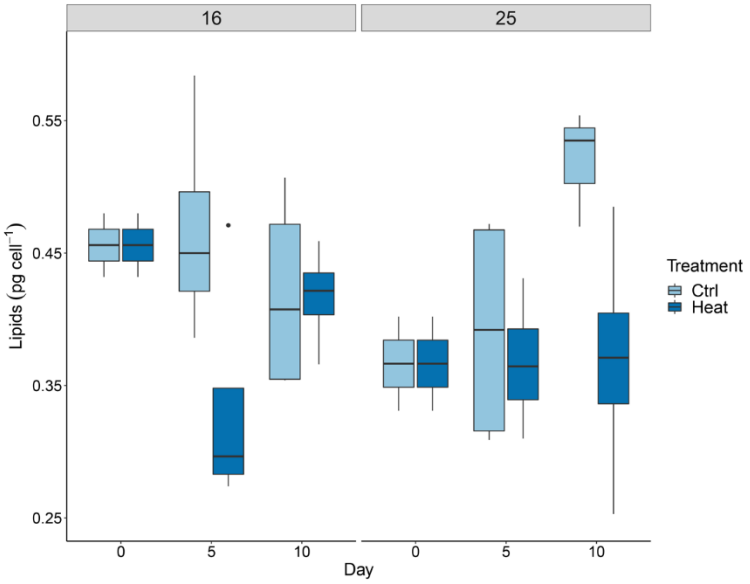

Figure 4.6: Cellular lipid content (pg cell^{-1}) of *P. tricornutum* in semi-continuous cultures. Cultures were grown in two temperature treatments (Ctrl, Heat) and two dissolved nutrient treatments (NP16, NP25). Samples were taken at three points (d0, d5, d10). Each treatment consisted of four replicates. Boxes represent 50 % of the central data and the median. Lower and upper whiskers represent minimum and maximum values, respectively, without outliers, which are represented as dots.

4.4. Discussion

In this study, we investigated the impact of a marine heatwave under two dissolved N:P ratios on the physiological traits of the diatom *P. tricornutum*. To test if phytoplankton cells were stressed, we assessed the AOX activity i.e., the ratio between SHAM-inhibited respiration and routine respiration. Additionally, we analyzed changes in growth rate and cell size as well as POC and the cellular lipid content. Overall, we did not detect a significant effect of dissolved N:P ratios on cellular properties, except for respiration, which was lower under elevated N:P ratio. We hypothesized that an elevated N:P ratio would increase cellular stress responses due to increasing temperatures because higher growth rates at elevated temperatures increase P requirements, but it appears that the fact that nutrients were not limited in our experiment played a greater role than the actual nutrient ratio. At the same time, we observed for several parameters that were assessed in this study changes in the control after the first dilution at d0. These changes could only be explained by an inappropriate acclimation period, although cultures were kept for at least seven days in experimental culture conditions prior to the experiment.

Nevertheless, we found that the heatwave significantly affected several cellular traits of *P. tricornutum*, which we discuss below.

According to the metabolic theory of ecology, an increase in temperature leads to increased metabolic activity, such as respiration, of aerobic organisms (Brown *et al.*, 2004). In support of our hypothesis, higher temperatures in the heatwave treatment resulted in significantly higher respiration rates of *P. tricornutum*. Our results are also consistent with other studies that found an increase in phytoplankton respiration rates at elevated temperatures (González-Olalla *et al.*, 2021, Staehr & Birkeland, 2006). However, compared to the control, higher total respiration of *P. tricornutum* was observed only after the acclimation phase of five days at 20 °C, but not directly after the temperature increase phase at d5. In addition to higher total respiration of *P. tricornutum* in the heatwave treatment, we also expected an increase in AOX activity since a temperature increase may lead to thermal stress. However, the AOX activities of *P. tricornutum* in both N:P treatments were, was higher only after the acclimation phase at d10 and not directly after the temperature rise at d5, where we expected the highest AOX activity. In fact, the AOX activity was lowest at d5 in the heatwave treatments, which indicates that the cells were not stressed by the rapid temperature increase. Alternatively, metabolic activities may have focused on the most productive respiratory pathway in terms of energy efficiency, which, in turn, could increase the production of reactive oxygen species and potentially lead to damage to cell structures (Møller, 2001). In favor of the latter explanation, AOX activity increased significantly after acclimation to the higher temperature. Other studies have found that temperature fluctuations can cause an increase in AOX activity (Oakley et al., 2014, Zalutskaya *et al.*, 2015, Murik *et al.*, 2019). However, in all these studies, the temperature changes were much more severe than in our study.

Although we did not find that an increase in temperature led to thermal stress in our study, we observed changes in growth rate, cell size, POC, and total lipid content of *P. tricornutum*. Supporting our hypothesis and in line with the metabolic theory of ecology (Brown et al., 2004), as well as previous observations that phytoplankton growth increases at higher temperatures until an optimal temperature is reached (Eppley, 1972), we observed higher growth rates in the heatwave treatment and higher POC content per cell. The heatwave treatment also resulted in significant changes in cell size. As we had hypothesized, cell size of

P. tricornutum decreased at higher temperatures and higher growth rates. However, also for this trait, changes were observed only after the acclimation period. In phytoplankton, carbon is mostly stored as lipids and carbohydrates (Geider & La Roche, 2002). However, the cellular lipid content in our study was significantly lower when cells grew at higher temperatures. It has also been shown that cellular lipid content increases under abiotic stress such as limiting nutrients or ocean acidification (Geider & La Roche, 2002, Liefer et al., 2019, Feng et al., 2015, Gao et al., 2018), which might be a further indication that cells in our experiment were not stressed. Because we found increased metabolic rates, stored lipids may have been used as a carbon source, leading to the observed decrease in cellular lipid content. At the same time, cellular POC increased at elevated temperature, which was also observed by (Feng *et al.*, 2009). Since we observed a lower cellular lipid content, higher POC might be caused by an increase in carbohydrates as structural components in cell walls (Geider & La Roche, 2002).

As the oceans continue to warm (IPCC, 2019), marine heatwaves could lead to future exceedances of optimal growth temperatures, affecting the response of phytoplankton cells to changes in abiotic parameters. In a multiple driver experiment manipulating temperature and turbidity, Remy *et al.* (2017) tested the effect of marine heatwaves on an assemblage of 18 marine phytoplankton species and found that the intensity of temperature increase played a large role in the phytoplankton response. While the community response in the moderate heatwave scenario was similar to that in the control group, the effect in the more severe treatment was markedly different, resulting in an overall loss of biomass and a sharp decline of diatom abundances in the phytoplankton community. Here, it is important to note that we tested the effects of a marine heatwave with an initial temperature of 15°C and a final temperature of 20°C, which are favorable to the growth of *P. tricornutum* (Goldman, 1977). Furthermore, in the study by (Remy et al., 2017), the addition of sediment coincided with an increase in nutrient concentrations, which mitigated the effects of heatwaves on community stability, while in our study, slight changes in dissolved N:P ratio did not result in significant differences except for respiration. This indicates that the intensity of heatwaves, as well as simultaneous changes in other parameters such as dissolved nutrient concentrations, play an important role. In this context, a study by Hayashida *et al.* (2020) recently found that the intensity of phytoplankton blooms during marine heatwaves is strongly dependent on the concentration of dissolved nutrients. Additionally, we have seen that changes in cellular traits often do not respond directly

to the increase in temperature but occur after an acclimation period at elevated temperature. Considering that marine heatwaves only last for a certain period before abiotic conditions return to their initial state, it could also be important how long marine heatwaves last and how much time the cells have to adapt to the conditions. In this context, cell size and lipid content of cells, in particular, may be crucial. Smaller cells, for example, have a shorter generation time and can adapt more quickly. However, these cells have lower storage capacities, for example, the storage of lipids, which can help the cells if the environmental conditions do not meet their requirements. Furthermore, changes in cellular traits, in turn, play an important role in ecosystem functioning. On the one hand, food quality for grazers may change, for example, due to changes in cellular carbon or lipid content, and on the other hand, shifts in phytoplankton community structure due to changes in growth rate and cell size may lead to a mismatch between primary production and consumers.

Our study shows that phytoplankton growing under current abiotic conditions might be able to cope with marine heatwaves without experiencing cellular stress. However, this also highlights the importance of mitigating global warming, as marine heatwaves at a higher average ocean temperature could lead to an exceedance of suitable growth conditions for marine phytoplankton. This stresses the importance of monitoring and regulating nutrient-rich runoff to the oceans, as lower dissolved nutrient concentrations may dampen the effects of higher temperatures.

Acknowledgments

We would like to thank Ursula Ecker and Julia Haafke for their technical assistance, as well as Kai-Uwe Ludwichowski and his team from Bremerhaven for measuring our samples for dissolved nutrients. We are also grateful to Gabriela Torres for her help and advice in the lab.

Supplementary material

Suppl. Table 4.1: Dissolved inorganic nitrogen (DIN) and phosphorus (DIP) in µmol L^{-1} in two temperature treatments (Ctrl, Heat) and two dissolved nutrient treatments (NP16, NP25). Samples were taken at three points (d0, d5, d10) before dilution of cultures. Data are means of four replicates.

		DIN in µmol L^{-1}			DIP in µmol L^{-1}		
		d0	d5	d10	d0	d5	d10
Control							
	NP16	76,9	76,4	80,7	6,2	6,1	6,2
	NP25	68,9	58,5	51,9	3,8	3,3	3,2
Heatwave							
	NP16	76,9	69,1	58,0	6,2	5,1	5,1
	NP25	68,9	76,1	71,8	3,8	3,2	3,4

Chapter 5

Extreme weather events: potential consequences of abrupt increases in river discharge on North Sea phytoplankton communities.

Elisabeth Groß[1*], Julien Di Pane[1], Maarten Boersma[1,2], Cédric L. Meunier[1,2]

[1] Alfred-Wegener-Institut Helmholtz-Zentrum für Polar- und Meeresforschung, Biologische Anstalt Helgoland, Helgoland, Germany

[2] University of Bremen, FB2, Bremen, Germany

Under review in Journal of Plankton Research

Abstract

Under global change, extreme weather events will become more frequent, and heavy precipitation leading to high river discharge will cause regular abrupt increases of nutrient-rich freshwater into coastal zones. We investigated the potential consequences of nutrient-rich freshwater pulses on phytoplankton communities from three stations in the North Sea with increasing distance from the coast. After incubation along a gradient of nutrient-rich freshwater additions, we analyzed changes in community diversity, average cell size, growth rate, and elemental stoichiometry. Phytoplankton communities from two of the three stations responded positively with increasing growth rates to pulses of nutrient-rich freshwater. Additionally, we observed a decrease in cell size within the taxonomic groups flagellates and diatoms at all stations, indicating positive selection in favor of smaller taxa and a decrease in molar N:P ratio of the phytoplankton communities. Overall, the response of phytoplankton communities to pulses of nutrient-rich freshwater was highly dependent on the initial community structure at each sampling site. Our study demonstrates that the biomass and functional structure of North Sea phytoplankton can be altered by extreme weather events, which could have further consequences for higher trophic levels and short-term food web dynamics in the North Sea.

5.1. Introduction

As primary producers, phytoplankton form the basis of most marine food webs and respond directly to environmental change due to their short generation time (Collins et al., 2014). Since different phytoplankton species have different preferences for environmental conditions, changes in environmental parameters are usually reflected in a restructuring of the community composition. This rearrangement of communities can be observed as natural phytoplankton succession following seasonal environmental change, in such parameters as temperature, irradiation, and dissolved macro-nutrients availability (Caracciolo *et al.*, 2021) or on longer time scales by anthropogenically-induced global change (Spilling *et al.*, 2018, Hare *et al.*, 2007). The frequency with which phytoplankton is exposed to variation in abiotic parameters strongly depends on their habitat. Whereas environmental conditions in the open ocean are rather stable, phytoplankton inhabiting coastal areas experience frequent fluctuations in, for example, temperature, dissolved nutrient concentrations, and salinity. This is particularly true for areas subjected to high river discharge, such as the southern North Sea, as they receive large inputs of nutrients and freshwater, both of which vary in intensity throughout the year and as a function of storm and precipitation events (Ducrotoy *et al.*, 2000).

The North Sea is bordered by several European countries and their large coastlines and is only connected to the Atlantic Ocean with a wide opening in the north and a smaller opening through the Dover Strait and the English Channel in the south-west as well as to the Baltic Sea in the east. As such, the coastal areas of especially the southern North Sea, are strongly influenced by river discharge. The annual freshwater input from rivers is strongly variable (Quante *et al.*, 2016, Prandle *et al.*, 1997). Within a climate change context, in addition to warming and elevated pCO_2, greenhouse gas emissions are also expected to increase the frequency and intensity of extreme weather events (Collins et al., 2013). Heavy precipitation events can cause abrupt increases in river discharge, which reduce the salinity and increase the dissolved nutrient concentrations of coastal zones, subsequently affecting biological communities potentially up to dozens of kilometers from the coast (Ducrotoy et al., 2000, Núñez-Riboni & Akimova, 2017, Voynova *et al.*, 2017).

When river discharge enters coastal areas, the local biota, including phytoplankton as primary producers, are directly subjected to pulses of nutrient-rich freshwater. Whereas an

increase in nutrients can boost phytoplankton growth (Pinckney *et al.*, 1999), changes in salinity can be detrimental to phytoplankton cells due to osmotic stress (Kirst, 1990). Previous studies of phytoplankton communities that used salinity as an abiotic stressor reported large changes in community structures. However, the effect of salinity changes on phytoplankton depends strongly on species identity and the tolerance ranges of these species (Flöder *et al.*, 2010). As expected, coastal phytoplankton species are more euryhaline than oceanic species (Brand, 1984, Balzano *et al.*, 2011), and the osmotic acclimation potential of algal species determines their tolerance to different salinities (D'ors *et al.*, 2016).

To understand how changes in environmental conditions can affect the functional structure of phytoplankton communities, trait-based approaches are a useful tool. Functional traits are morpho-physio-phenological characteristics of living organisms that influence growth, reproduction, and survival (Violle *et al.*, 2007). Explicitly-defined traits, such as cell size, can be used to understand and predict changes in community composition and, ultimately, ecosystem functioning (Litchman & Klausmeier, 2008, Weithoff & Beisner, 2019). Some traits of phytoplankton cells can be considered master traits since they regulate several physiological characteristics. Cell size, elemental stoichiometry, and growth rate, for example, are strongly linked (Litchman & Klausmeier, 2008). The elemental stoichiometry of phytoplankton, which is an important trophodynamic driver, is, for example, not only affected by the availability of dissolved nutrients but also varies among taxonomic groups (Geider & La Roche, 2002, Hillebrand et al., 2013, Sterner & Elser, 2002). Additionally, it has been shown that higher growth rates can lead to a more restricted and overall lower cellular N:P ratio (Hillebrand et al., 2013) as well as a decrease in cell size variability (Groß *et al.*, 2021). In natural environments, also nutrient acquisition strategies play an important role. Among the different strategies which have been proposed (Sommer 1984), velocity-adapted species, or *r*-strategists, are likely to benefit most from abrupt increases in nutrient availability as these species, which are often small, have high maximum nutrient uptake rates and high maximum growth rates (Litchman et al., 2007). Larger, affinity-adapted species, or *K*-strategists, on the other hand, are better equipped to effectively take up and assimilate growth-limiting nutrients at low concentrations. The effects of different nutrient acquisition strategies can be well observed looking at the origin of phytoplankton communities. Areas with high nutrient loads and fluctuations such as coastal areas are dominated by smaller cells due to their larger surface-to-volume ratio and high growth

rates. Overall, trait-based approaches allow to understand why some species are positively selected in response to environmental changes, and what the consequences for ecosystem functioning may be.

Several studies investigated the impact of changing nutrient loads on phytoplankton communities, but these focused mostly on eutrophication considering the average annual nutrient input into the oceans (Radach & Pätsch, 2007, Van Beusekom *et al.*, 2019). Fewer studies assessed the effects of abrupt increases in nutrient input (Weisse *et al.*, 2016) and changes in salinity (D'ors et al., 2016). Given the potential influence of abrupt river discharge on phytoplankton communities through sudden changes in salinity as well as dissolved nutrient concentrations, it is crucial to investigate how phytoplankton communities and their functional traits respond to these extreme events. Additionally, it is important to understand what role initial community structures play, especially in the context of the environmental conditions that are typical for the different areas (more variable in near-coastal areas).

In this study, we exposed natural phytoplankton communities sampled in early May from three different stations in the North Sea with increasing distance from shore to pulses of nutrient-rich freshwater of varying intensity. This allowed us to examine the influence of an abrupt high river discharge on community structure as well as properties such as growth rate, stoichiometric ratios, and cell size. Specifically, we tested the following hypotheses:

I. Nearshore phytoplankton communities will react to the pulse of nutrient-rich freshwater positively, indicated by higher growth rates, whereas offshore communities will react negatively to pulses of freshwater.
II. Pulses of nutrient-rich freshwater and higher growth rates will specifically benefit smaller, fast-growing species.
III. In coastal areas, higher growth rates will lead to a shift in the elemental stoichiometry of phytoplankton communities and a decreasing N:P ratio.

5.2. Materials and methods

Experimental Setup

To assess the potential impact of an abrupt increase in river discharge on coastal phytoplankton communities, we conducted an experiment testing three levels of decreased salinity and increased dissolved nutrient concentrations on natural phytoplankton communities from three stations in the southern North Sea. As response variables, we focused on growth rate of the community, shifts in community composition and size structure, as well as elemental stoichiometry.

The sampling and experiment were conducted on board the research vessel Pelagia of the Royal Netherlands Institute for Sea Research (NIOZ). Seawater containing natural phytoplankton communities was collected from three stations (st1: 53° 11.23' N, 4° 47.67' E; st2: 53° 39.88' N, 4° 03.07' E; st3: 54° 49.02' N, 3° 45.98' E) along a gradient from the Dutch coast to the open North Sea from 8th to10th May 2019 (Fig. 5.1). The water was sampled from 2 m depth by a rosette sampler equipped with CTD sensing (Sea-Bird SBE 9, Sea-Bird Electronics, Bellevue, Washington) and 24 12 L Niskin bottles. Twenty liters of water were sieved through a 200 µm mesh to exclude larger grazers and were subsequently sampled for initial dissolved nutrient concentrations, particulate organic carbon (POC), nitrogen (PON), and phosphorus (POP), as well as phytoplankton community composition. The remaining water was used to conduct the experiments. To test the influence of different intensities of pulses of nutrient-rich freshwater, simulating an abrupt increase in river discharge, we filled 910 mL cell culture flasks (Falcon) to 10, 20, and 30 % in triplicate with freshwater medium and topped up the flasks with sieved seawater containing natural phytoplankton communities for the trt10, trt20, and trt30 treatments, respectively. The medium was prepared according to f/2 medium (Guillard & Ryther, 1962), including silicate (SiO4-), using MilliQ water. Salinity decreased by about 3-8 salinity units from the lowest to the most severe treatment (Table 5.1). Similar salinity changes after flood events with high river discharges have been observed in the southern North Sea (Voynova et al., 2017). The fourth group of bottles was filled with sieved seawater only and served as a control group. This experiment resulted in 3 (regions) x 4 (treatments) x 3 replicates, for a total of 36 experimental flasks. Nutrient concentrations for each treatment can

be found in Table 1. Increasing treatment intensity caused an increase in osmotic stress due to greater salinity changes but at the same time delivered larger amounts of dissolved inorganic nutrients for phytoplankton growth. The flasks were incubated on board for 72-hours with simulated natural light under a 16:8 day:night cycle, which is approximately the day:night duration on Texel, Netherlands at the beginning of May, and irradiance of 90 µmol photons m^{-2} s^{-1} (GHL Mitras Lightbar 2 Daylight, 6500 K, dimmed to 80 %) in a temperature-constant container at 10 °C, simulating the mean water temperature at the three stations. All cell culture flasks were carefully homogenized manually several times a day to prevent sedimentation of phytoplankton cells.

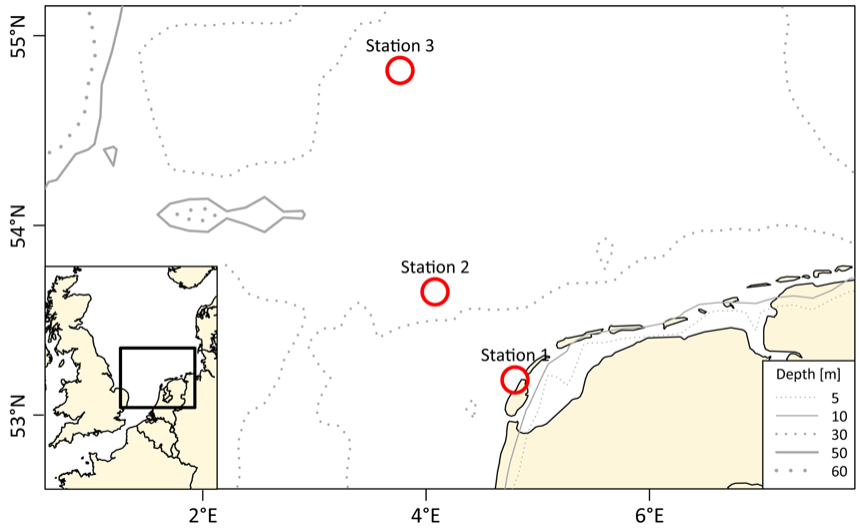

Figure 5.1: Location of the transect with the three sampling stations in the North Sea. Samples were taken from 8th to 10th May at the stations with the coordinates: st1: 53° 11.23' N, 4° 47.67' E; st2: 53° 39.88' N, 4° 03.07' E; st3: 54° 27.42' N, 3° 13.90'

N), phosphorus (DIP), and silicate (DSi) in µmol L^{-1} before and after 72-hour incubation with
t three stations. Total nitrogen (TN, DIN + particulate organic nitrogen (PON)) and total
phosphorus (POP)) in µmol L^{-1} at each station before and after 72-hours of experimental
ed with a '*' describe values above the calibration curve. Data are means of three replicates

		Initial				Final					
		DIN µmol L^{-1}	DIP µmol L^{-1}	DSi µmol L^{-1}	DIN µmol L^{-1}	DIP µmol L^{-1}	DSi µmol L^{-1}	TN µmol L^{-1}	TP µmol L^{-1}	TN µmol L^{-1}	TP µmol L^{-1}	Salinity
Station 1												
	ctrl	3.6	0.9	4.4	4.8	0.7	4.2	19.9	1.3	11.3	1.0	31.5
	trt10	77.8	2.4	6.4	75.3	2.1	6.0			87.8	2.8	28.7
	trt20	104.0*	3.9	8.6	99.3*	3.3	7.4			111.4*	3.9	26.2
	trt30	111.1*	4.7	9.5	110.7*	5.0	10.6			119.4*	5.6	24.3
Station 2												
	ctrl	3.2	0.9	1.8	3.2	0.7	1.1	5.9	1.1	7.7	0.8	31.6
	trt10	72.9	2.0	4.3	75.6	2.1	4.1			81.8	2.5	28.3
	trt20	104.9*	3.9	7.6	102.3*	3.6	6.6			107.7*	4.0	26.4
	trt30	115.1*	5.6	10.3	109.0*	4.7	8.8			113.3*	5.1	24.2
Station 3												
	ctrl	3.4	0.8	0.6	2.9	0.6	0.5	5.9	0.9	7.3	0.8	34.5
	trt10	78.3	2.3	4.3	76.4	2.2	4.2			86.3	2.8	31.4
	trt20	99.3*	3.3	5.8	98.5*	3.4	5.8			108.2*	4.0	28.6
	trt30	110.9*	5.1	8.9	110.4*	5.0	9.0			116.7*	5.6	26.3

Growth rate

To calculate the growth rate of phytoplankton communities, we used POC, representing the biomass in µg L^{-1}. Final POC samples were taken from each cell culture flask. To avoid using a large volume of each flask at the start of the experiment, we used one set of replicates with only sieved seawater as the initial sample. Considering that the sampled communities were diluted by 10, 20, and 30 % depending on the treatment before the experiment, the initial POC content was multiplied by 0.9, 0.8, and 0.7, respectively, before calculating the growth rate µ (d^{-1}) using following equation:

$$\mu = \ln(N_t/N_0) \cdot \Delta t^{-1}$$

whereby N_0 and N_t describe initial and final POC (µg C L^{-1}) and Δt (Day) is 3 in this case since the experiment ended after 72 hours.

Additionally, we calculated the absolute change in growth rate relative to the control from each treatment.

Community analysis

Initial and final samples for phytoplankton community composition were obtained by fixing 200 mL of water from the incubation flasks with acidic Lugol's iodine solution (final concentration 0.5 %). Phytoplankton cells were counted using the Utermöhl method (Utermöhl, 1958) and identified to genus or species level when possible, or otherwise grouped into size-dependent groups or 'morphotypes'. To assess changes in community composition when exposed to our treatments, we used the most abundant taxa having a cumulative abundance of up to 95%. This was done for clarity and to avoid focusing on a large number of taxa that make up only a small percentage of the frequently occurring taxa. The biovolume of each taxonomic unit was calculated using cell dimensions and geometric formulas (Hillebrand *et al.*, 1999) and used to assess changes in size structure of the phytoplankton communities. We used the entire community to calculate the community-weighted mean (CMW) cell volume.

Particulate and dissolved nutrient analyses

To assess the impact of the treatments on the elemental stoichiometry of phytoplankton communities, samples of 200 mL were filtered at the onset and the end of the incubation period on pre-combusted and pre-washed GF/F glass microfiber filters (Whatman, 25 mm, pore size 0.7 µm). All filters were stored individually in Eppendorf tubes at -20 °C. For POC and PON analyses, filters were dried for at least 48 h at 60 °C in a drying chamber before being wrapped in tin foil and analyzed with an elemental analyzer (Elementar vario MICRO cube). Particulate P was measured by spectrometric determination (Thermo Scientific Multiskan Spectrum) of orthophosphate (Grasshoff *et al.*, 1999). Dissolved inorganic nitrogen (DIN), phosphorus (DIP), and silicate (DSi) were measured at the beginning of the experiment and after the 72-hour incubation period to evaluate nutrient changes in our treatments. A volume of 50 mL was filtered through nylon membrane filters (Merck, 47 mm, pore size 0.2 µm) and stored at -20 °C. The samples were measured with an autoanalyzer (Alliance Instruments GmbH) after a modified method after Grasshoff (Seal/Alliance methods; (Grasshoff et al., 1999).

Data analysis

The software R (R Core Team, 2013) was used for all statistical analyses and to draw the figures. For the community analyses, we used the most abundant taxa having a cumulative abundance of up to 95%. This threshold was chosen according to a compromise between representativeness and clarity of the graphic representation. Differences in CMW cell volume, growth rate, and elemental stoichiometry between the treatments and stations were tested using two-way analyses of variance (ANOVA) and Tukey's *post-hoc* comparison. For all statistical comparisons, normality (Shapiro) and variance homogeneity (Levene) tests were performed. Data were transformed (square root) if criteria of normal distribution or variance homogeneity were not met. The threshold of significance was set at 5% for all analyses.

5.3. Results

To investigate the potential effect of an abrupt increase in river discharge, we subjected phytoplankton communities from three stations in the North Sea with increasing distance from the coast to pulses of nutrient-rich freshwater.

Growth rate

The growth rates at station 1 varied between -0.29 ± 0.053 and -0.10 ± 0.020 d^{-1}, station 2 values ranged from 0.10 ± 0.059 to 0.14 ± 0.032 d^{-1}, and station 3 from 0.18 ± 0.006 to 0.40 ± 0.070 d^{-1} (Fig. 5.2). A two-way ANOVA revealed significant differences between stations and treatments as well as a statistically significant interaction between the effects of station and treatment (Table 5.2). Overall, the treatments had a positive effect on the growth rate of phytoplankton communities compared to the control (Tukey's post-hoc test, $p_{trt10} \leq 0.001$, $p_{trt20} \leq 0.001$, $p_{trt30} = 0.0036$). Additionally, growth rates in treatments trt10 and trt20 were significantly higher than growth rates in trt30 (Tukey's post-hoc test, $p_{trt10} = 0.027$, $p_{trt20} = 0.017$). Within station 2, we did not observe significant differences between the treatments (Tukey's post-hoc test, $p \geq 0.99$). Within station 1 and station 3, however, the pulse of nutrient-rich freshwater in treatments trt10 and trt20 led to a significant increase in growth rates (Tukey's post-hoc test, $p \leq 0.0041$). No significant differences were found between the most severe treatment trt30 and the control at station 1 and station 3 (Tukey's post-hoc test, $p \geq 0.098$).

Table 5.2: Two-way analysis of variance, with growth rate (day^{-1}) of phytoplankton communities as dependent variable and station and treatment as independent variables. Significant differences ($p<0.05$) are highlighted in bold.

Effect	df_1, df_2	*F*	*p*
Growth rate			
Station	2, 24	380.39	**<0.001*** **
Treatment	3, 24	22.36	**<0.001*** **
Station x treatment	6, 24	3.47	**0.013***

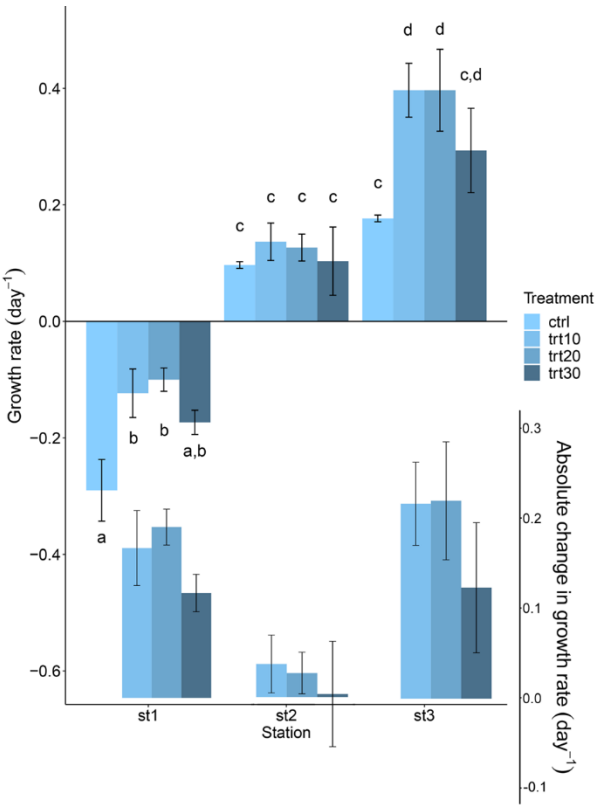

Figure 5.2: Influence of nutrient-rich freshwater pulses (10, 20, and 30 %) on the growth rate and the absolute change in growth rate relative to the control of phytoplankton communities (below) at three stations over a 72-hour incubation. Data presented are means and standard deviations of three replicates. Different letters above bars indicate significant differences (two-way ANOVA, Tukey post-hoc test, $p < 0.05$).

Taxonomic structure and cell size

We analyzed the relative abundance of the phytoplankton taxa between stations. The initial communities sampled at three stations in the North Sea in early May were dominated by flagellates (Fig 5.3). At station 1, closest to the coast, flagellates between 3 and 7 µm contributed 74.6 % of the relative abundance of cells in the community, with 42.5 % being flagellates of 3 µm cell size. In addition, *Phaeocystis globosa* and the diatom species *Pseudo-nitzschia delicatissima* contributed 9 % each to the phytoplankton community at station 1. At station 2, only flagellates of 3 µm cell size and *Phaeocystis globosa* contributed to 95% of the relative abundance of the community with 68.3 and 23.0%, respectively. The initial community at station 3 was also dominated by flagellates between 3 and 7 µm cell size with 82.8 %, whereas 3 µm cells contributed with 76.9 %. Several *Chaetoceros* species built up 8.6 % of the

relative abundance of the community and *Pseudo-nitzschia delicatissima* contributed with 4.3 %.

After the 72-hour incubation, a shift in community structure was observed at all stations, with the most pronounced changes occurring at station 1 and station 3 (Fig. 5.4). Comparing the control from station 1 after three days of incubation with the initial sample, the diatom species *Pseudo-nitzschia delicatissima* was much more abundant after the incubation with the addition of nutrient-rich freshwater, forming 62.8 % of the relative abundance of cells in the phytoplankton community with 52.2 % smaller cells of 40-60 µm and 10.6 % cells of 60-80 µm cell size. Also, cells of the diatom species *Chaetoceros socialis* contributed to 4.9 % of the community. The strong shift in community composition was caused by a simultaneous decrease in flagellates and an increase in *Pseudo-nitzschia delicatissima* (suppl. Fig. 5.1). However, as treatment intensity increased, the relative abundance of diatoms decreased from 67.7% in the control group to 32.4% in the most severe treatment trt30 due to a large increase in flagellates, including *Phaeocystis globosa*. Within the group of flagellates as well as for *Pseudo-nitzschia delicatissima*, we observed a shift towards smaller size. At station 2, we observed a similar pattern in terms of cell size change in response to treatment intensity. While 33.6% of the relative abundance of cells in the community was formed by 3 µm flagellates and 53.1% by 5 µm flagellates in the control, flagellates of 3 µm size increased with treatment intensity (suppl. Fig. 5.2) and built 95% of the cumulative abundance of the phytoplankton community in treatments trt20 and trt30. At station 3, the pulse of nutrient-rich freshwater led to an increase in the relative abundance of diatom species from 14.8 in the control to 36.3 % in trt20. The group of diatoms included *Pseudo-nitzschia delicatissima* of different cell sizes as well as several *Chaetoceros* species. Although the relative abundance of flagellates decreased with treatment intensity, it was almost exclusively flagellates of larger size and the relative abundance of 3 µm flagellates was not strongly affected (suppl. Fig. 5.3). The community structure in the most severe treatment was similar to the control, except with a greater relative abundance of flagellates with 3 µm cell size.

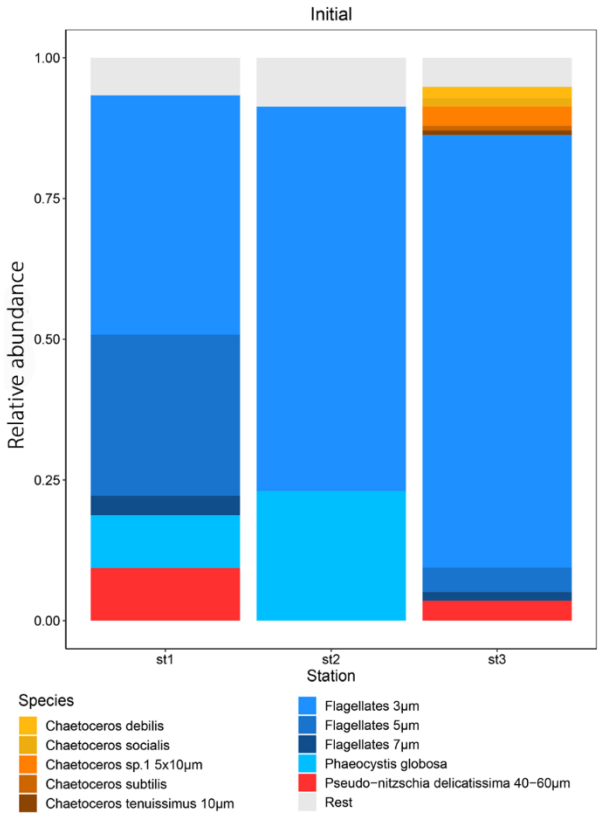

Figure 5.3: Relative abundances of the most abundant taxa at the three stations before incubation with nutrient-rich freshwater. Only taxa accounting for 95% of the cumulative abundance within the initial phytoplankton community composition were represented for the sake of clarity.

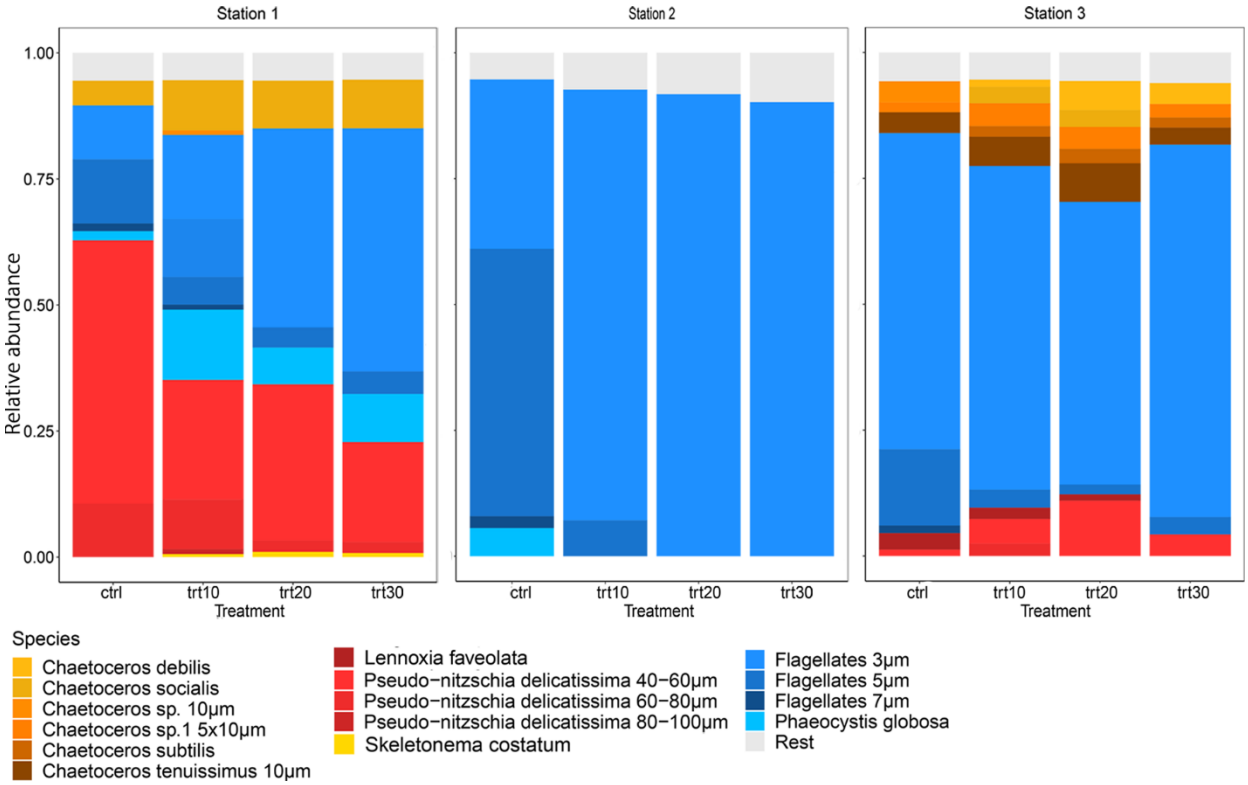

Figure 5.4: Influence of nutrient-rich freshwater pulses (10, 20, and 30%) on the phytoplankton community composition at three stations after a 72-hour incubation. Taxa shown are the most abundant contributing to 95 % of the communities.

In addition to the taxonomic structure, we assessed the CMW cell volume to investigate potential shifts. Contrary to what the relative abundance would suggest, in the initial samples, before we incubated the communities with nutrient-rich freshwater, we observed the lowest average cell volume at station 1, closest to the coast, and the highest at station 3, the most offshore station (Fig. 5.5). However, the CWM cell volume at station 1 and station 2 changed drastically after the 72-hour incubation with nutrient-rich freshwater. At station 1, the CMW cell volume increased from initially about 290 μm^3 to about 1470 μm^3 in the control and 590 μm^3 in trt30 (Fig. 5.6), suggesting a positive selection of larger cells. At station 2, the CWM cell volume decreased from initially about 510 μm^3 to about 200 μm^3 in the control and 50 μm^3 in trt30. At station 3, we observed an overall decrease in CWM cell volume from initially about 830 μm^3 to about 350 μm^3 in the control and 510 μm^3 in trt10. Only in trt20, the CMW cell volume remained about the same at 900 μm^3. Nevertheless, after incubation, changes in relative abundance are well represented by the changes in CWM cell volume of the phytoplankton communities.

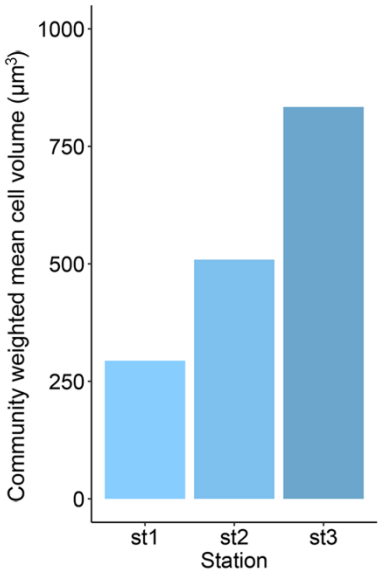

Figure 5.5: Community weighted mean cell volume (µm³) of phytoplankton communities at the three stations before incubation with nutrient-rich freshwater.

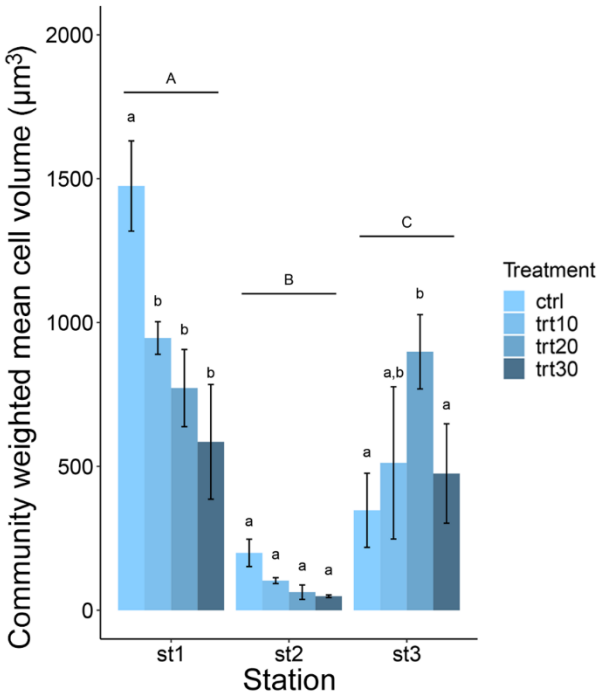

Figure 5.6: Influence of nutrient-rich freshwater pulses (10, 20, and 30%) on the community weighted mean cell volume (µm³) of phytoplankton communities at three stations after a 72-hour incubation. Data presented are means and standard deviations of three replicates. Different letters above bars indicate significant differences (two-way ANOVA, Tukey post-hoc test, $p < 0.05$). Capital letters (A, B, C) indicate significant differences between stations, and small letters (a, b) indicate significant difference

between treatments within one station. Significant differences in interactions between station and treatment can be found as Suppl. Table 1.

Elemental stoichiometry

In the last step, we tested the effect of pulses of nutrient-rich freshwater on the elemental stoichiometry of phytoplankton communities. We measured POC, PON, and POP (Suppl. Fig. 5.4) and calculated the molar ratios of C:N, C:P, and N:P for initial samples (Fig. 5.7) and after 72-hour incubations (Fig. 5.8). Additionally, we used the Redfield ratio (C:N:P = 106:16:1) and ranges of molar ratios reported by Geider and La Roche (2002) to assess possible nutrient limitations. Under optimal nutrient-replete conditions, values of cellular N:P range from 5 to 19, values of cellular C:N range from 3 to 17, and values of cellular C:P range from 27 to 135.

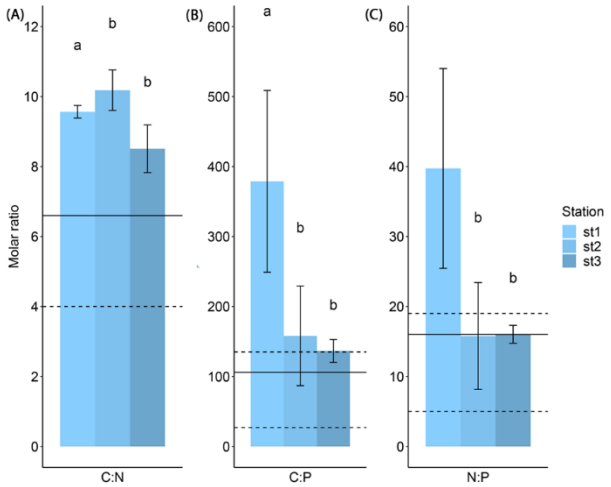

Figure 5.7: Molar C:N (A), C:P (B), and N:P (C) ratios of initial community samples from three stations. Data presented are means and standard deviations of three replicates. Horizontal lines represent the Redfield ratio of C:N:P = 106:16:1. The area between dashed lines represent C:N, C:P, and N:P ratios of phytoplankton growing under optimal nutrient-replete conditions (Geider & La Roche, 2002). In (A), the upper limit is C:N = 17. Different letters above bars indicate significant differences (two-way ANOVA, $p < 0.05$).

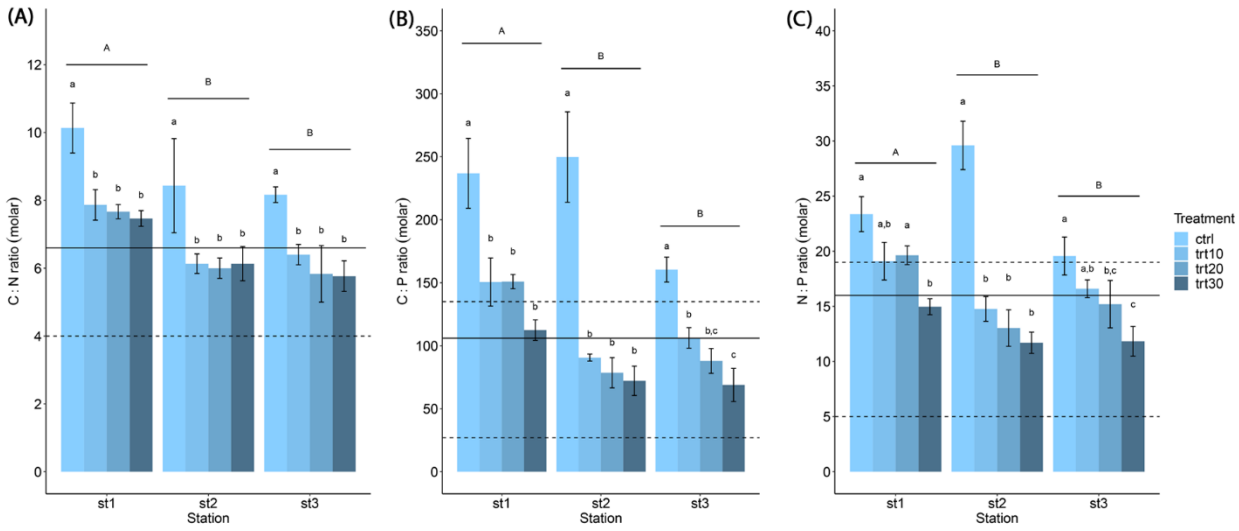

Figure 5.8: Influence of nutrient-rich freshwater pulses (10, 20, and 30%) on the molar C:N (A), C:P (B), and N:P (C) ratios of phytoplankton communities at three stations after a 72-hour incubation. Data presented are means and standard deviations of three replicates. Solid lines represent the Redfield ratio of C:N:P = 106:16:1. Areas below and above dashed lines represent C:N:P ratios indicative of nitrogen and phosphorus limited conditions for phytoplankton (Geider & La Roche, 2002). Different letters above bars indicate significant differences (two-way ANOVA, Tukey post-hoc test, $p < 0.05$). Capital letters (A, B) indicate significant differences between stations, and small letters (a, b) indicate significant difference between treatments within one station. Significant differences in interactions between station and treatment can be found as Suppl. Table 2.

Overall, the pulses of nutrient-rich freshwater led to a decrease in C:N, C:P, and N:P ratio of phytoplankton communities at all stations, with significant differences between the stations and treatments as well as their interaction (two-way ANOVA, Table 5.3). The molar C:N ratio of the phytoplankton communities ranged between 10.1 ± 0.7 in the control at station 1 and 5.8 ± 0.5 in trt30 at station 3 and therefore did not indicate an N-limitation. At all stations, the molar C:N ratio in the treatments with nutrient-rich freshwater was significantly lower than in the controls (Tukey's post-hoc test, $p \leq 0.05$). However, we did not observe a significant difference between the treatments trt10, trt20, and trt30 (Tukey's post-hoc test, $p \geq 0.124$). For both the molar C:P ratio and the molar N:P ratio of the communities, the controls exceeded the ratio of 135 mol C:mol P and 19 mol N:mol P at all stations, indicating P-limitation. The molar C:P ratio in the controls ranged between 249.7 ± 35.9 at station 2 and 160.4 ± 9.9 at station 3. The molar N:P ratio in the controls ranged between 29.6 ± 2.2 at station 2 and 19.6 ± 1.7 at station 3. From control to treatment trt10, a significant decrease in molar C:P was observed at all stations (Tukey's post-hoc test, $p \leq 0.046$). At station 1 and

station 2, no significant differences were observed between treatments trt10, trt20, and trt30 (Tukey's post-hoc test, $p \geq 0.163$). Only at station 3 the molar C:P ratio in trt30 was significantly lower than in trt10 (Tukey's post-hoc test, $p = 0.006$). For the molar N:P ratio, only at station 2 the control was significantly higher than the molar N:P ratio in trt10 (Tukey's post-hoc test, $p \leq 0.001$). At all stations, the molar N:P ratio in the most severe treatment trt30 was significantly lower than the controls (Tukey's post-hoc test, $p \leq 0.001$).

Table 5.3: Two-way analysis of variance, with the molar ratios (C:N, C:P, N:P) of phytoplankton communities as dependent variable, and station and treatment as independent variables. Significant differences ($p<0.05$) are highlighted in bold.

Effect	**df_1, df_2**	***F***	***p***
C:N ratio			
Station	2, 24	31.96	**<0.001*** **
Treatment	3, 24	35.10	**<0.001*** **
Station x treatment	6, 24	0.22	0.97
C:P ratio			
Station	2, 24	49.05	**<0.001*** **
Treatment	3, 24	103.99	**<0.001*** **
Station x treatment	6, 24	6.16	**<0.001*** **
N:P ratio			
Station	2, 24	17.55	**<0.001*** **
Treatment	3, 24	55.34	**<0.001*** **
Station x treatment	6, 24	5.73	**<0.001*** **

5.4. Discussion

In this study, we investigated the potential effect of an abrupt increase in river discharge on North Sea phytoplankton communities by exposing them to pulses of nutrient-rich freshwater using a trait-based approach. To assess how initial community structures affect the reaction to abrupt changes in environmental conditions, we tested the influence of pulses of nutrient-rich freshwater of varying intensity on three different phytoplankton communities

sampled with increasing distance from the coast and analyzed community structure and size distribution, growth rate, as well as the elemental stoichiometry of phytoplankton communities.

Overall, the addition of nutrient-rich freshwater had a positive effect on phytoplankton growth, but initial community structure played a large role in phytoplankton community response. We hypothesized that nearshore phytoplankton communities would respond positively to the pulses of nutrient-rich freshwater, as indicated by higher growth rates, whereas offshore communities respond negatively to pulses of nutrient-rich freshwater, which our results do not confirm. Representative of the high productivity of coastal waters (Cloern *et al.*, 2014), we observed about six times higher initial biomass at station 1, which is closest to the coast, compared to the other two stations (Suppl. Fig. 4), as well as the highest amount of total nitrogen and phosphorus (Table 1). However, although the nearshore and most offshore stations showed a large difference in initial biomass, we observed a positive response to pulses of nutrient-rich freshwater at both stations, resulting in higher growth rates in the least severe and intermediate treatments. In contrast, the second station showed no change in growth rate regardless of treatment. At the same time, for station 1 and station 3, we observed that both flagellates and diatoms contributed to 95% of the relative abundance, while at station 2, 95% of the phytoplankton community consisted of flagellates. This may also indicate that initial diversity plays an important role for phytoplankton communities when facing extreme weather events such as an abrupt increase in nutrient-rich freshwater, which supports the diversity-stability hypothesis (MacArthur, 1955, Otero *et al.*, 2020, Corcoran & Boeing, 2012).

In terms of initial community structure at station 1, flagellates comprise by far the most abundant taxa. The relatively high nutrient loads in coastal areas generally select for smaller, velocity-adapted species (Litchman et al., 2009), as we could also observe for the initial sample at station 1. Under the absence of fresh nutrients, larger, affinity-adapted species with storage capacities succeed (Litchman & Klausmeier, 2008). We could observe these dynamics in the control group of station 1 where the absolute and relative abundance of flagellates decreased within the 72-hour incubation, and the abundance of diatoms, especially the species *Pseudo-nitzschia delicatissima*, increased. This increase in diatoms was also likely the cause for the increase in CWM cell volume of the phytoplankton communities after incubation compared to before. In contrast, exposure to pulses of nutrient-rich freshwater caused an increase in the

abundance of flagellates at station 1, and within the flagellate group, a shift towards smaller size classes. These results support the concept that small, fast-growing taxa generally benefit most from abrupt increases in dissolved nutrient concentrations as they have high maximum nutrient uptake rates and high maximum growth rates (Litchman & Klausmeier, 2008, Sommer, 1984).

At station 2, the phytoplankton community was dominated by unicellular flagellates between 3 and 7 µm, as well as the species *Phaeocystis globosa*. Although no significant changes in biomass were observed between treatments at station 2, located about 70 km away from the coastal station, we also observed for this station a strong increase in small flagellates in response to pulses of nutrient-rich freshwater. In addition, the decline in CWM cell volume after incubation was likely due to the loss of the diatom species *Rhizosolenia imbricata*, which occurred at a very low absolute abundance of about 0.6% in the initial sample, but had a substantial influence on CWM cell volume due to its large size. We hypothesize that the overall lower biomass and diversity of phytoplankton communities at this offshore station in comparison to the coastal station 1 is related to the greater distance from the coast, and hence lower nutrient availability (Table 1), which has been observed previously in other North Sea studies (Stelfox-Widdicombe *et al.*, 2004, Burson et al., 2016).

At station 3, located close to the Dogger Bank and with the greatest distance from the coast, the pulses of nutrient-rich freshwater increased diatom abundances, both that of small diatoms of the genus *Chaetoceros* and larger diatoms of the species *Pseudo-nitzschia delicatissima*. This increase in diatoms, combined with the low dissolved Si concentrations we measured at station 3, as well as the increase in phytoplankton growth rate after the pulses of nutrient-rich freshwater, indicate that phytoplankton growth was likely Si-limited. Contrary to our expectations, the initial biomass at station 3 was not higher than the biomass at station 2, although the Dogger Bank region is known for high year-round primary production (Kröncke & Knust, 1995). However, nutrient upwelling in the Dogger Bank area and associated fluctuations in nutrient availability may have been the cause of the coexistence of taxa with smaller and larger cell sizes and their respective strategies for nutrient acquisition, as we observed for the initial community structure at station 3. Since only intermediate intensities of nutrient-rich freshwater pulses promoted phytoplankton growth, and especially that of

flagellates and diatoms, we hypothesize that these organisms benefit from the addition of nutrients but were not negatively affected by an enhanced drop in salinity in the least severe and intermediate treatment.

Our results suggest that the effects of extreme weather events and related river input on marine phytoplankton communities depend largely on initial community structure. While increases in dissolved nutrients enhanced primary production overall and significantly at two of three stations, phytoplankton taxa did not seem to suffer from changes in salinity, as growth rates in the treatments were higher or similar to those in the control. Also, Shikata *et al.* (2008), who investigated rapid changes in salinity on growth of diatoms and flagellates isolated from the field, did not observe changes in growth between 15 and 32. Although we found no difference between the control and the most severe treatment in terms of growth rate, suggesting no strong negative effects, it appears that phytoplankton do not benefit from nutrient additions when a more drastic decrease in salinity accompanies these. Additionally, we observed at all stations a decrease in cell size for flagellates as well as for diatoms, which supports our second hypothesis that pulses of nutrient-rich freshwater favor smaller, fast-growing species (Sommer, 1984). Former studies on the impact of increased river discharge mainly focused on the input of nutrients and terrestrial matter, which can potentially lead to light limitation. Deininger *et al.* (2016) observed an increase in biomass after adding soil and connecting nutrients to natural phytoplankton communities in a mesocosm experiment with diatom abundance increasing immediately after the addition of soil followed by an increase in dinoflagellates a few days later. Although in the study of Deininger et al. (2016), no negative effect of the browning of water was observed, Frigstad *et al.* (2020) stress the importance of light limitation as high river discharge is also connected to an input of terrestrial matter. Our study suggests that especially small flagellates of 3 µm cell size benefit from the addition of nutrient-rich freshwater. Taking potential light limitation into account, small cells could not only have an advantage over larger cells when subjected to pulses of nutrient-rich freshwater but also under light limitation since they are less affected by low light availability in comparison to larger cells (Litchman et al., 2010).

While phytoplankton growing at steady-state conditions in the laboratory can achieve a constant cellular C:N:P ratio, this is nearly impossible in the ocean due to short- and long-term

changes in abiotic conditions (Moore *et al.*, 2013). In our study, we hypothesized that the elemental stoichiometry of the phytoplankton community near the coast would shift and that the N:P ratio would decrease because pulses of nutrient-rich freshwater would promote phytoplankton growth rates, which leads to a more restricted and overall lower cellular N:P ratio (Hillebrand et al., 2013). The particulate N:P ratio of the phytoplankton community at station 1, closest to the coast, indicated a strong P limitation, which was also reported by Burson et al. (2016), and no strong nutrient limitation at stations 2 and 3. The particulate molar N:P ratio has widely been used to estimate whether phytoplankton growth is likely N- or P-limited (Tyrrell, 1999, Lenton & Watson, 2000). Although the Redfield ratio of N:P = 16 is sometimes referred to as the optimal growth molar ratio (Goldman *et al.*, 1979), it should be rather seen as the average stoichiometry of phytoplankton, weighted by the relative abundance of species with different N:P ratios (Klausmeier *et al.*, 2004). While Geider and La Roche (2002) reviewed that the values of cellular N:P ratios for phytoplankton growing under nutrient-replete conditions have a certain degree of variation, with N:P values under nutrient-replete conditions actually being below the Redfield ratio of 16, Hillebrand et al. (2013) indicated that variation in N:P decreases with increasing growth rate, and converge towards 16. In support of our hypothesis that pulses of nutrient-rich freshwater may alleviate nutrient limitation, we observed that our treatments resulted in decreased cellular C:N, C:P, and N:P ratios, which converged towards values in a range that was reported for non-limited growth conditions (Geider & La Roche, 2002). Similar to cell size, elemental stoichiometry of phytoplankton can also be considered a master trait, as it links environmental conditions to growth rates and food web interactions (Finkel et al., 2010). The C:N:P signature of phytoplankton cells is an important determinant of their nutritional quality for higher trophic levels. Consequently, by substantially and rapidly modifying the elemental stoichiometry of phytoplankton communities, abrupt nutrient-rich freshwater inputs may have important short-term effects on food web processes.

5.5. Conclusion

In this study, we investigated the possible effects of abrupt river discharge by subjecting natural phytoplankton communities from the North Sea to pulses of nutrient-rich freshwater. We found that initial community composition plays an important role in response to abrupt changes in dissolved nutrient concentration and salinity. The more diverse communities near

the coast and the Dogger Bank responded with an increase in biomass following pulses of nutrient-rich freshwater, while the community sampled between these stations was less affected in terms of community growth rate. At the same time, we did not observe any strongly negative impact of decreasing salinity, indicating a large salinity tolerance of North Sea phytoplankton communities, even though it appears that while phytoplankton benefit from nutrient additions, this is no longer the case when accompanied by a more drastic decrease in salinity. Furthermore, we demonstrate that pulses of nutrient-rich freshwater can lead to an overall decrease in cell size and an increasing abundance of small-celled flagellates. Together with the observed shifts in the elemental stoichiometry of phytoplankton, changes in community structure and cell size associated with extreme weather events could modulate short-term responses in higher trophic levels as they are exposed to sudden changes in their food sources.

Acknowledgments

This study was only possible due to the cooperation with the Royal Netherlands Institute for Sea Research (NIOZ). We would like to thank Herman Hummel, Jacco Kromkamp, and all NIOZ staff involved for the great organization of the cruise. The passing of Jacco Kromkamp has touched us deeply. We would also like to thank the entire crew of the *RV Pelagia* for ensuring a safe cruise and making this study possible. We thank Julia Haafke and Heike Rickels for the technical assistance.

Supplementary material

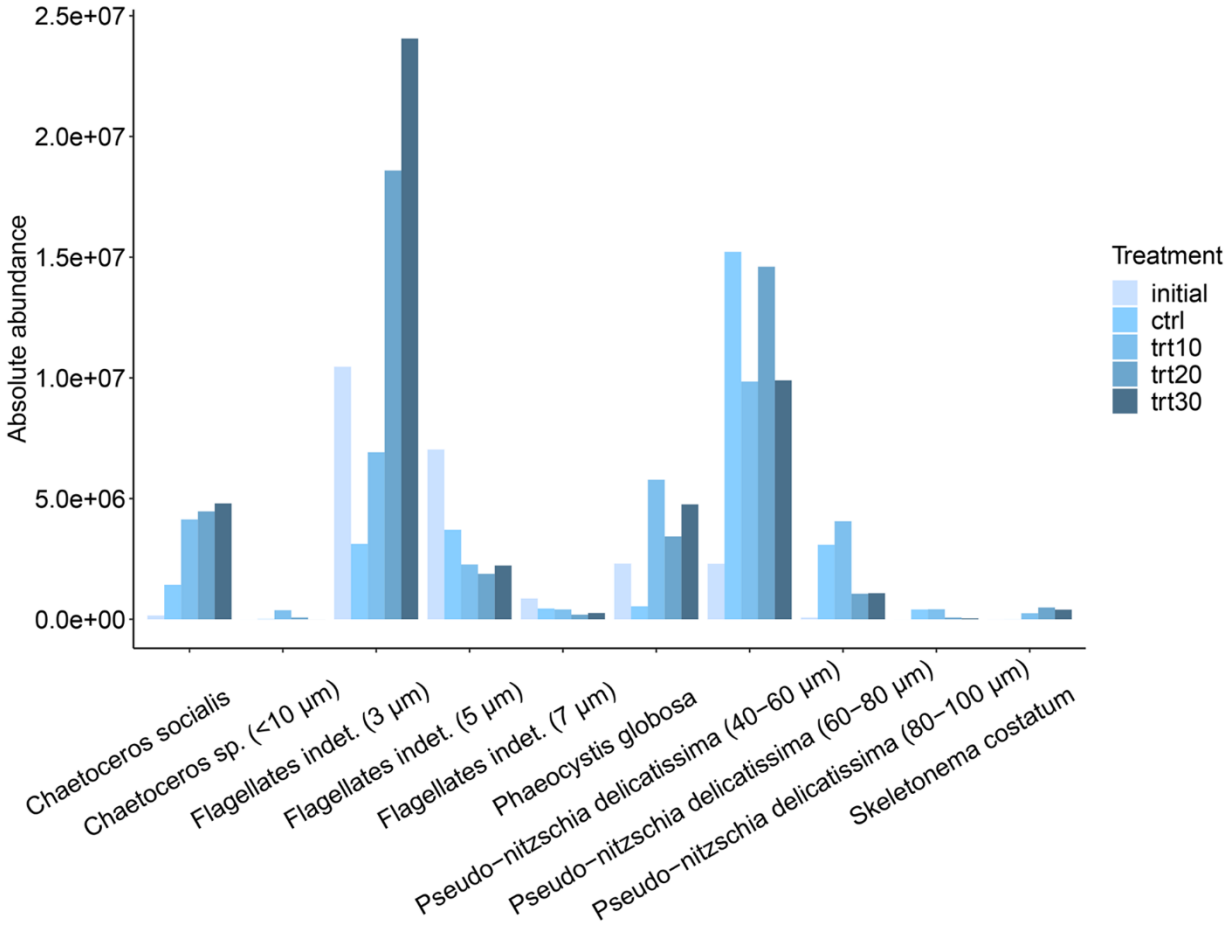

Suppl. Figure 5.1: Absolute abundances of the most abundant taxa at station 1 before and after a 72-hour incubation with nutrient-rich freshwater pulses (10, 20, and 30%). Taxa shown are the most abundant contributing to 95 % of the community at station 1.

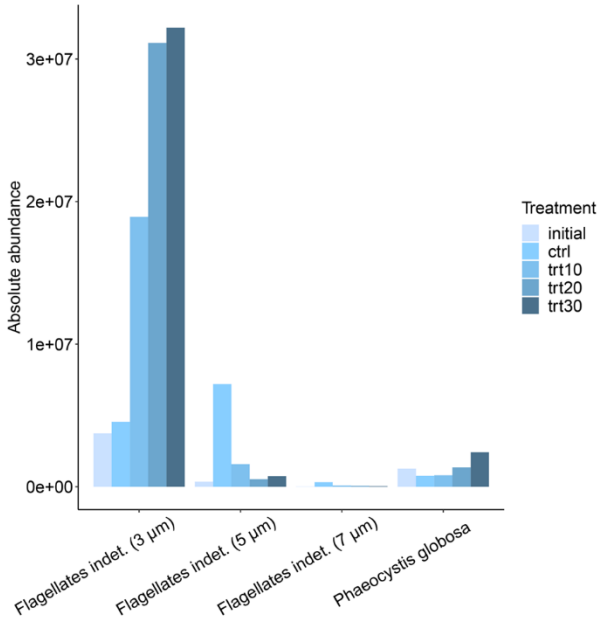

Suppl. Figure 5.2: Absolute abundances of the most abundant taxa at station 2 before and after a 72-hour incubation with nutrient-rich freshwater pulses (10, 20, and 30%). Taxa shown are the most abundant contributing to 95 % of the community at station 2.

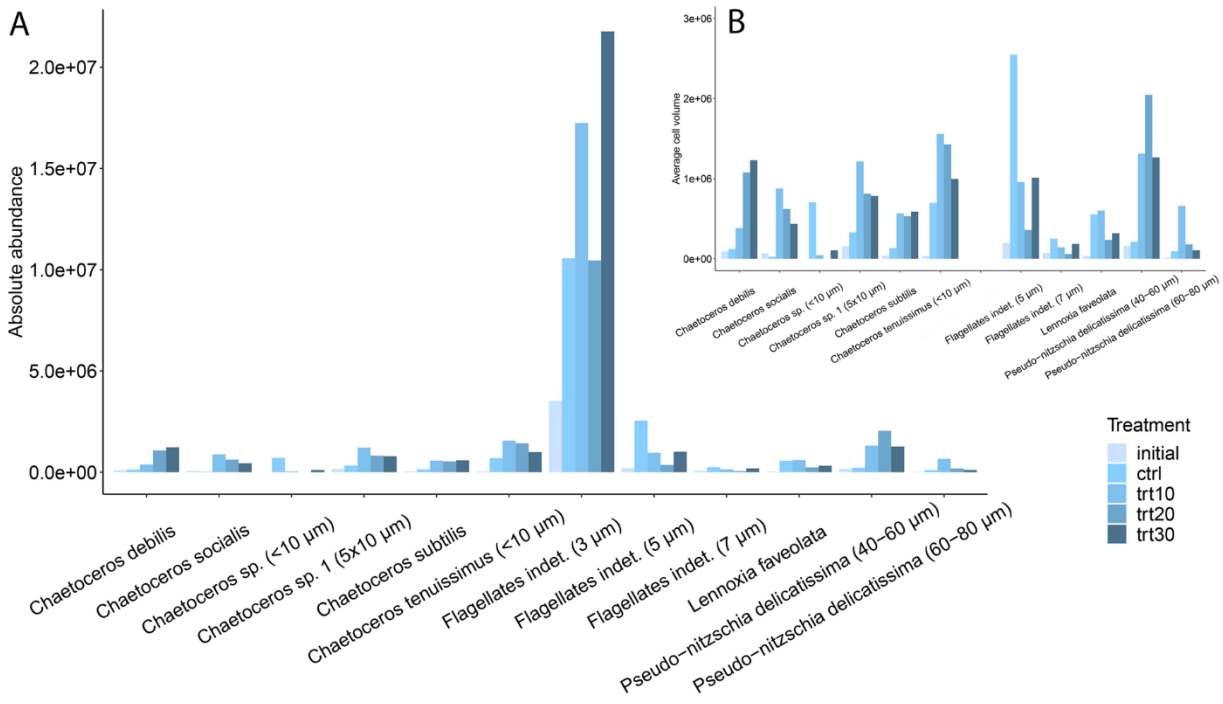

Suppl. Figure 5.3: Absolute abundances of the most abundant taxa at station 3 before and after a 72-hour incubation with nutrient-rich freshwater pulses (10, 20, and 30%). Taxa shown are the most abundant contributing to 95 % of the community at station 3 (A) and the most abundant contributing to 95 % of the community at station 3 without 3 µm flagellates (B).

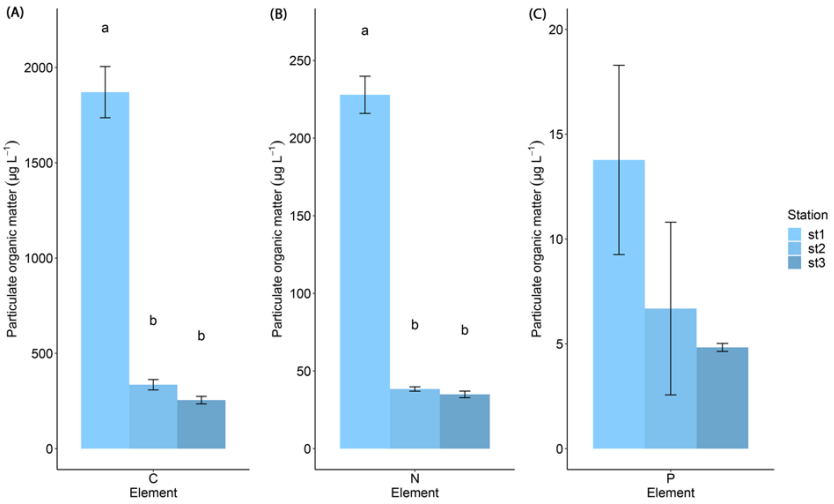

Suppl. Figure 5.4: Particulate organic carbon (A), nitrogen (B), and phosphorus (C) of initial community samples from three stations. Data presented are means and standard deviations of three replicates. Different letters (a, b) indicate significant differences (two-way ANOVA, $p < 0.05$).

Suppl. Table 5.1: Results of Tukey's *post-hoc* comparison after two-way ANOVA of average cell volume of phytoplankton communities after 72-hour incubation with interactions between stations (st1, st2, st3) and treatments (ctrl, trt10, trt20, trt30) with an initial dilution with nutrient-rich freshwater by 10, 20, and 30 %. The symbol '+' indicates a significant difference (Tukey's *post-hoc* comparison, $p < 0.05$) and the symbol '-' indicates the absence of significant difference.

Cell volume	st1: ctrl	st1: trt10	st1: trt20	st1: trt30	st2: ctrl	st2: trt10	st2: trt20	st2: trt30	st3: ctrl	st3: trt10	st3: trt20	st3: trt30
st1:ctrl												
st1:trt10	+											
st1:trt20	+	-										
st1:trt30	+	-	-									
st2:ctrl	+	+	+	-								
st2:trt10	+	+	+	+	-							
st2:trt20	+	+	+	+	-	-						
st2:trt30	+	+	+	+	-	-	-					
st3:ctrl	+	+	+	-	-	-	-	-				
st3:trt10	+	+	-	-	-	+	+	+	-			
st3:trt20	+	-	-	-	+	+	+	+	+	+		
st3:trt30	+	+	-	-	-	-	+	+	-	-	+	

Suppl. Table 5.2: Results of Tukey's *post-hoc* comparison after two-way ANOVA of molar C:N, C:P, and N:P ratio of phytoplankton communities after 72-hour incubation with interactions between stations (st1, st2, st3) and treatments (ctrl, trt10, trt20, trt30) with an initial dilution with nutrient-rich freshwater by 10, 20, and 30 %. The symbol '+' indicates a significant difference (Tukey's *post-hoc* comparison, $p < 0.05$) and the symbol '-' indicates the absence of significant difference.

C:N (molar)	st1: ctrl	st1: trt10	st1: trt20	st1: trt30	st2: ctrl	st2: trt10	st2: trt20	st2: trt30	st3: ctrl	st3: trt10	st3: trt20	st3: trt30
st1:ctrl												
st1:trt10	+											
st1:trt20	+	-										
st1:trt30	+	-	-									
st2:ctrl	-	-	-	-								
st2:trt10	+	-	-	-	+							
st2:trt20	+	+	-	-	+	-						
st2:trt30	+	-	-	-	+	-	-					
st3:ctrl	+	-	-	-	-	+	+	+				
st3:trt10	+	-	-	-	+	-	-	-	+			
st3:trt20	+	+	+	-	+	-	-	-	+	-		
st3:trt30	+	+	+	-	+	-	-	-	+	-	-	

C:P (molar)	st1: ctrl	st1: trt10	st1: trt20	st1: trt30	st2: ctrl	st2: trt10	st2: trt20	st2: trt30	st3: ctrl	st3: trt10	st3: trt20	st3: trt30
st1:ctrl												
st1:trt10	+											
st1:trt20	+	-										
st1:trt30	+	-	-									
st2:ctrl	-	+	+	+								
st2:trt10	+	+	+	-	+							
st2:trt20	+	+	+	+	+	-						
st2:trt30	+	+	+	+	+	-	-					

C:P (molar)	st1: ctrl	st1: trt10	st1: trt20	st1: trt30	st2: ctrl	st2: trt10	st2: trt20	st2: trt30	st3: ctrl	st3: trt10	st3: trt20	st3: trt30
st3:ctrl	+	-	-	+	+	+	+	+				
st3:trt10	+	-	-	-	+	-	-	+	+			
st3:trt20	+	+	+	-	+	-	-	-	+	-		
st3:trt30	+	+	+	+	+	-	-	-	+	+	-	

N:P (molar)	st1: ctrl	st1: trt10	st1: trt20	st1: trt30	st2: ctrl	st2: trt10	st2: trt20	st2: trt30	st3: ctrl	st3: trt10	st3: trt20	st3: trt30
st1:ctrl												
st1:trt10	-											
st1:trt20	-	-										
st1:trt30	+	-	+									
st2:ctrl	+	+	+	+								
st2:trt10	+	+	+	-	+							
st2:trt20	+	+	+	-	+	-						
st2:trt30	+	+	+	-	+	-	-					
st3:ctrl	-	-	-	+	+	+	+	+				
st3:trt10	+	-	-	-	+	-	-	+	-			
st3:trt20	+	-	+	-	+	-	-	-	+	-		
st3:trt30	+	+	+	-	+	-	-	-	+	+	-	

Chapter 6

General discussion

Phytoplankton are critical to the biogeochemical cycling of nutrients, and the oxygen produced by their photosynthetic activity accounts for half of the total oxygen production on Earth (Field et al., 1998). As the base of aquatic food webs, they also serve as food for herbivores, and changes in phytoplankton can have consequences for higher trophic levels up to fish and marine mammals (Beaugrand *et al.*, 2003, Frederiksen *et al.*, 2006). However, human activities cause simultaneous changes in a range of marine abiotic parameters (IPCC, 2014), and phytoplankton are directly affected by rising temperatures, increasing pCO_2 levels, and changes in dissolved nutrient concentrations (Collins et al., 2014, Finkel et al., 2010, Toseland et al., 2013). Therefore, it is of great importance to assess the impact of environmental changes on phytoplankton. Yet, evaluating the effects of global change on phytoplankton is not trivial because this group is highly diverse, and accounting for the variety of responses that can occur among species, as well as among strains of a species, is challenging. Trait-based approaches are a useful tool to reduce this complexity by focusing on functional traits of phytoplankton cells while providing a mechanistic explanation for the impact of environmental change. As such, trait-based approaches are a powerful tool to evaluate the impact of global change on phytoplankton ecophysiology (Litchman & Klausmeier, 2008).

In my thesis, I applied trait-based approaches to investigate the effects of increasing temperature, pCO_2, and dissolved N:P ratios on phytoplankton at the individual cell and the population levels on the one hand (**chapters two** and **three**) and, on the other hand, to investigate the effects of extreme weather events such as heatwaves and increased river discharge at the population level and on natural phytoplankton communities in the North Sea (**chapter four** and **five**). Below, I will highlight the key findings of this thesis and discuss the potential implications of global change for phytoplankton in coastal waters. Furthermore, I will

address in an outlook how changes in the functional traits of phytoplankton might affect ecosystem functioning as a whole.

6.1. Rising average temperature, pCO_2, and dissolved N:P ratio – phytoplankton living under future environmental conditions

Anthropogenic activities cause simultaneous changes in several abiotic parameters. While temperature and pCO_2 are globally increasing, coastal marine ecosystems have been shown to experience greater ocean warming than other habitats (Wiltshire et al., 2010). Temperature is a major driver affecting phytoplankton functional traits by influencing a number of ecophysiological processes (Eppley, 1972, Raven & Geider, 1988). Notably, studies reported that warming often increases phytoplankton growth (Montagnes & Franklin, 2001, Kremer et al., 2017) and photosynthesis rates (Staehr & Birkeland, 2006) and can cause a decrease in phytoplankton cell size (Atkinson *et al.*, 2003, Montagnes & Franklin, 2001). Higher pCO_2 might lead to increased growth rates as current CO_2 concentrations are not saturating for Rubisco, the enzyme that catalyzed primary fixation of inorganic carbon (Badger et al., 1998). In addition to warming and increasing pCO_2, industrial and agricultural development influence dissolved N:P ratios in coastal ecosystems through terrestrial runoff such as river discharge (Radach & Pätsch, 2007). As autotrophs, the growth of phytoplankton is directly linked to dissolved nutrients and changes in N:P ratios will consequently influence phytoplankton growth rates (Geider & La Roche, 2002, Ågren, 2004). While the individual influence of abiotic parameters on phytoplankton has long been studied, the assessment of concurrent effects of multiple global change drivers, which is necessary to evaluate the consequences of future scenarios realistically, is still in its infancy (Gunderson et al., 2016). Interestingly, temperature, pCO_2, and dissolved N:P ratio all influence phytoplankton growth rate, which is a master functional trait directly linked to other cellular traits (Litchman et al., 2007). Overall, this interdependency between abiotic conditions and traits is likely to influence the ecological functions played by phytoplankton. Hence, in my thesis, I aimed to evaluate the impact of rising average temperature, pCO_2 and dissolved N:P ratios on the growth rate and further influence other functional traits. In chapter two, I evaluated the effects of increasing temperature, pCO_2, and dissolved N:P ratios on the variability of traits between individual cells of a single diatom

strain, and in chapter three, I focused on diatom metabolic processes and stress responses to these environmental drivers.

6.1.1. Growth rate

In both studies presented in chapters two and three, where temperature, pCO_2, and dissolved inorganic N:P ratio were manipulated simultaneously, growth rates were positively affected by future environmental conditions. Furthermore, the full factorial approach used in chapter three showed that temperature was the main driver influencing the growth rate of *Phaeodactylum tricornutum,* whereas elevated pCO_2 dampened the positive effect of higher temperature on growth rate. The increase in dissolved N:P ratio from 16 to 25 had only a minor effect. I could not observe any significant impact of increased N:P ratio on the growth of the diatoms *Thalassiosira weissflogii,* and the growth rate of *P. tricornutum* was only significantly affected by higher N:P ratios under elevated pCO_2. The observation that temperature was the strongest driver for phytoplankton growth is not unexpected as temperature can affect several physiological processes (Eppley, 1972). The positive correlation between temperature and growth rates is anchored in the metabolic theory of ecology (Brown et al., 2004), which posits that organisms in warm conditions exhibit higher metabolic rates than those at colder temperatures. This pattern has been found in a number of studies that tested the growth response of several phytoplankton groups and species over a broad temperature range (Montagnes & Franklin, 2001, Staehr & Birkeland, 2006, Edwards *et al.*, 2016). In chapters two and three testing temperature increases of + 1.5 and + 3 °C, I was also able to show that even a relatively small increase in temperature can affect phytoplankton growth, although the increase in growth rate was not significant at + 1.5 °C in contrast to + 3 °C. These results highlight the respective impact that the different scenarios of the IPCC may yield (IPCC, 2021), as well as the importance of conducting experiments with realistic conditions expected for the next decades. In support of my work, Beardall and Raven (2004) highlighted the importance of even a 2 - 3 °C increase as a small temperature increase might push some species beyond their temperature optima.

In contrast to temperature responses which are well studied, responses of phytoplankton to elevated pCO_2 vary significantly among species and are often correlated to other

environmental drivers (Häder & Gao, 2015, Flynn et al., 2015, Seifert et al., 2020, Collins et al., 2014). The results from studies testing the influence of pCO_2 range from a negative impact on the growth of individual phytoplankton species (Hattich et al., 2017) to very little or no effect (Burkhardt *et al.*, 1999) to a positive impact on phytoplankton growth. The large differences in phytoplankton responses to elevated pCO_2 are likely correlated to the different CO_2 requirements and the differences in CO_2 sensitivity between phytoplankton groups (Riebesell, 2004). Even between replicates, Hattich et al. (2017) observed a high variability masking potential differences in growth rate between CO_2 treatments. Interestingly, a recent meta-analysis on a dataset compiled from 42 studies identified that pCO_2 modulates phytoplankton responses to global change, as increasing pCO_2 levels reduce the growth-enhancing effects of high temperature (Seifert et al., 2020). These results are in line with the experiment described in chapter three which did not reveal an individual impact of elevated pCO_2 on phytoplankton growth, but in which elevated pCO_2 dampened the effect of higher temperature on growth rate. Cross et al. (2015) reviewed different hypotheses that describe how growth is influenced by temperature and nutrients and concluded that the relative influence of dissolved nutrients on growth rate increases with temperature. This supports the observations in chapter three of increased growth sensitivity toward a higher N:P ratio under elevated temperature.

Overall, results from chapters two and three indicate that phytoplankton growth rate may increase under future environmental conditions, particularly under the influence of temperature increases beyond +1.5°C, but that additional and simultaneous changes in dissolved N:P ratios and pCO_2 may have an antagonistic effect.

6.1.2. Trait variability

I have shown that phytoplankton growth rate may be significantly affected by global change, and as several phytoplankton traits are linked to growth rate, they might also be directly and indirectly influenced by changing environmental conditions. Unlike the correlation between growth rate and cell size or the biochemical composition of cells, which have been measured at the population level (Costello & Chisholm, 1981, Flynn *et al.*, 2018, Marañón et al., 2013), much less attention has been paid to the correlation between growth rate and the cell-to-cell variability of different phytoplankton traits. Assessing the variability within individual

strains, or even between single cells, provides important insight into how phytoplankton species cope with environmental change. Under suboptimal growth conditions, high phenotypic variability may enable phytoplankton to adjust to new environmental conditions and can thus ensure their survival (Godhe & Rynearson, 2017). Based on the work of Hillebrand et al. (2013), which showed that increasing growth rates can lead to lower and converging N:P ratios at the population level, I hypothesized that not only the variability between species but also the variability within one strain decreases with increasing growth rate (chapter two). My results partially supported the hypothesis. While variability in cellular protein content was not affected by growth rate, neither at the single strain population level nor at the individual cell level, variability in cellular chlorophyll *a* content between different populations of one strain decreased significantly with increasing growth rate, and cell-to-cell variability in cell size also decreased with increasing growth rate. Similar patterns were observed by Fontana et al. (2019) who found in an experimental study that light limitation can increase the phenotypic heterogeneity of two phytoplankton species, and by Anderson and Rynearson (2020) who measured intraspecific thermal trait variation and observed the lowest variation at maximum growth rate. Cell size and chlorophyll *a* play an important physiological role for phytoplankton because they are strongly correlated with nutrient acquisition and photosynthesis (Litchman & Klausmeier, 2008), and, as growth rates may increase under future environmental conditions, reduced variability in these traits may reflect optimization of physiological processes supporting fast growth.

Additionally, the results from chapter two showed that higher temperatures and pCO_2 can cause an overall decrease in cell-to-cell variability of cell size, which was not correlated with growth rate. Cell size has been shown to be influenced by abiotic conditions or predation pressure, and high phenotypic plasticity in cell size is a key aspect determining the ability of phytoplankton to respond to environmental changes (Godhe & Rynearson, 2017). However, the subsistence of a species in a community depends not only on trait variability but also on how important traits are for the functioning and the coexisting of a species (Hillebrand & Matthiessen, 2009). Indeed, how well a single strain copes with changing environmental conditions depends on the tolerance range of individual cells. The sum of the tolerance ranges of different strains within a population determines whether the population can cope with environmental change. However, this field of research still needs to be further explored, and

more studies are needed to assess the phenotypic variability within species, conducting experiments not only with different populations but also with different strains of one species to evaluate the impact of environmental change on phytoplankton (Kremp et al. (2012).

6.1.3. Strain-specific responses

Although increased phytoplankton growth under future environmental conditions may indicate more favorable conditions, growth enhancement is often associated with trade-offs in other cell physiological mechanisms. Chapter three shows that temperature and, to a lesser extent, pCO_2 and dissolved N:P ratios significantly affect the growth of the diatom *P. tricornutum*. However, the AOX activity as a ratio of AOX-dependent respiration to total dark respiration, for example, which can be activated when cells experience stress (Vanlerberghe, 2013) and reduce the overproduction of reactive oxygen species formed in cells (Møller, 2001), significantly increased for *P. tricornutum* growing under elevated temperatures. Also, the ratio between photoprotective to light-harvesting pigments increased and the energy flow to the photosystem decreased, which can be interpreted as a strategy to prevent the formation of reactive oxygen species (Dubinsky & Stambler, 2009). Additionally, higher temperatures caused an increase in photosynthetic activity whereas dark respiration decreased. To compensate for the higher photosynthetic production of particulate organic carbon (POC) and lower consumption by mitochondrial respiration, dissolved organic carbon (DOC) excretion increased at higher temperatures. The positive correlation between growth rates and DOC excretion resulted in an overall lower POC content per cell, which might have consequences for food web processes, the microbial loop, and overall carbon cycling.

6.1.4. Synthesis

Under long-term environmental changes, including rising temperatures, increased pCO_2, and shifts in dissolved N:P ratios, temperature might be the most important driver affecting phytoplankton growth and other functional traits. The results of my thesis also indicate that phytoplankton responses to long-term environmental changes are strongly dependent on the interactive effect of multiple global change drivers, which is supported by other studies (Seifert et al., 2020, Cabrerizo *et al.*, 2014, Van de Waal & Litchman, 2020). For phytoplankton

species that are currently growing below their thermal limits, growth rates will likely increase with global warming, but the degree of growth enhancement may be dampened by simultaneous increases in pCO_2 and N:P ratios. The increased growth rate could also be accompanied by physiological stress. Phytoplankton cells might activate several processes, such as the increased activity of AOX-dependent respiration or an increased ratio between photoprotective to light-harvesting pigments when exposed to higher temperatures, pCO_2, and dissolved N:P ratios. I could also show in this thesis that higher growth rates might be associated with a reduction in cell-to-cell trait variability. Future studies should further address the relationship between trait variability and growth rate using chemostat experiments. In chemostats, growth rates can be precisely adjusted and held constant over a long period by adjusting the dilution rate. Correlations between growth rate and trait variability could be studied, through experiments manipulating temperature or nutrient ratios, providing new insight into the effects of long-term environmental changes.

6.2. Extreme weather events – Phytoplankton coping with extremes

In the context of global change, phytoplankton are not only subjected to gradual average changes in abiotic parameters but also an increasing number of extreme weather events (IPCC, 2021). Jentsch *et al.* (2007) proposed that extreme events can be characterized by statistical extremity, timing, and abruptness relative to the life cycles of the organisms affected. Marine heatwaves, for example, are defined as discrete, anomalously warm water events that occur in a particular location for at least five days (Hobday et al., 2016). This rapid increase in seawater temperature can drastically impact marine organisms, for instance, by causing a loss of genetic diversity (Gurgel et al., 2020) or by promoting the local extinction of a species (Thomsen et al., 2019). Such changes may lead to a restructuring of phytoplanktonic communities, with shifts in diversity toward communities dominated by fewer species that are better adapted to endure warmer and irregular temperature conditions. Abrupt temperature changes can also lead to changes in several physiological processes, and studies have reported a negative influence of heatwaves on photosynthetic and lipid metabolism associated with increased antioxidant responses (Murik et al., 2019, Feijão *et al.*, 2018). In addition to heatwaves, heavy precipitation events are also predicted to increase in frequency and intensity in the decades to come (IPCC, 2021). Intense precipitation substantially increases river discharge and leads to abrupt increases

of freshwater into coastal areas. In addition to suddenly decreasing seawater salinity, riverine inflow also fertilizes coastal areas with nutrients drained from terrestrial systems, influencing coastal marine phytoplankton biomass and community composition (Andersen *et al.*, 2020, Pecqueur *et al.*, 2011). Although the emissions of agricultural nutrients to European seas have largely been reduced over the past decades due to national/international measures and EU legislation, rivers continue to transport large amounts of nutrients (Bouraoui & Grizzetti, 2011). Hence, phytoplankton in coastal areas will face abrupt changes in salinity as well as dissolved nutrient concentrations when heavy precipitation events cause sudden increase in river discharge. Therefore, I investigated in the second part of my thesis the effect of a sudden increase in temperature on ecophysiological traits of the diatom *Phaeodactylum tricornutum*, mimicking a marine heatwave (chapter four), and the effect of abrupt changes in salinity and dissolved nutrient concentrations on natural North Sea phytoplankton communities to simulate an abrupt increase in river discharge (chapter five).

6.2.1. Heatwaves

Temperature fluctuations and marine heatwaves can modulate the intensity of phytoplankton blooms (Hayashida et al., 2020) and can induce changes in functional traits such as cell size (Remy et al., 2017), but can also cause cellular stress (González-Olalla et al., 2021). The results of my thesis indicate that phytoplankton may not react immediately to an abrupt temperature increase, as most significant changes in cellular traits were observed only after a few days at higher temperatures. While in chapter three, AOX activity was significantly higher for *P. tricornutum* growing under elevated average temperatures, the abrupt increase in temperature induced in chapter four resulted in an immediate reduction in AOX activity. The decrease in AOX-dependent respiration in response to a sudden temperature increase may have served to rapidly meet the increased demands on mitochondrial metabolism (Vanlerberghe, 2013), which in turn can damage cellular structures due to increased production of reactive oxygen species in cells (Møller, 2001). While I did not detect increased AOX activity in my thesis indicating cellular stress, several stress responses and a negative effect on photosynthesis and nutritional value of *P. tricornutum* were observed in other studies when it was exposed to a more severe heatwave (Feijão et al., 2018), highlighting the importance of the range of temperature fluctuations.

The growth rate of *P. tricornutum* increased significantly after acclimation to higher temperatures, in line with the results obtained in chapters one to three. The size of *P. tricornutum* cells and the cellular lipid content were negatively affected by a sudden increase in temperature. Because the elevated temperature caused an increase in metabolic rates, stored lipids may have been used as a carbon source, leading to the observed decrease in cellular lipid content. A decrease in cell size, which is commonly associated with increased growth rate, may be advantageous for cells growing under nutrient limitation due to the higher surface-to-volume ratio as well as under intensified stratification, as they exhibit lower sink rates (Finkel et al., 2010). At the same time, however, smaller cell size is typically associated with lower storage capacity, which can be a disadvantage under fluctuating environmental conditions (Litchman & Klausmeier, 2008). Remy et al. (2017) found that heatwaves can also negatively affect biovolume at the community level by favoring small species. Furthermore, their study showed that the addition of nutrients can offset the negative effects of a moderate heatwave of + 4 °C, while a more intense heatwave of + 8 °C could not be buffered by nutrient addition and negative effects on biodiversity were observed. As emphasized by Bergkemper *et al.* (2018), phytoplankton diversity may be even more sensitive to temperature changes than biomass.

Whether individual phytoplankton species exposed to temperature fluctuations caused by marine heatwaves experience severe thermal stress or have the potential to buffer the temperature increase may depend on the intensity of the temperature fluctuations in relation to their thermal window. In addition, other parameters, such as dissolved nutrients, are likely to play an important role (Gerhard *et al.*, 2019, Remy et al., 2017, Hayashida et al., 2020). If global warming is already pushing phytoplankton to their thermal limits and individual species can no longer buffer temperature fluctuations, marine heatwaves are very likely to cause severe changes in community structure and a decline in phytoplankton diversity.

6.2.2. Increased river discharge

I found an overall increase in phytoplankton growth rate in three natural phytoplankton communities from the North Sea when exposed to pulses of nutrient-rich freshwater. These results are supported by previous studies by Deininger et al. (2016) and Paczkowska *et al.* (2020) on heavy precipitation events and increased river discharge which obtained similar

results. Furthermore, I observed that the positive effect on growth, likely driven by nutrient addition, ceased in the most intense freshwater input treatment, indicating a certain degree of salinity tolerance of coastal phytoplankton communities, as previously observed by Brand (1984). Furthermore, my results suggest that the response of phytoplankton communities to the abrupt discharge of nutrient-rich freshwater rather depends on their initial composition than on their origin, which is supported by other studies on the effects of environmental factors on community structure (Striebel *et al.*, 2016, Eggers et al., 2014). While more diverse communities showed a positive response to pulses of nutrient-rich freshwater, the less diverse community was not significantly affected. Interestingly, the increase in growth rates was driven by small flagellates and small diatoms, and even within a phytoplankton species classified into different size classes, a shift towards smaller cells was observed. These results support the concept that small, fast-growing taxa generally benefit most from an abrupt increase in dissolved nutrient concentration because they have high maximum nutrient uptake rates and high maximum growth rates (Litchman & Klausmeier, 2008, Sommer, 1984).

6.2.3. Synthesis

In my thesis, I showed that extreme weather events can cause major changes in the functional properties of phytoplankton at the population and community levels. Rising temperatures due to marine heatwaves and pulses of nutrient-rich freshwater due to increased river discharge could lead to an increase in growth rates and an overall decrease in phytoplankton cell size. If and how extreme weather events can negatively affect individual phytoplankton species and entire communities may depend strongly on the intensity of environmental fluctuations, as shown by Remy et al. (2017), who found that the addition of nutrients has the potential to buffer negative effects of moderate heatwaves but not more drastic temperature fluctuations. In addition, I showed that for community stability, initial community structure has a determinant role when facing extreme events. Corcoran and Boeing (2012) emphasized that species combination might be the driving factor for productivity, while species richness is important for phytoplankton community stability.

To assess the impacts of extreme weather events, future studies should also consider the additional impacts of long-term average environmental change. Although phytoplankton might

be able to buffer the effects of moderate heatwaves and heavy precipitation events when growing under current abiotic conditions, this might no longer be possible if increasing temperatures, pCO_2, or changes in nutrient availability push phytoplankton toward the edge of their tolerance windows. Hayashida et al. (2020), for example, stated that an overall decline in nutrient availability in a future ocean might weaken phytoplankton blooms due to marine heatwaves but may also cause severe changes in community composition. In turn, a restructuring of the phytoplankton community could lead to a mismatch between predators and prey, which can have serious consequences for higher trophic levels (Jones *et al.*, 2018).

6.3. Potential consequences for ecosystem functioning

This thesis provides a comprehensive picture of the effects of environmental changes on the functional traits of phytoplankton, from single cells to phytoplankton communities. Long-term environmental changes, as well as extreme weather events, can lead to substantial changes in cell size, carbon fluxes, and the biochemical composition of phytoplankton, which are linked to changes in growth rates. As they form the basis of most marine food webs, changes in phytoplankton will affect higher trophic levels. I show in my thesis that especially global warming and an increasing number of marine heatwaves can have significant effects on metabolic fluxes and lead to higher growth rates of phytoplankton. This could be further enhanced by an increasing number of heavy precipitation events and overall higher nutrient inputs into coastal areas. Although increasing phytoplankton growth rates in surface waters may increase the conversion of carbon into biomass, organic carbon could be released in dissolved form and promote bacterial growth rather than transported to higher trophic levels. In addition, a general decrease in phytoplankton size could further weaken trophic transfers (see below), and the carbon sink into deeper ocean layers as smaller cells remain longer in surface waters due to a lower sinking velocity (Finkel et al., 2010). Consequently, long-term environmental changes, as well as an increase in the frequency and intensity of extreme events, have the potential to strengthen the microbial loop due to smaller cell sizes and increased exudation of dissolved organic carbon.

Cell size also plays an important role in micro- and mesozooplankton grazing. An overall decrease in phytoplankton cell size due to environmental change could promote the

growth of heterotrophic dinoflagellates or ciliates as microzooplankton is more efficient in consuming small prey items than mesozooplankton. In turn, enhanced energy flows through microzooplankton may extend the food chain and lead to additional carbon loss, weakening energy transfer to larger grazers (Aberle *et al.*, 2015, Fenchel, 2008). A decrease in mesozooplankton and an increase in microzooplankton biomass have already been observed in a mesocosm study by Moreno et al. (2022), who used the same environmental drivers as I did for my thesis. The authors suggested that lower energy transfer to higher trophic levels may occur when the direct link from phytoplankton to mesozooplankton is relocated through an intermediary trophic level comprised of microzooplankton. In addition, higher temperatures also lead to increasing metabolic rates in zooplankton and can increase grazing pressure (Lewandowska & Sommer, 2010), especially the pressure exerted on phytoplankton which is a preferred food source under warmer temperatures (Boersma *et al.*, 2016). However, if, as noted above, the available phytoplankton is not adequate, we may expect severe consequences for food web functioning overall. Since fluctuations in abiotic conditions can lead to serious changes in phytoplankton traits within a very short time, it is crucial to further investigate the effects of extreme weather events, especially in conjunction with long-term environmental changes. Knowing whether long-term changes will push individual species to their growth limits, and how communities may have already been altered, is necessary to realistically assess the effects of environmental fluctuations on ecosystem functioning in a future ocean.

Bibliography

Aberle, N., Malzahn, A. M., Lewandowska, A. M. & Sommer, U. 2015. Some like it hot: the protozooplankton-copepod link in a warming ocean. *Marine Ecology Progress Series* **519**:103-13.

Abraham, E. R. 1998. The generation of plankton patchiness by turbulent stirring. *Nature* **391**:577-80.

Aebi, H. 1984. [13] Catalase in vitro. *Methods in Enzymology.* Academic Press/Elsevier, pp. 121-26.

Ågren, G. I. 2004. The C:N:P stoichiometry of autotrophs - theory and observations. *Ecology Letters* **7**:185-91.

Ahmad, S. & Pardini, R. S. 1988. Evidence for the presence of glutathione peroxidase activity toward an organic hydroperoxide in larvae of the cabbage looper moth, *Trichoplusia ni*. *Insect Biochemistry* **18**:861-66.

Alipanah, L., Rohloff, J., Winge, P., Bones, A. M. & Brembu, T. 2015. Whole-cell response to nitrogen deprivation in the diatom *Phaeodactylum tricornutum*. *Journal of Experimental Botany* **66**:6281-96.

Allen, A. E., LaRoche, J., Maheswari, U., Lommer, M., Schauer, N., Lopez, P. J., Finazzi, G., Fernie, A. R. & Bowler, C. 2008. Whole-cell response of the pennate diatom *Phaeodactylum tricornutum* to iron starvation. *Proceedings of the National Academy of Sciences* **105**:10438-43.

Allesson, L., Ström, L. & Berggren, M. 2016. Impact of photochemical processing of DOC on the bacterioplankton respiratory quotient in aquatic ecosystems. *Geophysical Research Letters* **43**:7538-45.

Alvarez-Fernandez, S., Bach, L. T., Taucher, J., Riebesell, U., Sommer, U., Aberle, N., Brussaard, C. P. D. & Boersma, M. 2018. Plankton responses to ocean acidification: the role of nutrient limitation. *Progress in Oceanography* **165**:11-18.

Amato, A., Orsini, L., D'Alelio, D. & Montresor, M. 2005. Life cycle, size reduction patterns, and ultrastructure of the pennate planktonic diatom *Pseudo-nitzschia delicatissima* (Bacillariophyceae). *Journal of Phycology* **41**:542-56.

Andersen, J. H., Al-Hamdani, Z., Harvey, E. T., Kallenbach, E., Murray, C. & Stock, A. 2020. Relative impacts of multiple human stressors in estuaries and coastal waters in the North Sea-Baltic Sea transition zone. *Sci. Total Environ.* **704**:135316.

Anderson, S. I. & Rynearson, T. A. 2020. Variability approaching the thermal limits can drive diatom community dynamics. *Limnology and Oceanography* **65**:1961-73.

Anderson, T. R., Hawkins, E. & Jones, P. D. 2016. CO_2, the greenhouse effect and global warming: from the pioneering work of Arrhenius and Callendar to today's Earth System Models. *Endeavour* **40**:178-87.

Arbones, B., Figueiras, F. G. & Varela, R. 2000. Action spectrum and maximum quantum yield of carbon fixation in natural phytoplankton populations: implications for primary production estimates in the ocean. *Journal of Marine Systems* **26**:97-114.

Armbrust, E. V. 2009. The life of diatoms in the world's oceans. *Nature* **459**:185-92.

Atkinson, D., Ciotti, B. J. & Montagnes, D. J. S. 2003. Protists decrease in size linearly with temperature: ca. 2.5% C^{-1}. *Proceedings of the Royal Society of London. Series B: Biological Sciences* **270**:2605-11.

Azam, F., Fenchel, T., Field, J. G., Gray, J. S., Meyer-Reil, L.-A. & Thingstad, F. 1983. The ecological role of water-column microbes in the sea. *Marine Ecology Progress Series*:257-63.

Bach, L. T., Hernández-Hernández, N., Taucher, J., Spisla, C., Sforna, C., Riebesell, U. & Arístegui, J. 2019. Effects of elevated CO_2 on a natural diatom community in the subtropical NE Atlantic. *Frontiers in Marine Science* **6**:75.

Badger, M. R., Andrews, T. J., Whitney, S. M., Ludwig, M., Yellowlees, D. C., Leggat, W. & Price, G. D. 1998. The diversity and coevolution of Rubisco, plastids, pyrenoids, and chloroplast-based CO2-concentrating mechanisms in algae. *Can. J. Bot.-Rev. Can. Bot.* **76**:1052-71.

Bailleul, B., Berne, N., Murik, O., Petroutsos, D., Prihoda, J., Tanaka, A., Villanova, V., Bligny, R., Flori, S. & Falconet, D. 2015. Energetic coupling between plastids and mitochondria drives CO_2 assimilation in diatoms. *Nature* **524**:366-69.

Baines, S. B. & Pace, M. L. 1991. The production of dissolved organic matter by phytoplankton and its importance to bacteria: patterns across marine and freshwater systems. *Limnology and Oceanography* **36**:1078-90.

Balzano, S., Sarno, D. & Kooistra, W. H. C. F. 2011. Effects of salinity on the growth rate and morphology of ten *Skeletonema* strains. *Journal of Plankton Research* **33**:937-45.

Barros, M. P., Pedersén, M., Colepicolo, P. & Snoeijs, P. 2003. Self-shading protects phytoplankton communities against H_2O_2-induced oxidative damage. *Aquatic Microbial Ecology* **30**:275-82.

Beardall, J. & Raven, J. A. 2004. The potential effects of global climate change on microalgal photosynthesis, growth and ecology. *Phycologia* **43**:26-40.

Beaugrand, G., Brander, K. M., Lindley, J. A., Souissi, S. & Reid, P. C. 2003. Plankton effect on cod recruitment in the North Sea. *Nature* **426**:661-64.

Beliaeff, B. & Burgeot, T. 2002. Integrated biomarker response: a useful tool for ecological risk assessment. *Environmental Toxicology and Chemistry: An International Journal* **21**:1316-22.

Berges, J. A., Franklin, D. J. & Harrison, P. J. 2001. Evolution of an artificial seawater medium: improvements in enriched seawater, artificial water over the last two decades. *Journal of Phycology* **37**:1138-45.

Bergkemper, V., Stadler, P. & Weisse, T. 2018. Moderate weather extremes alter phytoplankton diversity - A microcosm study. *Freshwater Biology* **63**:1211-24.

Bitaubé Pérez, E., Pina, I. C. & Pérez Rodríguez, L. 2008. Kinetic model for growth of *Phaeodactylum tricornutum* in intensive culture photobioreactor. *Biochemical Engineering Journal* **40**:520-25.

Boersma, M., Mathew, K. A., Niehoff, B., Schoo, K. L., Franco-Santos, R. M. & Meunier, C. L. 2016. Temperature driven changes in the diet preference of omnivorous copepods: no more meat when it's hot? *Ecology Letters* **19**:45-53.

Bohlin, K. H. 1897. *Zur Morphologie und Biologie einzelliger Algen.* Nabu Press, Stockholm, 507-29.

Bouraoui, F. & Grizzetti, B. 2011. Long term change of nutrient concentrations of rivers discharging in European seas. *Sci. Total Environ.* **409**:4899-916.

Bowler, C., Vardi, A. & Allen, A. E. 2010. Oceanographic and biogeochemical insights from diatom genomes. *Annual Review of Marine Science* **2**:333-65.

Bradford, M. M. 1976. A rapid and sensitive method for the quantitation of microgram quantities of protein utilizing the principle of protein-dye binding. *Analytical Biochemistry* **72**:248-54.

Brand, L. E. 1984. The salinity tolerance of forty-six marine phytoplankton isolates. *Estuarine, Coastal and Shelf Science* **18**:543-56.

Brown, J. H., Gillooly, J. F., Allen, A. P., Savage, V. M. & West, G. B. 2004. Toward a metabolic theory of ecology. *Ecology* **85**:1771-89.

Brutemark, A., Engström-Öst, J., Vehmaa, A. & Gorokhova, E. 2015. Growth, toxicity and oxidative stress of a cultured cyanobacterium (*Dolichospermum* sp.) under different CO_2/pH and temperature conditions. *Phycological Research* **63**:56-63.

Buesseler, K. O. 1998. The decoupling of production and particulate export in the surface ocean. *Glob. Biogeochem. Cycle* **12**:297-310.

Burkhardt, S., Riebesell, U. & Zondervan, I. 1999. Effects of growth rate, CO2 concentration, and cell size on the stable carbon isotope fractionation in marine phytoplankton. *Geochim. Cosmochim. Acta* **63**:3729-41.

Burson, A., Stomp, M., Akil, L., Brussaard, C. P. D. & Huisman, J. 2016. Unbalanced reduction of nutrient loads has created an offshore gradient from phosphorus to nitrogen limitation in the North Sea. *Limnology and Oceanography* **61**:869-88.

Burson, A., Stomp, M., Greenwell, E., Grosse, J. & Huisman, J. 2018. Competition for nutrients and light: testing advances in resource competition with a natural phytoplankton community. *Ecology* **99**:1108-18.

Cabrerizo, M. J., Carrillo, P., Villafañe, V. E. & Helbling, E. W. 2014. Current and predicted global change impacts of UVR, temperature and nutrient inputs on photosynthesis and respiration of key marine phytoplankton groups. *Journal of Experimental Marine Biology and Ecology* **461**:371-80.

Caracciolo, M., Beaugrand, G., Hélaouët, P., Gevaert, F., Edwards, M., Lizon, F., Kléparski, L. & Goberville, E. 2021. Annual phytoplankton succession results from niche-environment interaction. *Journal of Plankton Research* **43**:85-102.

Chen, J., Guo, K., Thornton, D. C. & Wu, Y. 2020. Effect of temperature on the release of transparent exopolymer particles (TEP) and aggregation by marine diatoms (*Thalassiosira weissflogii* and *Skeletonema marinoi*). *Journal of Ocean University of China*:1-11.

Chisholm, S. W. 1992. Phytoplankton Size. *In*: Falkowski, P. G., Woodhead, A. D. & Vivirito, K. [Eds.] *Primary Productivity and Biogeochemical Cycles in the Sea.* Springer US, Boston, MA, pp. 213-37.

Chisholm, S. W. & Costello, J. C. 1980. Influence of environmental factors and population composition on the timing of cell division in *Thalassiosira fluviatilis* (Bacillariopyceae) grown on light/dark cycles. *Journal of Phycology* **16**:375-83.

Choo, K.-s., Snoeijs, P. & Pedersén, M. 2004. Oxidative stress tolerance in the filamentous green algae *Cladophora glomerata* and *Enteromorpha ahlneriana*. *Journal of Experimental Marine Biology and Ecology* **298**:111-23.

Cloern, J. E., Foster, S. Q. & Kleckner, A. E. 2014. Phytoplankton primary production in the world's estuarine-coastal ecosystems. *Biogeosciences* **11**:2477-501.

Collins, M., Knutti, R., Arblaster, J., Dufresne, J.-L., Fichefet, T., Friedlingstein, P., Gao, X., Gutowski, W. J., Johns, T., Krinner, G., Shongwe, M., Tebaldi, C., Weaver, A. J. & Wehner, M. 2013. Long-term climate change: projections, commitments and irreversibility. *Climate Change 2013: The Physical Science Basis.* Cambridge University Press, Cambridge, United Kingdom and New York, NY, USA, pp. 1029-136.

Collins, S., Rost, B. & Rynearson, T. A. 2014. Evolutionary potential of marine phytoplankton under ocean acidification. *Evol. Appl.* **7**:140-55.

Connell, J. H. 1978. Diversity in tropical rain forests and coral reefs: high diversity of trees and corals is maintained only in a nonequilibrium state. *Science* **199**:1302-10.

Corcoran, A. A. & Boeing, W. J. 2012. Biodiversity increases the productivity and stability of phytoplankton communities. *PLoS ONE* **7**:e49397.

Cordell, D., Drangert, J.-O. & White, S. 2009. The story of phosphorus: global food security and food for thought. *Global environmental change* **19**:292-305.

Costello, J. C. & Chisholm, S. W. 1981. The influence of cell size on the growth rate of *Thalassiosira weissflogii*. *Journal of Plankton Research* **3**:415-19.

Cross, W. F., Hood, J. M., Benstead, J. P., Huryn, A. D. & Nelson, D. 2015. Interactions between temperature and nutrients across levels of ecological organization. *Global Change Biology* **21**:1025-40.

D'ors, A., Bartolomé, M. C. & Sánchez-Fortún, S. 2016. Repercussions of salinity changes and osmotic stress in marine phytoplankton species. *Estuarine, Coastal and Shelf Science* **175**:169-75.

Day, D. A. & Wiskich, J. T. 1995. Regulation of alternative oxidase activity in higher plants. *Journal of Bioenergetics and Biomembranes* **27**:379-85.

De Martino, A., Bartual, A., Willis, A., Meichenin, A., Villazán, B., Maheswari, U. & Bowler, C. 2011. Physiological and molecular evidence that environmental changes elicit morphological interconversion in the model diatom *Phaeodactylum tricornutum*. *Protist* **162**:462-81.

Deininger, A., Faithfull, C. L., Lange, K., Bayer, T., Vidussi, F. & Liess, A. 2016. Simulated terrestrial runoff triggered a phytoplankton succession and changed seston stoichiometry in coastal lagoon mesocosms. *Marine Environmental Research* **119**:40-50.

Diaz, G., Melis, M., Batetta, B., Angius, F. & Falchi, A. M. 2008. Hydrophobic characterization of intracellular lipids in situ by Nile Red red/yellow emission ratio. *Micron* **39**:819-24.

Dickson, A. G. 1981. An exact definition of total alkalinity and a procedure for the estimation of alkalinity and total inorganic carbon from titration data. *Deep Sea Research* **28**:609-23.

Dickson, A. G. & Millero, F. J. 1987. A comparison of the equilibrium constants for the dissociation of carbonic acid in seawater media. *Deep Sea Research* **34**:1733-43.

Donald, K. M., Scanlan, D. J., Carr, N. G., Mann, N. H. & Joint, I. 1997. Comparative phosphorus nutrition of the marine cyanobacterium *Synechococcus* WH7803 and the marine diatom *Thalassiosira weissflogii*. *Journal of Plankton Research* **19**:1793-813.

Doney, S. C. 2010. The growing human footprint on coastal and open-ocean biogeochemistry. *Science* **328**:1512-16.

Doney, S. C., Fabry, V. J., Feely, R. A. & Kleypas, J. A. 2009. Ocean acidification: the other CO_2 problem. *Annual Review of Marine Science* **1**:169-92.

Duarte, C. M. & Cebrián, J. 1996. The fate of marine autotrophic production. *Limnology and Oceanography* **41**:1758-66.

Dubinsky, Z. & Stambler, N. 2009. Photoacclimation processes in phytoplankton: mechanisms, consequences, and applications. *Aquatic Microbial Ecology* **56**:163-76.

Ducrotoy, J.-P., Elliott, M. & de Jonge, V. N. 2000. The North Sea. *Marine Pollution Bulletin* **41**:5-23.

Edwards, K. F., Thomas, M. K., Klausmeier, C. A. & Litchman, E. 2016. Phytoplankton growth and the interaction of light and temperature: a synthesis at the species and community level. *Limnology and Oceanography* **61**:1232-44.

Eggers, S. L., Lewandowska, A. M., Barcelos e Ramos, J., Blanco-Ameijeiras, S., Gallo, F. & Matthiessen, B. 2014. Community composition has greater impact on the functioning of marine phytoplankton communities than ocean acidification. *Global Change Biology* **20**:713-23.

Engel, A., Händel, N., Wohlers, J., Lunau, M., Grossart, H.-P., Sommer, U. & Riebesell, U. 2011. Effects of sea surface warming on the production and composition of dissolved organic matter during phytoplankton blooms: results from a mesocosm study. *Journal of Plankton Research* **33**:357-72.

Eppley, R. W. 1972. Temperature and phytoplanton growth in the sea. *Fishery Bulletin* **70**.

Falkowski, P. G. & LaRoche, J. 1991. Acclimation to spectral irradiance in algae. *Journal of Phycology* **27**:8-14.

Feijão, E., Gameiro, C., Franzitta, M., Duarte, B., Caçador, I., Cabrita, M. T. & Matos, A. R. 2018. Heat wave impacts on the model diatom *Phaeodactylum tricornutum*: searching for photochemical and fatty acid biomarkers of thermal stress. *Ecological Indicators* **95**:1026-37.

Fenchel, T. 2008. The microbial loop - 25 years later. *Journal of Experimental Marine Biology and Ecology* **366**:99-103.

Feng, T.-Y., Yang, Z.-K., Zheng, J.-W., Xie, Y., Li, D.-W., Murugan, S. B., Yang, W.-D., Liu, J.-S. & Li, H.-Y. 2015. Examination of metabolic responses to phosphorus limitation via proteomic analyses in the marine diatom *Phaeodactylum tricornutum*. *Scientific Reports* **5**:1-10.

Feng, Y., Hare, C. E., Leblanc, K., Rose, J. M., Zhang, Y., DiTullio, G. R., Lee, P. A., Wilhelm, S. W., Rowe, J. M. & Sun, J. 2009. Effects of increased pCO_2 and temperature on the

North Atlantic spring bloom. I. The phytoplankton community and biogeochemical response. *Marine Ecology Progress Series* **388**:13-25.

Field, C. B., Behrenfeld, M. J., Randerson, J. T. & Falkowski, P. 1998. Primary production of the biosphere: integrating terrestrial and oceanic components. *Science* **281**:237-40.

Finkel, Z. V., Beardall, J., Flynn, K. J., Quigg, A., Rees, T. A. V. & Raven, J. A. 2010. Phytoplankton in a changing world: cell size and elemental stoichiometry. *Journal of Plankton Research* **32**:119-37.

Flöder, S., Jaschinski, S., Wells, G. & Burns, C. W. 2010. Dominance and compensatory growth in phytoplankton communities under salinity stress. *Journal of Experimental Marine Biology and Ecology* **395**:223-31.

Flynn, K. J., Clark, D. R., Mitra, A., Fabian, H., Hansen, P. J., Glibert, P. M., Wheeler, G. L., Stoecker, D. K., Blackford, J. C. & Brownlee, C. 2015. Ocean acidification with (de) eutrophication will alter future phytoplankton growth and succession. *Proceedings of the Royal Society B: Biological Sciences* **282**:20142604.

Flynn, K. J., Skibinski, D. O. F. & Lindemann, C. 2018. Effects of growth rate, cell size, motion, and elemental stoichiometry on nutrient transport kinetics. *PLoS Comput. Biol.* **14**:30.

Fogg, G. E. 1957. Relationships between metabolism and growth in plankton algae. *Microbiology* **16**:294-97.

Fontana, S., Thomas, M. K., Reyes, M. & Pomati, F. 2019. Light limitation increases multidimensional trait evenness in phytoplankton populations. *The ISME Journal* **13**:1159-67.

Frederiksen, M., Edwards, M., Richardson, A. J., Halliday, N. C. & Wanless, S. 2006. From plankton to top predators: bottom-up control of a marine food web across four trophic levels. *Journal of Animal Ecology* **75**:1259-68.

Frigstad, H., Kaste, Ø., Deininger, A., Kvalsund, K., Christensen, G., Bellerby, R. G. J., Sørensen, K., Norli, M. & King, A. L. 2020. Influence of riverine input on Norwegian coastal systems. *Frontiers in Marine Science*.

Gao, K. & Campbell, D. A. 2014. Photophysiological responses of marine diatoms to elevated CO_2 and decreased pH: a review. *Functional Plant Biology* **41**:449-59.

Gao, K., Zhang, Y. & Häder, D.-P. 2018. Individual and interactive effects of ocean acidification, global warming, and UV radiation on phytoplankton. *Journal of Applied Phycology* **30**:743-59.

Gechev, T. S., Van Breusegem, F., Stone, J. M., Denev, I. & Laloi, C. 2006. Reactive oxygen species as signals that modulate plant stress responses and programmed cell death. *Bioessays* **28**:1091-101.

Geider, R. & La Roche, J. 2002. Redfield revisited: variability of C:N:P in marine microalgae and its biochemical basis. *European Journal of Phycology* **37**:1-17.

Geider, R. J., La Roche, J., Greene, R. M. & Olaizola, M. 1993. Response of the photosynthetic apparatus of *Phaeodactylum tricornutum* (Bacillariophyceae) to nitrate, phosphate, or iron starvation. *Journal of Phycology* **29**:755-66.

Gerhard, M., Koussoroplis, A. M., Hillebrand, H. & Striebel, M. 2019. Phytoplankton community responses to temperature fluctuations under different nutrient concentrations and stoichiometry. *Ecology* **100**:e02834.

Gillespie, K. M., Rogers, A. & Ainsworth, E. A. 2011. Growth at elevated ozone or elevated carbon dioxide concentration alters antioxidant capacity and response to acute oxidative stress in soybean (*Glycine max*). *Journal of Experimental Botany* **62**:2667-78.

Giordano, M., Beardall, J. & Raven, J. A. 2005. CO_2 concentrating mechanisms in algae: mechanisms, environmental modulation, and evolution. *Annu. Rev. Plant Biol.* **56**:99-131.

Godhe, A. & Rynearson, T. 2017. The role of intraspecific variation in the ecological and evolutionary success of diatoms in changing environments. *Philosophical Transactions of the Royal Society B: Biological Sciences* **372**.

Goldman, J. A. L., Bender, M. L. & Morel, F. M. M. 2017. The effects of pH and pCO_2 on photosynthesis and respiration in the diatom *Thalassiosira weissflogii*. *Photosynthesis Research* **132**:83-93.

Goldman, J. C. 1977. Temperature effects on phytoplankton growth in continuous culture. *Limnology and Oceanography* **22**:932-36.

Goldman, J. C. 1986. On phytoplankton growth rates and particulate C:N:P ratios at low light. *Limnology and Oceanography* **31**:1358-63.

Goldman, J. C., McCarthy, J. J. & Peavey, D. G. 1979. Growth rate influence on the chemical composition of phytoplankton in oceanic waters. *Nature* **279**:210-15.

González-Olalla, J. M., Medina-Sánchez, J. M. & Carrillo, P. 2021. Fluctuation at high hemperature combined with nutrients alters the thermal dependence of phytoplankton. *Microbial Ecology*:1-13.

Grasshoff, K. 1976. Methods of seawater analysis. Verlag Chemie.

Grasshoff, K., Ehrhardt, M. & Kremling, K. 1999. Methods of seawater analysis. 3 ed. Weinheim: Verlag Chemie GmbH.

Grizzetti, B., Bouraoui, F. & Aloe, A. 2012. Changes of nitrogen and phosphorus loads to European seas. *Glob. Change Biol.* **18**:769-82.

Groß, E., Boersma, M. & Meunier, C. L. 2021. Environmental impacts on single-cell variation within a ubiquitous diatom: the role of growth rate. *PLoS ONE* **16**:e0251213.

Grover, J. P. 1991. Resource competition in a variable environment: phytoplankton growing according to the variable-internal-stores model. *The American Naturalist* **138**:811-35.

Guillard, R. R. & Ryther, J. H. 1962. Studies of marine planktonic diatoms. I. *Cyclotella nana* Hustedt, and *Detonula confervacea* (cleve) Gran. *Canadian Journal of Microbiology* **8**:229-39.

Guillard, R. R. L. 1975. Culture of phytoplankton for feeding marine invertebrates. *Culture of Marine Invertebrate Animals.* Springer, pp. 29-60.

Gunderson, A. R., Armstrong, E. J. & Stillman, J. H. 2016. Multiple Stressors in a Changing World: the Need for an Improved Perspective on Physiological Responses to the Dynamic Marine Environment. *In*: Carlson, C. A. & Giovannoni, S. J. [Eds.] *Annual Review of Marine Science, Vol 8.* Annual Reviews, Palo Alto, pp. 357-+.

Gurgel, C. F. D., Camacho, O., Minne, A. J. P., Wernberg, T. & Coleman, M. A. 2020. Marine heatwave drives cryptic loss of genetic diversity in underwater forests. *Current Biology* **30**:1199-206. e2.

Habig, W. H. & Jakoby, W. B. 1981. [27] Glutathione S-transferases (rat and human). *Methods in Enzymology.* Elsevier, pp. 218-31.

Häder, D.-P. & Gao, K. 2015. Interactions of anthropogenic stress factors on marine phytoplankton. *Frontiers in Environmental Science* **3**.

Halliwell, B. 1987. Oxidative damage, lipid peroxidation and antioxidant protection in chloroplasts. *Chemistry and Physics of Lipids* **44**:327-40.

Halpern, B. S., Walbridge, S., Selkoe, K. A., Kappel, C. V., Micheli, F., D'Agrosa, C., Bruno, J. F., Casey, K. S., Ebert, C. & Fox, H. E. 2008. A global map of human impact on marine ecosystems. *Science* **319**:948-52.

Hancke, K., Hancke, T. B., Olsen, L. M., Johnsen, G. & Glud, R. N. 2008. Temperature effects on microalgal photosynthesis-light responses measured by O_2 production, pulse-amplitude-modulated fluorescence, and ^{14}C assimilation. *Journal of Phycology* **44**:501-14.

Hardin, G. 1960. The competitive exclusion principle. *Science* **131**:1292-97.

Hare, C. E., Leblanc, K., DiTullio, G. R., Kudela, R. M., Zhang, Y., Lee, P. A., Riseman, S. & Hutchins, D. A. 2007. Consequences of increased temperature and CO_2 for phytoplankton community structure in the Bering Sea. *Marine Ecology Progress Series* **352**:9-16.

Harley, C. D. G., Randall Hughes, A., Hultgren, K. M., Miner, B. G., Sorte, C. J. B., Thornber, C. S., Rodriguez, L. F., Tomanek, L. & Williams, S. L. 2006. The impacts of climate change in coastal marine systems. *Ecology Letters* **9**:228-41.

Harrison, P. J., Waters, R. E. & Taylor, F. J. R. 1980. A broad spectrum artificial sea water medium for coastal and open ocean phytoplankton. *Journal of Phycology* **16**:28-35.

Hattich, G. S. I., Listmann, L., Raab, J., Ozod-Seradj, D., Reusch, T. B. H. & Matthiessen, B. 2017. Inter-and intraspecific phenotypic plasticity of three phytoplankton species in response to ocean acidification. *Biology Letters* **13**:20160774.

Hayashida, H., Matear, R. J. & Strutton, P. G. 2020. Background nutrient concentration determines phytoplankton bloom response to marine heatwaves. *Global Change Biology* **26**:4800-11.

Heraud, P., Wood, B. R., Tobin, M. J., Beardall, J. & McNaughton, D. 2005. Mapping of nutrient-induced biochemical changes in living algal cells using synchrotron infrared microspectroscopy. *FEMS Microbiology Letters* **249**:219-25.

Herrera-Estrella, L. & López-Arredondo, D. 2016. Phosphorus: the underrated element for feeding the world. *Trends in Plant Science* **21**:461-63.

Hillebrand, H., Dürselen, C. D., Kirschtel, D., Pollingher, U. & Zohary, T. 1999. Biovolume calculation for pelagic and benthic microalgae. *Journal of Phycology* **35**:403-24.

Hillebrand, H. & Matthiessen, B. 2009. Biodiversity in a complex world: consolidation and progress in functional biodiversity research. *Ecology Letters* **12**:1405-19.

Hillebrand, H., Steinert, G., Boersma, M., Malzahn, A., Meunier, C. L., Plum, C. & TPtacnik, R. 2013. Goldman revisited: faster-growing phytoplankton has lower N:P and lower flexibility. *Limnology and Oceanography* **58**:2076-88.

Hobday, A. J., Alexander, L. V., Perkins, S. E., Smale, D. A., Straub, S. C., Oliver, E. C. J., Benthuysen, J. A., Burrows, M. T., Donat, M. G. & Feng, M. 2016. A hierarchical approach to defining marine heatwaves. *Progress in Oceanography* **141**:227-38.

Hofmann, P., Chatzinotas, A., Harpole, W. S. & Dunker, S. 2019. Temperature and stoichiometric dependence of phytoplankton traits. *Ecology* **100**:14.

Honjo, S. & Manganini, S. J. 1993. Annual biogenic particle fluxes to the interior of the North Atlantic Ocean; studied at 34°N 21°W and 48°N 21°W. *Deep Sea Research Part II: Topical Studies in Oceanography* **40**:587-607.

Hutchinson, G. E. 1961. The paradox of the plankton. *The American Naturalist* **95**:137-45.

Hutter, K.-J. & Eipel, H. E. 1978. Flow cytometric determinations of cellular substances in algae, bacteria, moulds and yeasts. *Antonie Van Leeuwenhoek* **44**:269-82.

Hyka, P., Lickova, S., Přibyl, P., Melzoch, K. & Kovar, K. 2013. Flow cytometry for the development of biotechnological processes with microalgae. *Biotechnology Advances* **31**:2-16.

IPCC 2014. Summary for policymakers. *In*: Field, C. B., Barros, V. R., Dokken, D. J., Mach, K. J., Mastrandrea, M. D., Bilir, T. E., Chatterjee, M., Ebi, K. L., Estrada, Y. O., Genova, R. C., Girma, B., Kissel, E. S., Levy, A. N., MacCracken, S., Mastrandrea, P. R. & White, L. L. [Eds.] *Climate change 2014: Impacts, Adaptation, and Vulnerability. Part A: Global and Sectoral Aspects. Contribution of Working Group II to the Fifth Assessment Report of the Intergovernmental Panel on Climate Change.* Cambridge University Press, pp. 1-32.

IPCC 2019. *Summary for Policymakers.* AGU,

IPCC 2021. Summary for Policymakers. *In*: MassonDelmotte, V., Zhai, P., Pirani, A., Connors, S. L., Péan, C., Berger, S., Caud, N., Chen, Y., Goldfarb, L., Gomis, M. I., Huang, M., Leitzell, K., Lonnoy, E., Matthews, J. B. R., Maycock, T. K., Waterfield, T., Yelekçi, O., Yu, R. & Zhou, B. [Eds.] *Climate Change 2021: The Physical Science Basis. Contribution of Working Group I*

to the Sixth Assessment Report of the Intergovernmental Panel on Climate Change. Cambridge University Press.

Irwin, A. J. & Finkel, Z. V. 2008. Mining a sea of data: deducing the environmental controls of ocean chlorophyll. *PLoS ONE* **3**:e3836.

Irwin, A. J., Finkel, Z. V., Schofield, O. M. E. & Falkowski, P. G. 2006. Scaling-up from nutrient physiology to the size-structure of phytoplankton communities. *Journal of Plankton Research* **28**:459-71.

Janknegt, P. J., Van de Poll, W. H., Visser, R. J. W., Rijstenbil, J. W. & Buma, A. G. J. 2008. Oxidative stress responses in the marine Antarctic diatom *Chaetoceros brevis* (bacillariophyceae) during photoacclimation. *Journal of Phycology* **44**:957-66.

Jaschinski, T., Helfrich, E. J. N., Bock, C., Wolfram, S., Svatoš, A., Hertweck, C. & Pohnert, G. 2014. Matrix-free single-cell LDI-MS investigations of the diatoms *Coscinodiscus granii* and *Thalassiosira pseudonana*. *Journal of Mass Spectrometry* **49**:136-44.

Jentsch, A., Kreyling, J. & Beierkuhnlein, C. 2007. A new generation of climate-change experiments: events, not trends. *Frontiers in Ecology and the Environment* **5**:365-74.

Jiao, N., Herndl, G. J., Hansell, D. A., Benner, R., Kattner, G., Wilhelm, S. W., Kirchman, D. L., Weinbauer, M. G., Luo, T. & Chen, F. 2010. Microbial production of recalcitrant dissolved organic matter: long-term carbon storage in the global ocean. *Nature Reviews Microbiology* **8**:593-99.

Jochem, F. J. 2000. Probing the physiological state of phytoplankton at the single-cell level. *Scientia Marina* **64**:183-95.

Jones, T., Parrish, J. K., Peterson, W. T., Bjorkstedt, E. P., Bond, N. A., Ballance, L. T., Bowes, V., Hipfner, J. M., Burgess, H. K. & Dolliver, J. E. 2018. Massive mortality of a planktivorous seabird in response to a marine heatwave. *Geophysical Research Letters* **45**:3193-202.

Juan, Y., Tang, X.-X., Zhang, P.-Y., Tian, J.-Y. & Cai, H.-J. 2004. Effects of CO_2 enrichment on photosynthesis, lipid peroxidation and activities of antioxidative enzymes of *Platymonas subcordiformis* subjected to UV-B radiation stress. *Acta Botanica Sinica* **46**:682-90.

Kaeppel, E. C., Gärdes, A., Seebah, S., Grossart, H.-P. & Ullrich, M. S. 2012. *Marinobacter adhaerens* sp. nov., isolated from marine aggregates formed with the diatom *Thalassiosira weissflogii*. *International Journal of Systematic and Evolutionary Microbiology* **62**:124-28.

Kirst, G. O. 1990. Salinity tolerance of eukaryotic marine algae. *Annu. Rev. Plant Biol.* **41**:21-53.

Klausmeier, C. A., Litchman, E., Daufresne, T. & Levin, S. A. 2004. Optimal nitrogen-to-phosphorus stoichiometry of phytoplankton. *Nature* **429**:171-4.

Knight, J. A., Anderson, S. & Rawle, J. M. 1972. Chemical basis of the sulfo-phospho-vanillin reaction for estimating total serum lipids. *Clinical Chemistry* **18**:199-202.

Kremer, C. T., Thomas, M. K. & Litchman, E. 2017. Temperature-and size-scaling of phytoplankton population growth rates: reconciling the Eppley curve and the metabolic theory of ecology. *Limnology and Oceanography* **62**:1658-70.

Kremp, A., Godhe, A., Egardt, J., Dupont, S., Suikkanen, S., Casabianca, S. & Penna, A. 2012. Intraspecific variability in the response of bloom-forming marine microalgae to changed climate conditions. *Ecology and Evolution* **2**:1195-207.

Kröncke, I. & Knust, R. 1995. The Dogger Bank: a special ecological region in the central North Sea. *Helgoländer Meeresuntersuchungen* **49**:335-53.

Kuczynska, P., Jemiola-Rzeminska, M. & Strzalka, K. 2015. Photosynthetic pigments in diatoms. *Marine Drugs* **13**:5847-81.

Kvernvik, A. C., Rokitta, S. D., Leu, E., Harms, L., Gabrielsen, T. M., Rost, B. & Hoppe, C. J. M. 2020. Higher sensitivity towards light stress and ocean acidification in an Arctic sea-ice-associated diatom compared to a pelagic diatom. *New Phytologist* **226**:1708-24.

Lamb, J. J., Røkke, G. & Hohmann-Marriott, M. F. 2018. Chlorophyll fluorescence emission spectroscopy of oxygenic organisms at 77 K. *Photosynthetica* **56**:105-24.

Launay, H., Huang, W., Maberly, S. C. & Gontero, B. 2020. Regulation of carbon metabolism by environmental conditions: a perspective from diatoms and other chromalveolates. *Frontiers in Plant Science*:1033.

Laws, E. & Caperon, J. 1976. Carbon and nitrogen metabolism by *Monochrysis lutheri*: measurement of growth-rate-dependent respiration rates. *Mar. Biol.* **36**:85-97.

Lee, S. & Fuhrman, J. A. 1987. Relationships between biovolume and biomass of naturally derived marine bacterioplankton. *Applied and Environmental Microbiology* **53**:1298-303.

Lenton, T. M. & Watson, A. J. 2000. Redfield revisited: regulation of nitrate, phosphate, and oxygen in the ocean. *Glob. Biogeochem. Cycle* **14**:225-48.

Lesser, M. P. 1997. Oxidative stress causes coral bleaching during exposure to elevated temperatures. *Coral Reefs* **16**:187-92.

Lewandowska, A. & Sommer, U. 2010. Climate change and the spring bloom: a mesocosm study on the influence of light and temperature on phytoplankton and mesozooplankton. *Marine Ecology Progress Series* **405**:101-11.

Li, J. & Sun, X. 2016. Effects of different phosphorus concentrations and N/P ratios on the growth and photosynthetic characteristics of *Skeletonema costatum* and *Prorocentrum donghaiense*. *Chinese Journal of Oceanology and Limnology* **34**:1158-72.

Liefer, J. D., Garg, A., Fyfe, M. H., Irwin, A. J., Benner, I., Brown, C. M., Follows, M. J., Omta, A. W. & Finkel, Z. V. 2019. The macromolecular basis of phytoplankton C:N:P under nitrogen starvation. *Frontiers in Microbiology* **10**:763.

Litchman, E., De Tezanos Pinto, P., Klausmeier, C. A., Thomas, M. K. & Yoshiyama, K. 2010. Linking traits to species diversity and community structure in phytoplankton. *Hydrobiologia*:15-28.

Litchman, E. & Klausmeier, C. A. 2008. Trait-based community ecology of phytoplankton. *Annual Review of Ecology, Evolution, and Systematics* **39**:615-39.

Litchman, E., Klausmeier, C. A., Schofield, O. M. & Falkowski, P. G. 2007. The role of functional traits and trade-offs in structuring phytoplankton communities: scaling from cellular to ecosystem level. *Ecology Letters* **10**:1170-81.

Litchman, E., Klausmeier, C. A. & Yoshiyama, K. 2009. Contrasting size evolution in marine and freshwater diatoms. *Proceedings of the National Academy of Sciences* **106**:2665-70.

Liu, H., Bidigare, R. R., Laws, E., Landry, M. R. & Campbell, L. 1999. Cell cycle and physiological characteristics of *Synechococcus* (WH7803) in chemostat culture. *Marine Ecology Progress Series* **189**:17-25.

MacArthur, R. 1955. Fluctuations of animal populations and a measure of community stability. *Ecology* **36**:533-36.

Mallick, N., Mohn, F. H., Soeder, C. J. & Grobbelaar, J. U. 2002. Ameliorative role of nitric oxide on H_2O_2 toxicity to a chlorophycean alga *Scenedesmus obliquus*. *The Journal of General and Applied Microbiology* **48**:1-7.

Marañón, E. 2015. Cell size as a key determinant of phytoplankton metabolism and community structure.

Marañón, E., Cermeno, P., López-Sandoval, D. C., Rodríguez-Ramos, T., Sobrino, C., Huete-Ortega, M., Blanco, J. M. & Rodríguez, J. 2013. Unimodal size scaling of phytoplankton growth and the size dependence of nutrient uptake and use. *Ecology Letters* **16**:371-79.

Margalef, R. 1978. Life-forms of phytoplankton as survival alternatives in an unstable environment. *Oceanologica Acta* **1**:493-509.

Markina, Z. V. 2019. Flow cytometry as a method to study marine unicellular algae: development, problems, and prospects. *Russian Journal of Marine Biology* **45**:333-40.

Marra, J. & Barber, R. T. 2004. Phytoplankton and heterotrophic respiration in the surface layer of the ocean. *Geophysical Research Letters* **31**.

Martinez, R. 1992. Respiration and respiratory electron transport activity in marine phytoplankton: growth rate dependence and light enhancement. *Journal of Plankton Research* **14**:789-97.

McGinnis, K. M., Dempster, T. A. & Sommerfeld, M. R. 1997. Characterization of the growth and lipid content of the diatom *Chaetoceros muelleri*. *Journal of Applied Phycology* **9**:19-24.

Mehrbach, C., Culberson, C. H., Hawley, J. E. & Pytkowicx, R. M. 1973. Measurement of the apparent dissociation constants of carbonic acid in seawater at atmospheric pressure. *Limnology and Oceanography* **18**:897-907.

Meunier, C. L., Boersma, M., El-Sabaawi, R., Halvorson, H. M., Herstoff, E. M., Van de Waal, D. B., Vogt, R. J. & Litchman, E. 2017. From elements to function: Toward unifying ecological stoichiometry and trait-based ecology. *Frontiers in Environmental Science* **5**:10.

Mittler, R., Vanderauwera, S., Gollery, M. & Van Breusegem, F. 2004. Reactive oxygen gene network of plants. *Trends in Plant Science* **9**:490-98.

Mohamed, Z. A. 2008. Polysaccharides as a protective response against microcystin-induced oxidative stress in *Chlorella vulgaris* and *Scenedesmus quadricauda* and their possible significance in the aquatic ecosystem. *Ecotoxicology* **17**:504-16.

Møller, I. M. 2001. Plant mitochondria and oxidative stress: electron transport, NADPH turnover, and metabolism of reactive oxygen species. *Annu. Rev. Plant Biol.* **52**:561-91.

Montagnes, D. J. S. & Franklin, M. 2001. Effect of temperature on diatom volume, growth rate, and carbon and nitrogen content: reconsidering some paradigms. *Limnology and Oceanography* **46**:2008-18.

Moore, C. M., Mills, M. M., Arrigo, K. R., Berman-Frank, I., Bopp, L., Boyd, P. W., Galbraith, E. D., Geider, R. J., Guieu, C. & Jaccard, S. L. 2013. Processes and patterns of oceanic nutrient limitation. *Nature Geoscience* **6**:701-10.

Morán, X. A. G., López-Urrutia, Á., Calvo-Diaz, A. & Li, W. K. 2010. Increasing importance of small phytoplankton in a warmer ocean. *Global Change Biology* **16**:1137-44.

Moreira-Turcq, P. F. & Martin, J. M. 1998. Characterisation of fine particles by flow cytometry in estuarine and coastal Arctic waters. *Journal of Sea Research* **39**:217-26.

Moreno, H. D., Köring, M., Di Pane, J., Tremblay, N., Wiltshire, K. H., Boersma, M. & Meunier, C. L. 2022. An integrated multiple driver mesocosm experiment reveals the effect of global change on planktonic food web structure. *Communications Biology* **5**:179.

Murik, O., Tirichine, L., Prihoda, J., Thomas, Y., Araújo, W. L., Allen, A. E., Fernie, A. R. & Bowler, C. 2019. Downregulation of mitochondrial alternative oxidase affects chloroplast function, redox status and stress response in a marine diatom. *New Phytologist* **221**:1303-16.

Nelson, D. M., Treguer, P., Brzezinski, M. A., Leynaert, A. & Queguiner, B. 1995. Production and dissolution of biogenic silica in the ocean - revised global estimates, comparison with regional data and relationship to biogenic sedimentation. *Glob. Biogeochem. Cycle* **9**:359-72.

Neori, A. & Holm-Hansen, O. 1982. Effect of temperature on rate of photosynthesis in Antarctic phytoplankton. *Polar Biology* **1**:33-38.

Núñez-Riboni, I. & Akimova, A. 2017. Quantifying the impact of the major driving mechanisms of inter-annual variability of salinity in the North Sea. *Progress in Oceanography* **154**:25-37.

Oakley, C. A., Hopkinson, B. M. & Schmidt, G. W. 2014. Mitochondrial terminal alternative oxidase and its enhancement by thermal stress in the coral symbiont *Symbiodinium*. *Coral Reefs* **33**:543-52.

Ober, J. A. 2016. Mineral commodity summaries 2016. *Mineral Commodity Summaries.* Reston, VA, pp. 205.

Obernosterer, I. & Herndl, G. J. 1995. Phytoplankton extracellular release and bacterial growth:dependence on the inorganic N:P ratio. *Marine Ecology Progress Series* **116**:247-57.

Olenina, I., Hajdu, S., Edler, L., Andersson, A., Wasmund, N., Busch, S., Göbel, J., Gromisz, S., Huseby, S., Huttunen, M., Jaanus, A., Kokkonen, P., Ledaine, I. & Niemkiewicz, E.

2006. *Biovolumes and size-classes of phytoplankton in the Baltic Sea.* HELCOM Balt.Sea Environ. Proc., 144.

Otero, J., Álvarez-Salgado, X. A. & Bode, A. 2020. Phytoplankton diversity effect on ecosystem functioning in a coastal upwelling system. *Frontiers in Marine Science* **7**:959.

Paau, A. S., Oro, J. & Cowles, J. R. 1978. Application of flow microflorometry to the study of algal cells and isolated chloroplasts. *Journal of Experimental Botany* **29**:1011-20.

Paczkowska, J., Brugel, S., Rowe, O., Lefébure, R., Brutemark, A. & Andersson, A. 2020. Response of coastal phytoplankton to high inflows of terrestrial matter. *Frontiers in Marine Science* **7**:80.

Padfield, D., Yvon-Durocher, G., Buckling, A., Jennings, S. & Yvon-Durocher, G. 2016. Rapid evolution of metabolic traits explains thermal adaptation in phytoplankton. *Ecology Letters* **19**:133-42.

Paerl, H. W., Hall, N. S., Peierls, B. L. & Rossignol, K. L. 2014. Evolving paradigms and challenges in estuarine and coastal eutrophication dynamics in a culturally and climatically stressed world. *Estuaries and Coasts* **37**:243-58.

Paerl, H. W., Valdes-Weaver, L. M., Joyner, A. R. & Winkelmann, V. 2007. Phytoplankton indicators of ecological change in the eutrophying Pamlico Sound system, North Carolina. *Ecological Applications* **17**:S88-S101.

Passow, U. & Laws, E. A. 2015. Ocean acidification as one of multiple stressors: growth response of *Thalassiosira weissflogii* (diatom) under temperature and light stress. *Marine Ecology Progress Series* **541**:75-90.

Pecqueur, D., Vidussi, F., Fouilland, E., Le Floc'h, E., Mas, S., Roques, C., Salles, C., Tournoud, M.-G. & Mostajir, B. 2011. Dynamics of microbial planktonic food web components during a river flash flood in a Mediterranean coastal lagoon. *Hydrobiologia* **673**:13-27.

Peñuelas, J., Poulter, B., Sardans, J., Ciais, P., Van Der Velde, M., Bopp, L., Boucher, O., Godderis, Y., Hinsinger, P. & Llusia, J. 2013. Human-induced nitrogen-phosphorus imbalances alter natural and managed ecosystems across the globe. *Nature Communications* **4**:1-10.

Peñuelas, J., Sardans, J., Rivas-ubach, A. & Janssens, I. A. 2012. The human-induced imbalance between C, N and P in Earth's life system. *Global Change Biology* **18**:3-6.

Perelman, A., Dubinsky, Z. & Martínez, R. 2006. Temperature dependence of superoxide dismutase activity in plankton. *Journal of Experimental Marine Biology and Ecology* **334**:229-35.

Pierrot, D., Lewis, E. & Wallace, D. W. R. 2006. MS Excel program developed for CO_2 system calculations. *ORNL/CDIAC-105a. Carbon dioxide information analysis center, oak ridge national laboratory, US Department of Energy, Oak Ridge, Tennessee* **10**.

Pinckney, J. L., Paerl, H. W. & Harrington, M. B. 1999. Responses of the phytoplankton community growth rate to nutrient pulses in variable estuarine environments. *Journal of Phycology* **35**:1455-63.

Ploug, H., Stolte, W., Epping, E. H. G. & Jorgensen, B. B. 1999. Diffusive boundary layers, photosynthesis, and respiration of the colony-forming plankton algae, *Phaeocystis sp. Limnology and Oceanography* **44**:1949-58.

Pogorzelec, N. M., Mundy, C. J., Findlay, C. R., Campbell, K., Diaz, A., Ehn, J. K., Rysgaard, S. & Gough, K. M. 2017. FTIR imaging analysis of cell content in sea-ice diatom taxa during a spring bloom in the lower Northwest Passage of the Canadian Arctic. *Marine Ecology Progress Series* **569**:77-88.

Pomroy, A. J. 1984. Direct counting of bacteria preserved with Lugol iodine solution. *Applied and Environmental Microbiology* **47**:1191-92.

Prandle, D., Hydes, D. J., Jarvis, J. & McManus, J. 1997. The seasonal cycles of temperature, salinity, nutrients and suspended sediment in the southern North Sea in 1988 and 1989. *Estuarine, Coastal and Shelf Science* **45**:669-80.

Prihoda, J., Tanaka, A., de Paula, W. B. M., Allen, J. F., Tirichine, L. & Bowler, C. 2012. Chloroplast-mitochondria cross-talk in diatoms. *Journal of Experimental Botany* **63**:1543-57.

Quante, M., Colijn, F., Bakker, J. P., Härdtle, W., Heinrich, H., Lefebvre, C., Nöhren, I., Olesen, J. E., Pohlmann, T. & Sterr, H. 2016. Introduction to the assessment-characteristics of the region. *North Sea Region Climate Change Assessment.* Springer, pp. 1-52.

R Core Team 2013. R: A language and environment for statistical computing. R Foundation for Statistical Computing, Vienna, Austria.

R Core Team 2021. R: A language and environment for statistical computing. R Foundation for Statistical Computing, Vienna, Austria.

Radach, G. & Pätsch, J. 2007. Variability of continental riverine freshwater and nutrient inputs into the North Sea for the years 1977–2000 and its consequences for the assessment of eutrophication. *Estuaries and Coasts* **30**:66-81.

Rajagopal, S., Murthy, S. D. S. & Mohanty, P. 2000. Effect of ultraviolet-B radiation on intact cells of the cyanobacterium *Spirulina platensis*: characterization of the alterations in the thylakoid membranes. *Journal of Photochemistry and Photobiology B: Biology* **54**:61-66.

Ras, M., Steyer, J.-P. & Bernard, O. 2013. Temperature effect on microalgae: a crucial factor for outdoor production. *Reviews in Environmental Science and Bio/Technology* **12**:153-64.

Rasdi, N. W. & Qin, J. G. 2015. Effect of N:P ratio on growth and chemical composition of *Nannochloropsis oculata* and *Tisochrysis lutea*. *Journal of Applied Phycology* **27**:2221-30.

Raven, J. A. & Geider, R. J. 1988. Temperature and algal growth. *New Phytologist* **110**:441-61.

Remy, M., Hillebrand, H. & Flöder, S. 2017. Stability of marine phytoplankton communities facing stress related to global change: interactive effects of heat waves and turbidity. *Journal of Experimental Marine Biology and Ecology* **497**:219-29.

Riebesell, U. 2004. Effects of CO_2 enrichment on marine phytoplankton. *J. Oceanogr.* **60**:719-29.

Riebesell, U., Schulz, K. G., Bellerby, R. G. J., Botros, M., Fritsche, P., Meyerhöfer, M., Neill, C., Nondal, G., Oschlies, A. & Wohlers, J. 2007. Enhanced biological carbon consumption in a high CO_2 ocean. *Nature* **450**:545-48.

Rokitta, S. D., Kranz, S. A. & Rost, B. in press. Inorganic carbon aquisition by aquatic primary producers. *In*: Maberly, S. C. & Gontero, B. [Eds.] *Blue planet, red and green photosynthesis.* ISTE-Wiley.

Rokitta, S. D. & Rost, B. 2012. Effects of CO_2 and their modulation by light in the life-cycle stages of the coccolithophore *Emiliania huxleyi*. *Limnology and Oceanography* **57**:607-18.

Schindler, D. W. 1987. Detecting ecosystem responses to anthropogenic stress. *Canadian Journal of Fisheries and Aquatic Sciences* **44**:s6-s25.

Seifert, M., Rost, B., Trimborn, S. & Hauck, J. 2020. Meta-analysis of multiple driver effects on marine phytoplankton highlights modulating role of pCO_2. *Global Change Biology* **26**:6787-804.

Sett, S., Bach, L. T., Schulz, K. G., Koch-Klavsen, S., Lebrato, M. & Riebesell, U. 2014. Temperature modulates coccolithophorid sensitivity of growth, photosynthesis and calcification to increasing seawater pCO_2. *PLoS ONE* **9**:9.

Sett, S., Schulz, K. G., Bach, L. T. & Riebesell, U. 2018. Shift towards larger diatoms in a natural phytoplankton assemblage under combined high-CO_2 and warming conditions. *Journal of Plankton Research* **40**:391-406.

Sharma, K. K., Schuhmann, H. & Schenk, P. M. 2012. High lipid induction in microalgae for biodiesel production. *Energies* **5**:1532-53.

Sherwood, T. K., Pigford, R. L. & Wilke, C. R. 1975. *Mass Transfer.* McGraw-Hill Book Company,

Shi, D., Hong, H., Su, X., Liao, L., Chang, S. & Lin, W. 2019. The physiological response of marine diatoms to ocean acidification: differential roles of seawater pCO_2 and pH. *Journal of Phycology* **55**:521-33.

Shikata, T., Nagasoe, S., Oh, S.-J., Matsubara, T., Yamasaki, Y., Shimasaki, Y., Oshima, Y. & Honjo, T. 2008. Effects of down-and up-shocks from rapid changes of salinity on survival and growth of estuarine phytoplankters. *Journal-Faculty of Agriculture Kyushu University* **53**:81.

Siron, R., Giusti, G. & Berland, B. 1989. Changes in the fatty acid composition of *Phaeodactylum tricornutum* and *Dunaliella tertiolecta* during growth and under phosphorus deficiency. *Marine Ecology Progress Series*:95-100.

Smayda, T. J. 1970. The suspension and sinking of phytoplankton in the sea. *Oceanography and Marine Biology - An Annual Review* **8**:353-414.

Smetacek, V. 1999. Diatoms and the ocean carbon cycle. *Protist* **150**:25-32.

Sommer, U. 1984. The paradox of the plankton: fluctuations of phosphorus availability maintain diversity of phytoplankton in flow-through cultures. *Limnology and Oceanography* **29**:633-36.

Sommer, U., Paul, C. & Moustaka-Gouni, M. 2015. Warming and ocean acidification effects on phytoplankton-from species shifts to size shifts within species in a mesocosm experiment. *PLoS ONE* **10**:e0125239.

Spilling, K., Olli, K., Lehtoranta, J., Kremp, A., Tedesco, L., Tamelander, T., Klais, R., Peltonen, H. & Tamminen, T. 2018. Shifting diatom-dinoflagellate dominance during spring bloom in the Baltic Sea and its potential effects on biogeochemical cycling. *Frontiers in Marine Science* **5**:327.

Staehr, P. A. & Birkeland, M. J. 2006. Temperature acclimation of growth, photosynthesis and respiration in two mesophilic phytoplankton species. *Phycologia* **45**:648-56.

Stelfox-Widdicombe, C. E., Archer, S. D., Burkill, P. H. & Stefels, J. 2004. Microzooplankton grazing in *Phaeocystis* and diatom-dominated waters in the southern North Sea in spring. *Journal of Sea Research* **51**:37-51.

Sterner, R. W. & Elser, J. J. 2002. *Ecological stoichiometry: the biology of elements from molecules to the biosphere.* Princeton University Press,

Stoll, M. H. C., Bakker, K., Nobbe, G. H. & Haese, R. R. 2001. Continuous-flow analysis of dissolved inorganic carbon content in seawater. *Analytical Chemistry* **73**:4111-16.

Stolte, W. & Riegman, R. 1996. A model approach for size-selective competition of marine phytoplankton for fluctuating nitrate and ammonium. *Journal of Phycology* **32**:732-40.

Strickland, J. D. H. & Parsons, T. R. 1972. A practical handbook of seawater analysis.

Striebel, M., Schabhüttl, S., Hodapp, D., Hingsamer, P. & Hillebrand, H. 2016. Phytoplankton responses to temperature increases are constrained by abiotic conditions and community composition. *Oecologia* **182**:815-27.

Sugie, K. & Yoshimura, T. 2016. Effects of high CO_2 levels on the ecophysiology of the diatom *Thalassiosira weissflogii* differ depending on the iron nutritional status. *ICES J. Mar. Sci.* **73**:680-92.

Taniguchi, N. & Gutteridge, J. 2000. *Experimental protocols for reactive oxygen and nitrogen species.* OUP Oxford,

Tanioka, T. & Matsumoto, K. 2020. A meta-analysis on environmental drivers of marine phytoplankton C:N:P. *Biogeosciences* **17**:2939-54.

Taucher, J., Jones, J., James, A., Brzezinski, M. A., Carlson, C. A., Riebesell, U. & Passow, U. 2015. Combined effects of CO2 and temperature on carbon uptake and partitioning by the marine diatoms *Thalassiosira weissflogii* and *Dactyliosolen fragilissimus*. *Limnology and Oceanography* **60**:901-19.

Thangaraj, S. & Sun, J. 2020. The biotechnological potential of the marine diatom *Skeletonema dohrnii* to the elevated temperature and pCO_2. *Marine Drugs* **18**:259.

Thangaraj, S. & Sun, J. 2021. Transcriptomic reprogramming of the oceanic diatom *Skeletonema dohrnii* under warming ocean and acidification. *Environmental Microbiology* **23**:980-95.

Thingstad, T. F., Ovreas, L., Egge, J. K., Lovdal, T. & Heldal, M. 2005. Use of non-limiting substrates to increase size; a generic strategy to simultaneously optimize uptake and minimize predation in pelagic osmotrophs? *Ecology Letters* **8**:675-82.

Thomsen, M. S., Mondardini, L., Alestra, T., Gerrity, S., Tait, L., South, P. M., Lilley, S. A. & Schiel, D. R. 2019. Local extinction of bull kelp (*Durvillaea* spp.) due to a marine heatwave. *Frontiers in Marine Science* **6**:84.

Thornton, D. C. O. 2014. Dissolved organic matter (DOM) release by phytoplankton in the contemporary and future ocean. *European Journal of Phycology* **49**:20-46.

Tilman, D. 1977. Resource competition between plankton algae: an experimental and theoretical approach. *Ecology* **58**:338-48.

Tilman, D. 1985. The resource-ratio hypothesis of plant succession. *The American Naturalist* **125**:827-52.

Tong, S., Xu, D., Wang, Y., Zhang, X., Li, Y., Wu, H. & Ye, N. 2021. Influence of ocean acidification on thermal reaction norms of carbon metabolism in the marine diatom *Phaeodactylum tricornutum*. *Marine Environmental Research* **164**:105233.

Torstensson, A., Hedblom, M., Mattsdotter Björk, M., Chierici, M. & Wulff, A. 2015. Long-term acclimation to elevated pCO_2 alters carbon metabolism and reduces growth in the Antarctic diatom *Nitzschia lecointei*. *Proceedings of the Royal Society B: Biological Sciences* **282**:20151513.

Tortell, P. D., Payne, C., Gueguen, C., Strzepek, R. F., Boyd, P. W. & Rost, B. 2008. Inorganic carbon uptake by Southern Ocean phytoplankton. *Limnology and Oceanography* **53**:1266-78.

Toseland, A. D. S. J., Daines, S. J., Clark, J. R., Kirkham, A., Strauss, J., Uhlig, C., Lenton, T. M., Valentin, K., Pearson, G. A. & Moulton, V. 2013. The impact of temperature on marine phytoplankton resource allocation and metabolism. *Nature Climate Change* **3**:979-84.

Tyrrell, T. 1999. The relative influences of nitrogen and phosphorus on oceanic primary production. *Nature* **400**:525-31.

Uchiyama, M. & Mihara, M. 1978. Determination of malonaldehyde precursor in tissues by thiobarbituric acid test. *Analytical Biochemistry* **86**:271-78.

Utermöhl, H. 1958. Zur vervollkommnung der quantitativen phytoplankton-methodik: Mit 1 Tabelle und 15 abbildungen im Text und auf 1 Tafel. *Internationale Vereinigung für theoretische und angewandte Limnologie: Mitteilungen* **9**:1-38.

Van Beusekom, J., Carstensen, J., Dolch, T., Grage, A., Hofmeister, R., Kerimoglu, O., Kolbe, K., Lenhart, H., Pätsch, J. & Rick, J. 2019. Wadden Sea Eutrophication: long-term trends and regional differences. *Frontiers in Marine Science* **6**:370.

Van de Waal, D. B. & Litchman, E. 2020. Multiple global change stressor effects on phytoplankton nutrient acquisition in a future ocean. *Philosophical Transactions of the Royal Society B* **375**:20190706.

Vanlerberghe, G. C. 2013. Alternative oxidase: a mitochondrial respiratory pathway to maintain metabolic and signaling homeostasis during abiotic and biotic stress in plants. *International Journal of Molecular Sciences* **14**:6805-47.

Vega-López, A., Ayala-López, G., Posadas-Espadas, B. P., Olivares-Rubio, H. F. & Dzul-Caamal, R. 2013. Relations of oxidative stress in freshwater phytoplankton with heavy metals and polycyclic aromatic hydrocarbons. *Comparative Biochemistry and Physiology Part A: Molecular & Integrative Physiology* **165**:498-507.

Villanova, V., Fortunato, A. E., Singh, D., Bo, D. D., Conte, M., Obata, T., Jouhet, J., Fernie, A. R., Marechal, E. & Falciatore, A. 2017. Investigating mixotrophic metabolism in the model diatom *Phaeodactylum tricornutum*. *Philosophical Transactions of the Royal Society B: Biological Sciences* **372**:20160404.

Violle, C., Navas, M. L., Vile, D., Kazakou, E., Fortunel, C., Hummel, I. & Garnier, E. 2007. Let the concept of trait be functional! *Oikos* **116**:882-92.

Von Dassow, P., Chepurnov, V. A. & Armbrust, E. V. 2006. Relationships between growth rate, cell size, and introduction of spermatogenesis in the centric diatom *Thalassiosira weissflogii* (Bacillariophyta). *Journal of Phycology* **42**:887-99.

Voynova, Y. G., Brix, H., Petersen, W., Weigelt-Krenz, S. & Scharfe, M. 2017. Extreme flood impact on estuarine and coastal biogeochemistry: the 2013 Elbe flood. *Biogeosciences* **14**:541-57.

Wagner, H., Jakob, T. & Wilhelm, C. 2006. Balancing the energy flow from captured light to biomass under fluctuating light conditions. *The New Phytologist* **169**:95-108.

Wagner, H., Liu, Z., Langner, U., Stehfest, K. & Wilhelm, C. 2010. The use of FTIR spectroscopy to assess quantitative changes in the biochemical composition of microalgae. *Journal of biophotonics* **3**:557-66.

Weisse, T., Gröschl, B. & Bergkemper, V. 2016. Phytoplankton response to short-term temperature and nutrient changes. *Limnologica* **59**:78-89.

Weithoff, G. & Beisner, B. E. 2019. Measures and approaches in trait-based phytoplankton community ecology - from freshwater to marine ecosystems. *Frontiers in Marine Science* **6**.

Wen, X., Geng, Y. & Li, Y. 2014. Enhanced lipid production in *Chlorella pyrenoidosa* by continuous culture. *Bioresource Technology* **161**:297-303.

Wernberg, T., Smale, D. A. & Thomsen, M. S. 2012. A decade of climate change experiments on marine organisms: procedures, patterns and problems. *Global Change Biology* **18**:1491-98.

Wetz, M. S. & Wheeler, P. A. 2007. Release of dissolved organic matter by coastal diatoms. *Limnology and Oceanography* **52**:798-807.

Wiltshire, K. H., Boersma, M., Möller, A. & Buhtz, H. 2000. Extraction of pigments and fatty acids from the green alga *Scenedesmus obliquus* (Chlorophyceae). *Aquatic Ecology* **34**:119-26.

Wiltshire, K. H., Kraberg, A., Bartsch, I., Boersma, M., Franke, H.-D., Freund, J., Gebühr, C., Gerdts, G., Stockmann, K. & Wichels, A. 2010. Helgoland roads, North Sea: 45 years of change. *Estuaries and Coasts* **33**:295-310.

Winder, M. & Sommer, U. 2012. Phytoplankton response to a changing climate. *Hydrobiologia* **698**:5-16.

Wolf, K. K. E., Hoppe, C. J. M. & Rost, B. 2018. Resilience by diversity: large intraspecific differences in climate change responses of an Arctic diatom. *Limnology and Oceanography* **63**:397-411.

Wolf, K. K. E., Romanelli, E., Rost, B., John, U., Collins, S., Weigand, H. & Hoppe, C. J. M. 2019. Company matters: the presence of other genotypes alters traits and intraspecific

selection in an Arctic diatom under climate change. *Global Change Biology* **25**:2869-84.

Wu, Y., Campbell, D. A., Irwin, A. J., Suggett, D. J. & Finkel, Z. V. 2014. Ocean acidification enhances the growth rate of larger diatoms. *Limnology and Oceanography* **59**:1027-34.

Wu, Y., Gao, K. & Riebesell, U. 2010. CO_2-induced seawater acidification affects physiological performance of the marine diatom *Phaeodactylum tricornutum*. *Biogeosciences* **7**:2915-23.

Yakovleva, I. M., Baird, A. H., Yamamoto, H. H., Bhagooli, R., Nonaka, M. & Hidaka, M. 2009. Algal symbionts increase oxidative damage and death in coral larvae at high temperatures. *Marine Ecology Progress Series* **378**:105-12.

Yodsuwan, N., Sawayama, S. & Sirisansaneeyakul, S. 2017. Effect of nitrogen concentration on growth, lipid production and fatty acid profiles of the marine diatom *Phaeodactylum tricornutum*. *Agriculture and Natural Resources* **51**:190-97.

Yoshida, K., Terashima, I. & Noguchi, K. 2007. Up-regulation of mitochondrial alternative oxidase concomitant with chloroplast over-reduction by excess light. *Plant Cell Physiology* **48**:606-14.

Young, J. N., Kranz, S. A., Goldman, J. A. L., Tortell, P. D. & Morel, F. M. M. 2015. Antarctic phytoplankton down-regulate their carbon-concentrating mechanisms under high CO_2 with no change in growth rates. *Marine Ecology Progress Series* **532**:13-28.

Zalutskaya, Z., Lapina, T. & Ermilova, E. 2015. The *Chlamydomonas reinhardtii* alternative oxidase 1 is regulated by heat stress. *Plant Physiology and Biochemistry* **97**:229-34.

Zlotnik, I. & Dubinsky, Z. 1989. The effect of light and temperature on DOC excretion by phytoplankton. *Limnology and Oceanography* **34**:831-39.

Acknowledgments

I would like to thank PD Dr. Cédric Meunier for making this thesis possible, his support as a supervisor, and the freedom he gave me to work on this topic. I thank Prof. Dr. Maarten Boersma for his advice and valuable feedback during my PhD. I would like to thank Prof. Dr. Tilmann Harder for the evaluation of this thesis and Prof. Dr. Marko Rohlfs and Dr. Marlis Reich for being part of my defense committee. I thank Prof. Dr. Georg Pohnert, PD Dr. Maren Striebel, and Dr. Gunnar Gerdts for their advice in different phases of my PhD as members of my thesis advisory committee.

I would like to thank the Federal Ministry of Education and Research (BMBF) for the financial support of my PhD. I thank the Royal Netherlands Institute for Sea Research (NIOZ) and the crew from the RV Pelagia for making my fieldwork possible. I would like to thank the AWI graduate school POLMAR for always having an open ear for the PhD students, for their help in all kinds of matters, and for the amazing program they created.

I would like to thank all my Helgoland colleagues who have helped me over the years, Nadine and Tanja, who have trusted me with the supervision of their master's theses, my fellow Helgoland PhDs who have always listened to me and cheered me up, and all the POGOnians I have had the pleasure to meet and who have inspired me. A big thanks goes to Bärbel and Susy, you helped me so much.

I thank Ursula and Julia with all my heart, also for their technical help, but especially for the many talks we had and for becoming my friends. You really are the best! A special thanks also goes to Zoran and Estela, you made my time on Helgoland so much better. Thank you!

Nelly, Laura, and Hugo, what can I say? I don’t know what I would have done without you. You have become the best friends I could have wished for, and I am deeply grateful for your trust and friendship! I am also incredibly grateful to my friends from the mainland, Esma and Laura, who have always been there for me, that I can call you my friends for so many years!

Thank you, Marcus, for being by my side, for always believing in me, and for all your emotional support. I love you!

Finally, I would like to thank my family, my parents, and my siblings, for always believing in me, encouraging me and supporting my decisions. No matter where I've been or what I've done these past years, you've always been there for me. I love you all!

Versicherung an Eides Statt

Ich, Elisabeth Groß,

.

versichere an Eides Statt durch meine Unterschrift, dass ich die vorstehende Arbeit selbständig und ohne fremde Hilfe angefertigt und alle Stellen, die ich wörtlich dem Sinne nach aus Veröffentlichungen entnommen habe, als solche kenntlich gemacht habe, mich auch keiner anderen als der angegebenen Literatur oder sonstiger Hilfsmittel bedient habe.

Ich versichere an Eides Statt, dass ich die vorgenannten Angaben nach bestem Wissen und Gewissen gemacht habe und dass die Angaben der Wahrheit entsprechen und ich nichts verschwiegen habe.

Die Strafbarkeit einer falschen eidesstattlichen Versicherung ist mir bekannt, namentlich die Strafandrohung gemäß § 156 StGB bis zu drei Jahren Freiheitsstrafe oder Geldstrafe bei vorsätzlicher Begehung der Tat bzw. gemäß § 161 Abs. 1 StGB bis zu einem Jahr Freiheitsstrafe oder Geldstrafe bei fahrlässiger Begehung.

_____

Ort, Datum Unterschrift